

Winter 2013

# Ultrasonication assisted Layer-by-Layer technology for the preparation of multi-functional anticancer drugs paclitaxel and lapatinib

Xingcai Zhang

Follow this and additional works at: <https://digitalcommons.latech.edu/dissertations>

 Part of the [Biomedical Engineering and Bioengineering Commons](#), [Nanoscience and Nanotechnology Commons](#), and the [Pharmacy and Pharmaceutical Sciences Commons](#)

---

**ULTRASONICATION ASSISTED LAYER-BY-LAYER TECHNOLOGY FOR THE  
PREPARATION OF MULTI-FUNCTIONAL ANTICANCER DRUGS  
PACLITAXEL AND LAPATINIB**

by

Xingcai Zhang, B. Engr., M. Engr., M. S. M. E., M. S.

A Dissertation Presented in Partial Fulfillment  
of the Requirements for the Degree  
Doctor of Philosophy

COLLEGE OF ENGINEERING AND SCIENCE  
LOUISIANA TECH UNIVERSITY

March 2013

UMI Number: 3570074

All rights reserved

INFORMATION TO ALL USERS

The quality of this reproduction is dependent upon the quality of the copy submitted.

In the unlikely event that the author did not send a complete manuscript and there are missing pages, these will be noted. Also, if material had to be removed, a note will indicate the deletion.

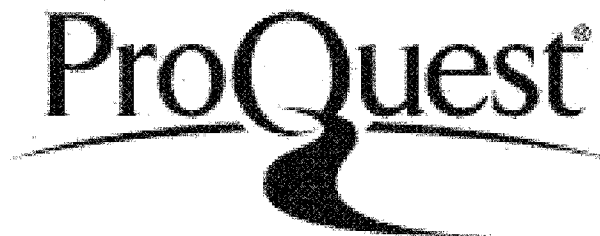


UMI 3570074

Published by ProQuest LLC 2013. Copyright in the Dissertation held by the Author.

Microform Edition © ProQuest LLC.

All rights reserved. This work is protected against unauthorized copying under Title 17, United States Code.



ProQuest LLC  
789 East Eisenhower Parkway  
P.O. Box 1346  
Ann Arbor, MI 48106-1346

LOUISIANA TECH UNIVERSITY

THE GRADUATE SCHOOL

07/17/2012

Date

We hereby recommend that the dissertation prepared under our supervision  
by XINGCAI ZHANG

entitled ULTRASONICATION ASSISTED LAYER-BY-LAYER TECHNOLOGY FOR  
THE PREPARATION OF MULTI-FUNCTIONAL ANTICANCER DRUGS  
PACLITAXEL AND LAPATINIB

be accepted in partial fulfillment of the requirements for the Degree of  
PH.D ENGINEERING

Yuri Lvov  
Supervisor of Dissertation Research  
Chad Shee  
Head of Department  
Engineering  
Department

Recommendation concurred in:

Jesse Palm  
Alan Chiappera  
S. Zivanovic  
Jim Feng

Advisory Committee

Approved: Bala Ramanathan  
Director of Graduate Studies

Approved: William Melorathy  
Dean of the Graduate School

Stan Nye  
Dean of the College

## ABSTRACT

In this dissertation, ultrasonication assisted Layer-by-Layer (LbL) technology for the preparation of multifunctional poorly water-soluble anticancer drug nanoparticles, paclitaxel and lapatinib, has been developed. Many FDA approved drugs are very low soluble in water; therefore, it is very difficult to load and control their release and targeting efficiently, which greatly confines their application. The development of this method will pave the way for the development and application of those low soluble anticancer drugs.

In the first part of this dissertation, the first approach for powerful ultrasonication, the top-down approach (sonicating bulk drug crystals in polyelectrolyte solution), was successfully applied for the preparation of the nanoparticles of paclitaxel. For this approach, a 200 nm diameter was a kind of “magic” barrier for colloidal particles prepared. This diameter barrier may be related to the nucleation size of the solvent vapor microbubbles. Consequently, agents enhancing bubbling formation (such as  $\text{NH}_4\text{HCO}_3$ ) were applied to decrease paclitaxel colloid particles to 100-120 nm. Those paclitaxel nanoparticles were Layer-by-Layer coated with a 10-20 nm polycation/polyanion shell to provide aqueous colloidal stability and slower particle dissolution. However, a large obstacle of these powerful ultrasonication methods was a necessity of long ca 45 minutes high power ultrasonication which resulted in  $\text{TiO}_2$  contamination from titanium electrode. The small amount of  $\text{TiO}_2$  contamination from ultrasonication did negatively affect the *in vivo* testing of

this system in mice, and had to be removed before low toxicity of the Layer-by-Layer coated paclitaxel nanoparticles were observed.

In the second part of the dissertation, the second approach for sonication, the bottom-up approach (sonicating drug in a water-miscible organic solvent followed by slow water add-in) was successfully applied for the preparation of the nanoparticles of lapatinib and paclitaxel with less powerful sonication. By using polymeric excipients combined with non-ionic and anionic surfactants along with regular sonication, the prepared particle sizes was uniform at around 140-150 nm. Less sonication time (ca 15 minutes) and lower sonication power avoided TiO<sub>2</sub> contamination. The amphiphiles attached to the hydrophobic nanoparticles and served as anchors for LbL shell. The inner LbL layers and surfactants minimized the surface free energy, thereby preventing crystal form changes and nanoparticles coalescence, while the outermost layers enhanced colloidal stability.

In the third part of the dissertation, LbL shells with PEGylation (using a block copolymer of poly-L-lysine (PLL) and PEG) for lapatinib were developed for enhanced colloidal stability in high molarity PBS buffer.

In the above proposed paclitaxel and lapatinib formulation, we obtained 150-200 nm with high drug content of 80-90% due to very thin capsule walls (ca 10 nm). The drug release time from the LbL capsules was found to be between 10 and 20 hours depending on the shell thickness. Washless Layer-by-Layer assembly was used: 1) addition of polycation in the amount that is enough to reverse surface charge of the dispersion to a high positive (+30 mV) value; 2) addition of polyanion in the amount that is enough to reverse surface charge of the dispersion to a high negative (-30 mV) value. No intermediate washing of nanoparticles was done until the shell was complete. The washless method had the advantage of time and energy saving, preservation of the sample structure and no losses of sample.

In the last part of the dissertation, we elaborated nanoformulation of two drugs in one nanocapsule locating paclitaxel in the core and lapatinib on the shell periphery. With this formulation, combining in one nanoparticle dual drugs, we reached the drugs' efficiency synergy. In a multidrug-resistant (MDR) ovarian cancer cell line, OVCAR-3, LbL lapatinib/paclitaxel nanocolloids mediated an enhanced cell growth inhibition in comparison with the LbL paclitaxel-only and LbL lapatinib-only treatment, not to say the free one drug treatment.

## APPROVAL FOR SCHOLARLY DISSEMINATION

The author grants to the Prescott Memorial Library of Louisiana Tech University the right to reproduce, by appropriate methods, upon request, any or all portions of this Dissertation. It is understood that "proper request" consists of the agreement, on the part of the requesting party, that said reproduction is for his personal use and that subsequent reproduction will not occur without written approval of the author of this Dissertation. Further, any portions of the Dissertation used in books, papers, and other works must be appropriately referenced to this Dissertation.

Finally, the author of this Dissertation reserves the right to publish freely, in the literature, at any time, any or all portions of this Dissertation.

Author Xingcai Zhang *Xingcai Zhang*  
Date 11/05/2012 *11/05/2012*

## TABLE OF CONTENTS

ABSTRACT .....	iii
ACKNOWLEDGEMENT .....	viii
CHAPTER ONE: INTRODUCTIONS .....	1
1.1 Motivation and Background .....	1
1.2 Methodology for Multifunctional Poorly Soluble Drugs .....	10
1.3 Outline .....	27
CHAPTER TWO: MATERIALS AND INSTRUMENTS .....	28
2.1 Materials .....	28
2.2 Instruments .....	29
CHAPTER THREE: TOP-DOWN APPROACH FOR PREPARING PACLITAXEL NANOCORES .....	38
3.1 Top-Down Approach .....	39
3.2 Top-Down With Bubbling Agent Approach.....	41
3.3 Zeta Potential Monitoring the Layer-by-Layer Process.....	43
3.4 Confocal Fluorescence Image.....	45
3.5 Efficiency of Bubbling Agent Method.....	46
3.6 Mechanism of Bubbling Agent for Enhancement of Ultrasonication Capability .....	47
3.7 Conclusions.....	50

CHAPTER FOUR: BOTTOM-UP APPROACH FOR DRUG NANOFORMULATION .....	51
4.1 Bottom-Up Approach With Powerful Ultrasonication .....	52
4.2 Bottom-Up With Surfactants Assisted Sonication Approach .....	61
4.3 Conclusions .....	63
CHAPTER FIVE: CAPSULE PEGYLATION AND CONTROLLED RELEASE STUDY FOR LAPATINIB AND PACLITAXEL .....	64
5.1 PEGylation .....	64
5.2 Controlled Release Study .....	67
CHAPTER SIX: DUAL DRUGS ENCAPSULATION OF PACLITAXEL AND LAPATINIB .....	71
6.1 Introduction .....	72
6.2 Methods .....	75
6.3 Results .....	79
6.4 Discussion .....	92
6.5 Conclusions .....	93
CHAPTER SEVEN: CONCLUSION AND FUTURE WORK .....	96
7.1 Conclusions .....	96
7.2 Future Work .....	98
REFERENCES .....	100
VITA .....	114
Book Chapter .....	115
Peer-Reviewed Journals .....	115
Conference Proceedings .....	116

## ACKNOWLEDGMENTS

I would like to show my respect and thankfulness to my advisor, Dr. Yuri. M. Lvov, for his support throughout my doctoral research and study. Also, my former and current advisory committee members: Dr. Sandra Zivanovic, Dr. James Palmer, Dr. Alan Chiu, Dr. June Feng, Dr. Weizhong Dai and Dr. Mark DeCoster gave me a lot of support and advice, which deserve great thankfulness. I would also like to express my thankfulness to my former lab mates, Dr. Tanya, Elshad, Kiril, and Zhiguo, and those who are still pursuing their degrees, Pravin, Gaurov, Anupam, Wenbo and Yafei, for their lab assistance and good advice. Thanks to IfM faculty Philip, Alfred and staff Debbie, and Dee for their assistance in SEM imaging, XRD study and other technical support. I would further like to acknowledge Dr. Stefano Leporatti, Ms. Viviana Vergaro (both from Italian Institute of Technology, Lecce, Italy), Dr. V. Torchilin, (Northeastern University, Boston) and Dr. Chery-Ann Nathan (Heath Center, LSU-Shreveport) for helping me in my research work for drug testing. This work was supported by research grants from NIH RO1 Grant Cancer drug nano-encapsulation with LbL.

I wish to express my heartfelt love and commendation to my grandparents, parents, younger brother, friends and relatives in China and USA for their love and support.

## CHAPTER 1

### INTRODUCTION

In this chapter, the motivation and background for the dissertation is described. The technology gaps for the existing drug delivery system, an introduction for sonication assisted Layer-by-Layer technology and how it may help in solving existing problems are described. The outline of the dissertation is also shown. Some sections of this chapter were published in a paper written by the author of this dissertation in co-authorship with Dr. Lvov and our Italian collaborators as “Drug-loaded polyelectrolyte microcapsules for sustained targeting of cancer cells,” in *Advanced Drug Delivery Reviews*, v 63, 847-864, 2011. The text sections cited from this paper is properly cited (see Ref. 27), and they are not in use in any other dissertation.

#### 1.1 Motivation and Background

##### 1.1.1 Statement of Problem and Significance

Cancer remains one of the most challenging diseases. In America, 11.4 million people alive have a cancer history. More than 1500 people die of cancer every day, accounting for one fourth of total deaths. More than 1,500,000 new cancer cases are diagnosed yearly. The NIH (National Institute of Health) estimated the costs of cancer for 2010 to be over 260 billion dollars. Among the costs, the direct medical costs were over 100 billion dollars; the indirect loss of productivity by illness costs was over 20 billion dollars; the indirect mortality cost was over 140 billion dollars [1-2].

Traditional cancer treatments often have side effects of killing healthy cells and causing toxicity to patients. Therefore, it is of great importance to develop new therapeutics which can effectively target cancerous cells [3]. The needed features of pharmaceutical drug delivery (small size, biodegradability, high content of a drug in preparation, prolonged circulation in the blood, and the ability to target required organs) are reasonably well met by liposomes, microcapsules, and nanoparticles for well water-soluble drugs. The development of nanoparticle drugs having all of these properties for low soluble pharmaceuticals represent a challenge.

Drug delivery systems (DDS) are designed to enhance the pharmacokinetics and therapeutic performance of drugs [4]. In fact, they may pave the way for achieving Nobel Prize winner Paul Erich's "magic bullet." One of the intensely studied DDS is the magnetic field manipulated drug delivery systems, because magnetic materials are biodegradable and can be given endovascular and act at a relatively long range [5]. This system also can be helpful for imaging [5]. However, the drug loading capacity of these systems is relatively low for cancer treatment, and this is even more conspicuous for the many poorly soluble drugs.

Many efficient cancer drugs (for example, paclitaxel, lapatinib, atovaquone, curcumin, camptothecin, and tamoxifenetc) approved by FDA are poorly soluble in water. However, their bioavailability is low for treatment, and many of them are not only toxic to cancer cell but also toxic to normal cells. Paclitaxel is a representative poorly soluble drug which could be used to treat various cancers such as lung, ovarian, and breastcancers [6]. However, it is very difficult to load and control its release target and rate efficiently by conventional technique [7-10]. Therefore, the application scope of poorly soluble drugs has been confined [11-12].

Layer-by-Layer (LbL) self-assembly has been a well-established method for nanofabrication and nanoarchitechure build-up. LbL's versatility can be very useful for

building up the drug delivery system. We used Layer-by-Layer coating technology to establish a simple, effective method for preparing multifunctional poorly soluble drug nanoparticles which can become stable, targeted releasable, traceable, aqueous and bioactive nanoparticles with high concentration (more than 50%) of the active drug. Due to these multifunctional properties, the poorly soluble drug nanoparticles could be used for achieving our object of early detection, diagnostics, and prognostics for cancer diseases. Here, we used paclitaxel and lapatinib as representative poorly soluble anticancer drugs and aimed at establishing simple, effective methods in cancer research and nanomedicine and to develop chemotherapeutics that can target cancerous cells. Our research was superior to micelle carriers and other techniques in universality of method (for micelle carrier technology, different drug requires different condition to become soluble), multifunction (targeting, imaging, proper usage of anti-angiogenesis agents), drug concentration (more than 50% compared with less than 5%), stability (high and low), and controllability of release rate (easy and difficult). Of course, in this work, we accomplished these goals only partially.

To sum up, our approach may be helpful for establishing simple in preparation stable nanocolloids of low soluble drugs which otherwise do not have means for delivery. For this research, we solved the following tasks: 1) forming of 200-300 nm nanocores of paclitaxel and lapatinib through ultrasonication and modified solvation methods; 2) making stable nano colloids of these drugs in water, 3) making this nanocolloids stable at 0.1 M NaCl solution and PBS buffer at concentration of 1-2 mg/ml through architectural design of LbL shells with PEGylation; 4) optimizing drug release rate through adjustment of the polyelectrolyte layer number in the capsule shell, and 5) combining these two drugs (paclitaxel and lapatinib) in one nanocapsules for enhanced anticancer efficiency. The nanocapsule targeting, though, which may be performed with this method of architectural shell through including immunoglobulins in the outermost shell, is out of the scope of this work.

### 1.1.2 Drug Delivery Systems (DDS)

Drug delivery systems are the development of tailored systems which help deliver a certain amount of one (or more) therapeutic drug(s) to a targeting point, at a certain controlled release rate, with or without the existence of a specific trigger [13].

The US demand for drug delivery systems (including the value of the delivered drugs) will increase over ten percentannually to \$132 billion in 2012 [14], which will well justify this work. In a further introductory section, we will use sections of our review paper in *Advanced Drug Delivery Reviews*, 2011, p. 847-864 with appropriate reference V. Vergaro, F. Scarlino, C. Bellomo, M. Maffia, X. Zhang, Y. Lvov, S. Leporatti, "Drug-loaded polyelectrolyte microcapsules for sustained targeting of cancer cells" *Advanced Drug Delivery Reviews*, v 63, 847-864, 2011.

Oral drug delivery systems will continue to account for the largest share (50%) of demand through 2012 due to favorable cost advantages, a wealth of potential new product applications and significant efficacy advantages over conventional dosage formulations. Parenteral preparations will provide the strongest growth opportunities for drug delivery systems, with demand expanding over 15% annually through 2012 (32% share). While the Inhalation & Other account for 18% of the total share. An increasing incidence of chronic respiratory conditions will keep demand for inhalation drug delivery systems advancing favorably [14].

Medicines adapted to a controlled-release matrix, diffusion and reservoir systems will post favorable sales gains as drug makers seek to gain competitive advantages by introducing new, improved formulations of off-patent pharmaceuticals. Improved solubility and pharmacokineticactions will lead to rapid growth both in the number and sales of drug nanoparticles [14].

Primary goals for drug delivery systems include (i) target drug delivery, (ii) drug toxicity reduction while maintaining therapeutic effects, (iii) greater safety and biocompatibility and (iv) faster and lasting development of medicines. To reach these purposes, a deep investigation about drug incorporation and release, in order to maximize drug loaded into nanocarriers, as well as biocompatibility and bio-distribution information are also essential [13, 15].

The major drug delivery systems developed are micellar nanocarriers, magnetic field manipulated DDS, liposomes, dendrimers, solid lipid nanoparticles (SLN) and nanostructured lipid carriers (NLC), fullerenes and nanotubes (CNT & Halloysite) etc. They are briefly discussed below.

#### 1.1.2.1 Magnetic Field Manipulated DDS

One of the intensely studied DDS is the magnetic field manipulated drug delivery system. Since magnetic materials are biodegradable and can be given endovascular and act at relatively long range [5]. Furthermore, this system can be helpful for imaging [5]. Most common magnetic nanoparticles are iron peroxide ( $\text{Fe}_3\text{O}_4$ ) NPs of 15-60 nm diameters [16]. They generally are made by a magnetic core and then coated with natural or synthetic polymers. Natural compounds widely used are carbohydrates, such as dextran, and proteins that are usually cross-linked to avoid their degradation in aqueous solutions. Synthetic coating materials are PEG, PLA and PVA, which have a higher mechanical strength than other natural chemicals [17].

Other metallic nanoparticles used are gold shell nanoparticles, which have a dielectric core covered by a thin metallic gold shell. Their properties make them useful mostly for biomedical imaging and therapeutic applications [16]. Recently, Lee et al. developed magnetism-engineered iron oxide (MEIO) nanoparticles for the detection of target biological molecules *in vivo* [18]. When conjugated with an antibody, MnMEIO-Herceptin conjugates

demonstrated enhanced sensitivity for cancer cell detection as well as for *in vivo* imaging of small tumors.

However, the drug loading capacity of these systems is relatively low for cancer treatment and this capacity is even more conspicuous for the many poorly soluble drugs. Besides, it is unclear how to remove inorganic components from the patient organism.

#### 1.1.2.2 Liposomes and Micelles

Micelles are nanoscopic self-assembling core-shell structural colloidal particles, one of the most commonly studied drug delivery system, and in some cases, micelles can serve as drug delivery systems for poorly soluble pharmaceuticals. Their hydrophobic cores can be used for encapsulation of many poorly soluble drugs with increased stability and good biocompatibility [7-10].

However, micelles are far from satisfactory because of their low loading efficacy, problems with controlling the release rate of the drug and other problems.

Liposomes are small vesicles composed by amphiphilic phospholipids enclosing an interior aqueous space, within the range of 50 to 1000 nm [19]. Phospholipids (phosphatidylcholines, usually called "lecithin") are the main constituents of liposomes, and due to their amphipathic properties, they readily form concentric bilayers. The most common laboratory protocol used to create liposomes consists of sonication, extrusion, reverse-phase evaporation, and solvent injection approaches [20]. Depending on their size and the number of bilayers, liposomes can be classified into three categories: multi-lamellar vesicles (MLV), large uni-lamellar vesicles (LUV) and small unilamellar vesicles (SUV). The major problems associated with liposomes are their stability, poor batch-to-batch reproducibility, difficulty in sterilization, and low drug loading capacity.

Liposomes and micelles are the most common nano/micro vehicle for delivery of low soluble anticancer drugs; however, their low stability and low 2-3% loading capacity confines

their application efficiency. In our research, we collaborated with the Pharmacy Department of Northeastern University, the group of experts who pioneered micellar formulation for anticancer drugs (V. Torchilin), and their experience allowed us to understand and exploit LbL technique abilities to add new features for nanocapsule formulation (e.g., higher stability, and higher drug loading).

#### 1.1.2.3 Dendrimers

Dendrimers are repeatedly branched polymeric macromolecules [19]. Dendrimers have three components: an initiator core, branches, and terminal functional groups. The core is frequently named (G0) to which are linked first generation monomers (G1), while second generation monomers (G2) are linked to corresponding G1 monomer in a 2:1 ratio and can be properly functionalized coherently with drug delivery application [19]. Further steps of generations create the dendrimer and its molecular weight doubles with each additional generation. The main advantages of the dendrimers are (i) nanoscale sizes, (ii) high numbers of terminal surface groups (Z) suitable for bioconjugation, (iii) an internal hollow space which can encapsulate small molecule drugs and (iv) Non- or low immunogenicity due to PEGylation.

#### 1.1.2.4 Solid lipid nanoparticles (SLN) and Nanostructured Lipid Carriers (NLC)

SLN and NLC have been developed very recently and can be easily synthesized. SLN are lipid-based drug-delivery carriers with nanometer to sub-micrometer scale size (50-1000 nm) after drug encapsulation; moreover, they have a lipid, biocompatible and biodegradable composition and do not require the use of organic solvents for their assembly. The SLN particle synthesis protocol, which involves high-pressure homogenization techniques, can be performed at a lower cost and can be easily scaled up [20]. NLC, similar to SLN, are colloidal particles that typically range in size from 100 to 500 nm. They are composed by solid- and liquid-phase lipids, but are generally solid at temperatures above 40 °C. In contrast

to the lipid crystal matrix of SLN, the lipid matrix of NLC has an imperfect crystal or amorphous structure. This structure allows for drug loading in both the molecular form and in clustered aggregates. Both SLN and NLC have been successfully multi-functionalized to target specific cells, and to release drugs in a controlled manner [20]. SLN and NLC advantages consist in i) controlled drug delivery and release ii) particularly feasible for synergistic multiple drugs encapsulation, and iii) increased blood circulation half time and exploiting EPR retention on tumor sites. Hydrophobic drugs with short circulation half-lives are ideal candidates for delivery via SLN and NLC [20].

#### 1.1.2.5 Fullerenes and Nanotubes (Carbon nanotubes & Halloysite)

Fullerenes have a polygonal structure made up by 60 carbon atoms and can be easily functionalized. Their diameter is 0.7 nm, but they have a poor solubility in aqueous solvents and are likely to create supramolecular aggregates, thus they are hardly used in biomedical applications. This problem has been solved functionalizing fullerenes. Amphifullerene compounds are functionalized fullerenes, based on a C<sub>60</sub> core, which contain both hydrophobic (water-insoluble) and hydrophilic (water-soluble) moieties, called AF-1 monomers, and self-assemble to form supramolecular structures referred to as “buckysomes” [21]. Buckysomes are self-assembled, water soluble fullerenes used for drug delivery approaches, such as the paclitaxel-embedded buckysomes (PEBs). Currently, *in vitro* and *in vivo* preclinical studies are available, since these structures have not been tested in clinic.

Carbon nanotubes (CNTs) consist of a single sheet of graphite rolled to form a cylinder [16]. CNTs can be used as carriers for the delivery of drugs, DNA, proteins and other molecular probes into cells [22]. Early experimental studies regarding interactions between MWNTs and proteins revealed that both biomacromolecules and synthetic molecules can be adsorbed over the CNTs' surface [23, 24] and/or fill the internal cavity of these cargo-carriers [25].

For drug delivery, these approaches seem more useful for introducing drugs into interior cavity of tube, whose open ends might be capped to generate a nanopill [25].

However, the main problem of Fullerenes and CNTs as drug nanocontainers is their toxicity and low drug encapsulated concentration. We do not foresee practical results based on these drug delivery nanosystems.

Halloysite clays are two-layered rolled aluminosilicate, chemically similar to kaolin, with hollow tubular structure in the submicrometer range. The size of halloysite particles varies from 50 to 70 nm in external diameter, 15 nm diameter lumen and 1-0.5  $\mu\text{m}$  length [26]. Their preparation can be made with inexpensive materials and simple protocols of fabrication. Moreover, halloysite nanotubes have different chemistry in the inner and outer surfaces, and this property can be exploited for different and peculiar modification of inner and outer walls [26]. Halloysite nanotubes are much more bio-friendly than carbon nanotubes (they are just clay used by people for thousand years); however, again, they are inorganic and cannot be used for intravein blood injection because they are not biodegradable.

### 1.1.3 Drug Delivery Mechanisms

There are mainly two types of drug delivery mechanisms: 1) passive targeting through the enhanced permeability and retention (EPR) effect and 2) active targeting through attachment of special targeting agents. Passive targeting is ubiquitous but it has some disadvantages such as low drug delivery efficiency and difficulty in controlling the process. The advantage of Layer-by-Layer self-assembly technology is the wide choice of materials for building up the architectures. Those active targeting agents can be used and incooperated into the nanoarchitectures for active targeting to the cancer cells and, therefore, improve the efficiency of cancer treatment and reduce of toxicity [28].

As can be seen from Figure 1.1 [27], in passive targeting, the vasculature supplying cancer lesions might have increased endothelial fenestrations and architectural anarchy,

resulting in the preferential extravasations and protracted lodging of injected particulates. The active targeting is conjugation of active recognition moieties to the surface of a nanovector. The active targeting requires specific drug delivery system. In our case, the versatility of Layer-by-Layer technology in choosing different compositions for building up the nanoarchitechure and the ability to control the size will provide a very powerful drug carrier system.

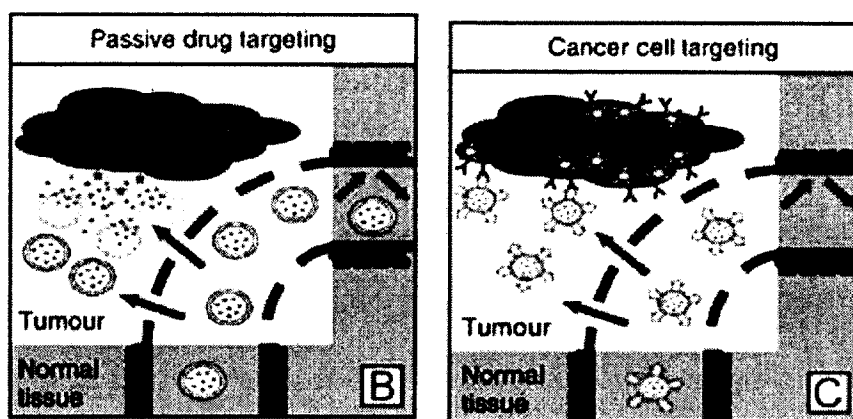


Figure 1.1 Passive targeting (left) and active targeting (right) [27]

## 1.2 Methodology for Multifunctional Poorly Soluble Drugs

The application scope of poorly soluble drugs has been confined due to the difficulty to load and control its release target and rate efficiently by conventional techniques. Here, the technology gaps and how our technology can solve these problems will be discussed.

### 1.2.1 Technology Gaps

Poorly soluble drugs are very difficult to load and control its release target and rate efficiently. The main gaps for enlarging the application of poorly soluble drugs are listed as follows: The first gap is to produce aqueous nanoparticles of poorly soluble drugs with high concentration (more than 50%) of the active drug [28]. The second gap is about endowing poorly soluble drugs with high targeting selectivity [28] and imaging capability. The third

gap is to simultaneous targeted released and imaged more than one drug or one drug and one anti-angiogenic agents at one time. (These drugs can be soluble or poorly soluble).

These three gaps have important theoretic and practical significance for enlarging use of drugs and recovery from disease. Because of the intrinsic poorly soluble property of many drugs, it is thus very difficult to load them and control their release target and rate efficiently. Targeting selectivity is mainly concerned with the technology to endow drugs' high differential uptake efficiency in the target cells over normal cells via specific ligands [3], while the biological solubility, stability and the ability to overcome the barriers are concerned with the technology for dissolving insoluble drugs effectively. These two directions are interrelated and have some influence on each other towards the purpose of this research. The target selectivity study is important for both soluble and poorly soluble drugs. The technology for dissolving insoluble drugs effectively so that they can be as effective as soluble drugs is even more important for the commercialization of these drugs, and through careful design of the Layer-by-Layer coating technology, these three goals may be well solved. To sum up, they are interrelated and synergistic goals to increase the efficacy of poorly soluble drugs, and they all are very important part of this research.

### 1.2.2 Layer-by-Layer Technique

Layer-by-Layer assembly is a unique technique for the fabrication of composite films with nanometer precision. The attractive feature of this approach is its ability to assemble complex structures from modular components, and integrate them into self-assembling constructions for a wide range of applications [29-35].

#### 1.2.2.1 Layer-by-Layer Approach

As can be seen from Figure 1.2, Layer-by-Layer self-assembly of multilayer films involves the construction of complex composite materials with precise film thickness, one layer at a time, enabling the development of novel structures and devices with properties

tailored by controlling the molecular makeup and arrangement. Early fundamental studies of multilayer assemblies on planar substrates demonstrated the practicality and versatility of the approach, and work over the past decade has included further investigation into the internal structure and composition of LbL films, including dynamic and long term interactions between film components, solvents, and solute, especially transport properties. Beyond assembly onto flat planar surfaces, the multilayer deposition via LbL has been extended to colloidal templates, leading to elaborate modification of particles and even to hollow capsules, both of which are exciting and attractive for many applications. While the bulk of work in LbL has been in experimental investigations, some efforts to generate theoretical descriptions for the multilayer assembly have also been undertaken, although much more work is needed in this area to establish useful models for design of devices based on this approach. Finally, applications for LbL films abound and are now being pursued at the academic level, with some examples of industrial applications for eye lens modification, improvement of cellulose fiber for better fabric and paper, microcapsules for insulin sustained release, and others [31-35].

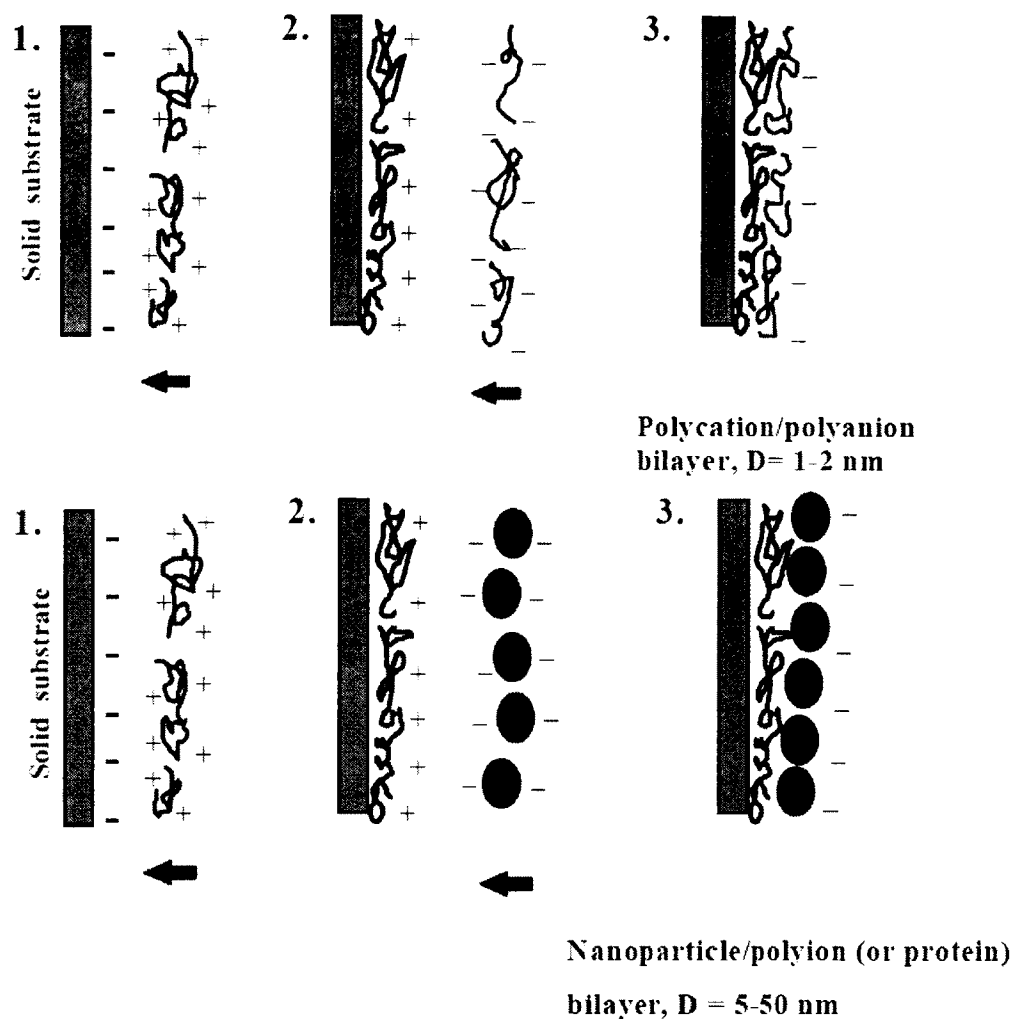


Figure 1.2 Layer-by-Layer (LbL) self-assembly ideology [34]

As was demonstrated by Decher et al. [31] in Figure 1.3, Layer-by-Layer self-assembly approach consists of alternate adsorption of polyanions, such as PSS (poly (styrene sulphonate)) and DXS (dextran sulphate), and polycations, like PAH (poly (allylamine hydrochloride)) and PRM (protamine dextran). The technique takes advantage of attractive electrostatic forces between charged polymers and oppositely charged surfaces, and film growth is achieved stepwise by the repetitive exposure of substrates to dilute polycation and polyanion solutions.

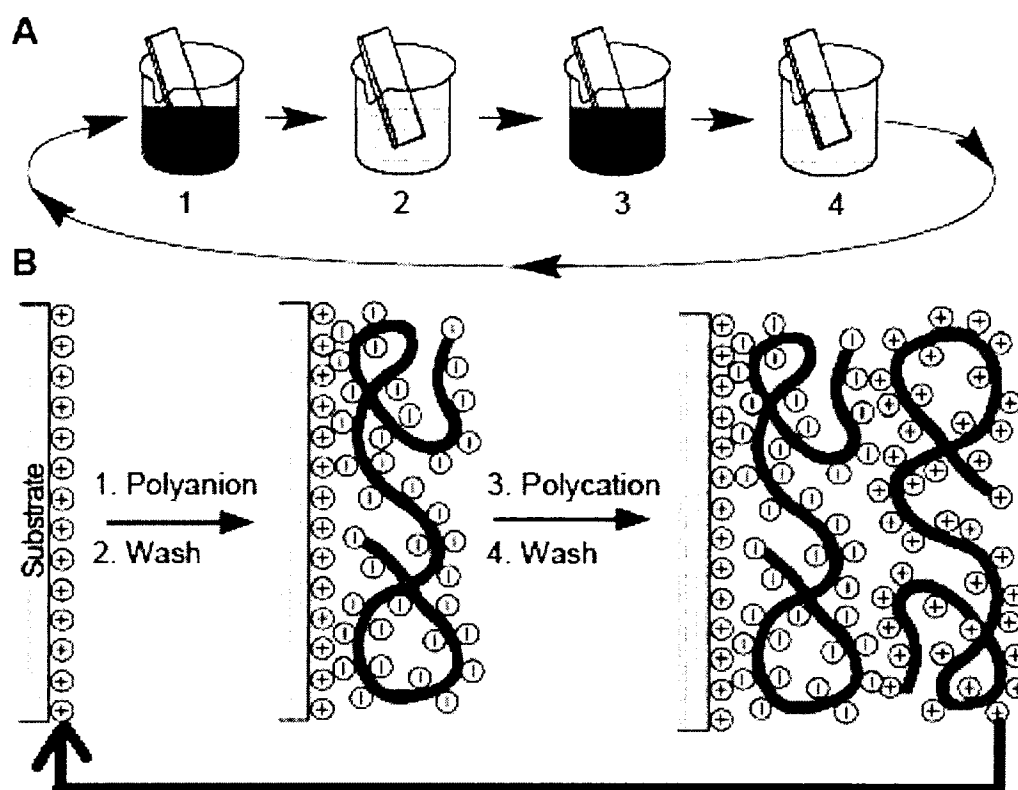


Figure 1.3 Layer-by-Layer (LbL) self-assembly set-up and process [31]

Hydrophilic and positively charged substrates are immersed into the solution of polyanion (negatively charged polymer, for example, PSS) for several minutes. As a result, a thin layer (thickness 1-2 nm) of the polymer is adsorbed on the surface. Charge overcompensation leads to a negative surface re-charging. Then, the substrate is washed (a washing step is needed to remove not adsorbed material) and placed into the solution with polycation (positively charged polymer, for example, PEI). The polymer is attached electrostatically to the charged surface. The process can be repeated several times to reach a defined multilayer thickness controlled by layer coating cycling. As depicted in Figure 1.3, the iterative dipping of a substrate (e.g. a glass microscope slide) into solutions of oppositely charged polyelectrolytes yields multilayered films composed of alternating layers of cationic and anionic polymers. The thicknesses of these films typically range from tens or hundreds of

nanometers to up to several micrometers, depending on the number of layers deposited and the solution conditions (e.g., pH, ionic strength, etc.) used during fabrication.

This polyelectrolyte multilayer coating can be easily and reproducibly formed on the surface of any charged substrate. By varying the charge density on each polymer or the number of coating cycles, substrates with a different surface charge and different composition of the polymeric coat can be prepared. Layer-by-Layer technique of assembly permits the deposition of thin films on a wide variety of macroscopic, microscopic, and nanoscopic objects [36-41].

#### 1.2.2.2 LbL Drug-Loaded Polyelectrolyte Microcapsules

Several groups have used templating Layer-by-Layer assembly to fabricate hollow multilayered capsules by depositing polyelectrolytes onto cores that can be dissolved, degraded, or otherwise removed after film formation. Experiments are reviewed by references [39, 41-49]. This approach has been used widely to develop approaches to either encapsulate or deliver a wide range of macromolecular agents. In fact, packaging of drugs into micro- or nanocarriers has sparked great interest on biological validation of micro-to-nanoscale delivery systems for targeted therapy [50-51]. For therapeutic purposes, there is a clear need to fabricate supramolecular assemblies of drug and functional carrier materials which would be biocompatible and biodegradable under physiological conditions [52-53]. In this respect, hollow microcapsules are of particular interest, as they can be fabricated via Layer-by-Layer (LbL) assembly of oppositely charged polyelectrolyte multilayers of dextran sulfate (DXS), protamine (PRM) or poly-L-arginine (PLA) that are degraded by intracellular proteases or hydrolytic enzymes, around a sacrificial core of calcium carbonate (of few hundred nm to several micrometers of diameter) that is dissolved by EDTA after deposition [54-55]. Due to the versatility of electrostatic interactions, properties and functionalities of the resulting hollow capsules (i.e. their encapsulation or

release efficiency), can be finely tuned in the nanometer range by varying capsule wall thickness and number and composition of the polymeric layers, hence their permeability in response to changes on the pH, ionic strength or solvent [42].

The intrinsic advantage of LbL fabrication method is unmet by any other technique, as it lies in the potential of entrapping simultaneously drugs, fluorescent probes or colloid nanoparticles (e.g. quantum dots or magnetic particles) with tunable functionalities into the biodegradable multilayers of one unique hollow capsule (post-loading method) [42, 56-57].

Polyelectrolyte microcapsules can be fabricated by LbL technique previously described. After the consecutive assembly of oppositely charged polymer layers around the  $\text{CaCO}_3$  core, the core itself is removed to obtain hollow and stable capsules whose inner cavity and polymer wall can be loaded and functionalized, respectively, with a variety of substances such as molecular dyes, drugs, biomolecules, which retain their distinctive properties after the embedding procedure [49, 58]. The resulting hollow capsule usually has a wall thickness of between a few tens and several hundred nanometers and have a diameter ranging from tens of nanometers to several micrometers, depending on the size of the original core [49, 58]. The forming of the hollow capsule is illustrated in Figure 1.4.

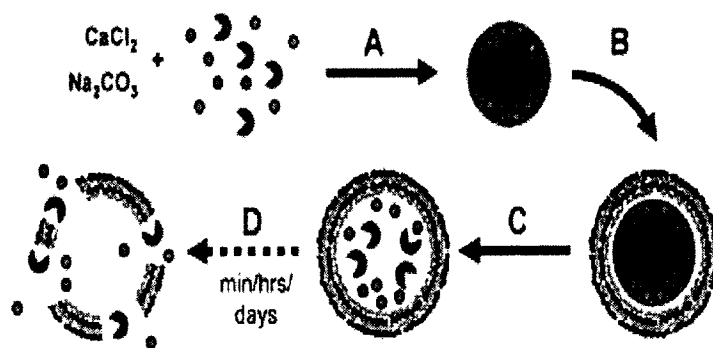


Figure 1.4 Formation and release of LbL assembly capsules [58]

Particularly, the initial step of nanoparticle formation is the creation of  $\text{CaCO}_3$  core mixing soluble salts of  $\text{Ca}^{2+}$ , as  $\text{CaCl}_2$ , and  $\text{CO}_3^{2-}$  compounds, like  $\text{Na}_2\text{CO}_3$ . The mixture results in an amorphous precipitate initially, which subsequently transforms into aggregated  $\text{CaCO}_3$  microcrystals with a particular morphology. The  $\text{CaCO}_3$  microparticles obtained by this simple route are uniform and homogeneously sized, non-aggregated, high porous spheres. The quality of the resultant microparticles was found to be strongly dependent on the experimental conditions such as type of salts used, their concentration, pH values, temperature, and rate of solution mixing and intensity agitation of the reaction mixture [59, 60]. After core building, the LbL covering occurs, using an alternate layering of polyanions and polycations (DXS-PRM and PSS-PAH). Once a multilayered layer has been created,  $\text{CaCO}_3$  core dissolution occurs by saline solutions (e.g. sodium hypochlorite solution) or ethylenediaminetetraacetic acid (EDTA). The core dissolution makes an empty cavity, subsequently loaded with a drug, like paclitaxel. Two fundamental components for capsule fabrication are the core templates and the polyelectrolyte pairs. An ideal template has to be stable under the LbL process, soluble in mild conditions and completely removable from the inside of the capsules without affecting the morphology and stability of the multilayer assembled on top of it. In recent years, numerous materials have been employed as sacrificial templates such as polystyrene latex, melamine formaldehyde (MF),  $\text{SiO}_2$ , carbonate particles ( $\text{MnCO}_3$ ,  $\text{CaCO}_3$ ,  $\text{CdCO}_3$ ) and biological cells like erythrocytes [49, 58]. The assembly of Latex is shown in Figure 1.5 as an example.

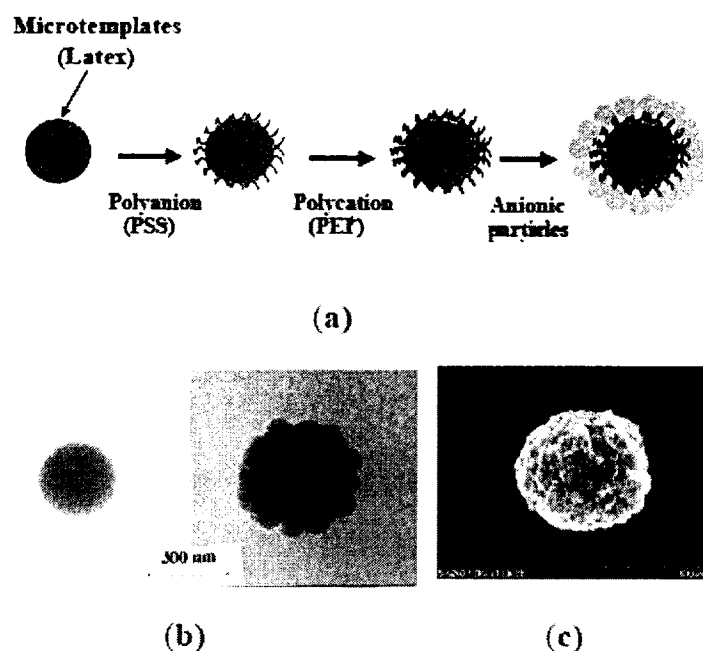


Figure 1.5 LbL assembly of Latex [34]

The capsule wall is also crucial for the fabrication of functional capsules, as their permeability or porosity strongly depends on the chemical structure and the molecular weight of the employed polyelectrolyte pairs. The majority of polyelectrolyte capsules described in literature are composed of pairs of synthetic biocompatible-not-biodegradable polyelectrolytes such as anionic poly (sodium) styrene sulphonate and cationic poly (allylamine) hydrochloride, or composed of biocompatible and biodegradable polyelectrolytes such as dextran sulphonate and protamine sulphate, which are more suited for therapeutic use. The mechanical/elastic properties of polyelectrolyte capsules are influenced by several parameters such as the chemical nature of the polymer used, which can cause weak or strong intermolecular interactions with the multilayer, and the molecular composition of the innerpart of the capsules [54].

LbL deposition onto charged polystyrene (PS) particles in solution was firstly exploited by Caruso and co-workers [54] to construct hollow polyelectrolyte shells through the

stepwise adsorption of polyelectrolytes onto a decomposable colloidal template. This template was subsequently removed after formation of the multilayer shells was realized. Instead of PS particles weakly cross-linked melamine formaldehyde (MF) colloidal particles were used by Donath et al. [55]. These particles decompose in aqueous media at pH values below 1.6. The PSS/PAH polyelectrolyte multilayer film was built up beginning with adsorption of the negatively charged polyelectrolyte onto the positively charged MF particles. When these coated MF particles were exposed to low pH, the core decomposed [55], and the residual MF oligomers were expelled from the core, since they could permeate through the polyelectrolyte layers that form the shell. These MF oligomers were separated from the hollow shells by centrifugation. MF particles are widely used as core templates and have been very well characterized. They are favored above PS particles because of their decomposable character but have several disadvantages, such as their low biocompatibility. Furthermore, the oligomers formed after decomposition can partially remain inside the polymer wall during the dissolution process, and there is an increased resistance or difficulty to decomposition upon time. In order to overcome these disadvantages, other biocompatible and decomposable templates for LbL techniques have been investigated [61]. The two mostly studied template materials are poly-DL-lactic acid (PDLA) and poly (DL-lactic-coglycolic acid) (PLGA). Degradable microparticles based on these biopolymers were prepared using the oil/water emulsion-solvent evaporation technique. PSS and PAH were chosen as polyelectrolytes to coat onto the biodegradable templates. The next step was the removal of the core by dissolution, which was achieved by dissolving the polymers in a mixture of NMP/acetone in a 1:1 volume ration [61]. Instead of an MF core, metal carbonate crystals were also used by Ma et al. [62]. These cores can be removed easily by EDTA solution. The advantage of using these organometallic polymers for incorporation into the capsule walls is that they allow changing the permeability of these walls. The  $\text{CaCO}_3$  template particle has

found use for encapsulation of biological compounds, since it can be dissolved under healthy conditions.

### 1.2.2.3 LbL Drug-Loaded Polyelectrolyte Nanocolloids

A natural extension of previously described approach is the deposition of polyelectrolyte films on nanoparticles (drug or inorganic) leading to coated nanocolloids. In this respect our group developed recently drug-nanocolloids [63]. These novel entities are stable aqueous polyelectrolyte multilayer shells built on drug particles with few nanometer wall thicknesses (up to 100 nm) and made through a LbL assembly, which consisted in an alternate adsorption of oppositely charged polyelectrolytes onto solid templates [63]. LbL coating technology was used to make stable aqueous nanocarriers of poorly soluble drugs with a high content of the active drug and controllable drug release rate. To achieve this goal, aqueous suspensions of poorly soluble drugs with micron range particles are subjected to the ultrasonic treatment in order to decrease the size of individual drug particles to the nano level (between 100 and 200 nm), while keeping the nanoparticles formed under the sonication to prevent their fast agglomeration, stabilize them in solution by applying the LbL coating (alternating addition of polycations and polyanions to the system) and assembling thin polyelectrolyte shells on their surface. In the assembly process, the highly charged polymeric layer was formed on the drug particle surface after the first polymer application, and this layer prevents drug particle aggregation after terminating the sonication. At the end of the process, stable coated nanocolloidal drug dispersions were formed with high drug content in each particle (between 50% and 90%) [63]. Moreover, it was also possible to functionalize nanocolloids using a polymer containing reactive groups (such as amino or carboxylic groups) for the last “outer” surface layer, thus allowing the linking of specific ligands, or reporter groups, and other moieties of interest to drug nanoparticles such as monoclonal antibodies [63].

### 1.2.3 Sonochemistry

One of the central problems for LbL nanoformulation is formation of the initial drug core of 200-300 nm in diameter. We solved this problem with bulk drug ultrasonication with simultaneous polycation deposition stabilizing formed dispersion. Sonochemistry will enable “green” chemistry without environmentally harmful chemical by-products. Compared to different sources of the energy input into the reaction, ultrasonic treatment can induce a wide range of chemical reactions in non-equilibrium state applicable for synthesis and modification of products with new physico-chemical characteristics and catalytic activity. The effects of ultrasound derive primarily from cavitation, where bubbles collapse in liquids, which results in an enormous concentration of spatially confined energy. This energy is derived from the surface and kinetic energy within the liquid converted into heat and chemical energy imparted to resulting materials [64-66]. Nanoparticle synthesis is often based on control of nucleation and crystallization [67-69]. The vision of the proposed project was to achieve a breakthrough in ultrasonic synthesis by employing surface-active materials (amphiphilic polymers, polyelectrolytes, surface-functionalized nanoparticles, etc.) as regulators to control the interfacial parameters of the cavitation process on nano level during formation and collapse of microbubbles. Introducing the surface-active materials at the cavitation interface will enable one to control the temperature and pressure inside bubbles, to control the energy balance and ways of energy dissipation. The proposed approach will help in controlling the structure and physical state of the cavitation interface and develop new methods for one-step sonochemical synthesis of nanoparticles with core-shell structures.

Figure 1.6 is the set-up for sonication study. Ultrasonication can be applied to create extreme physical-chemical conditions at the liquid/gas interface; whereas, the bulk solution can stay at room-temperature.

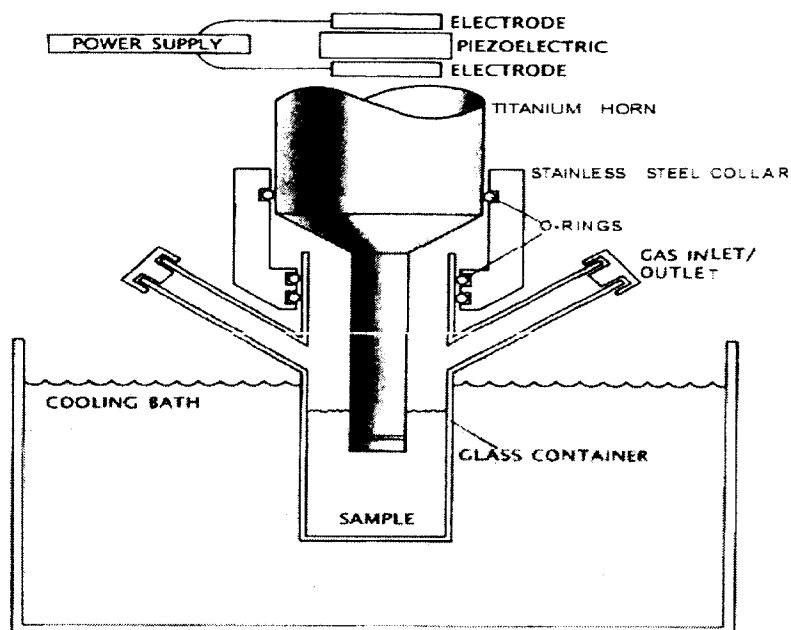


Figure 1.6 Set-up for sonication study [66]

During high-power ultrasonication (20 kHz, 50-100W), gas bubbles were formed and expanded, followed by cavity implosion and jet formation (Figure 1.7).

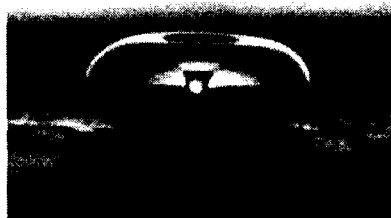


Figure 1.7 Cavity implosion and jet formation [66]

The cavity implosion created very high temperature (up to 5000 K) (Figure 1.8) and high pressure (up to  $10^3$  atmosphere) in the center of the cavity, while the bulk solution remained at low-temperature because of localized energy release and high cooling rate. This high pressure and the jet formation crushed solid materials into micro- and nanoparticles [64-68].

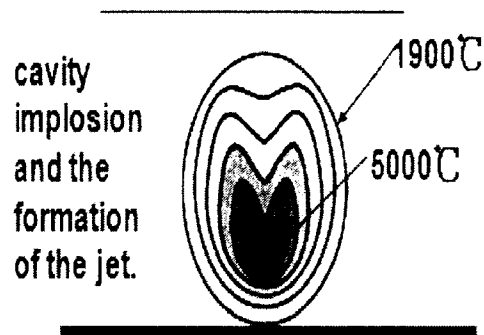


Figure 1.8 Cavity temperatures [66]

Figure 1.9 schematically illustrates the control mechanism over cavitation process. Initial mixture contains initial reagents and surface-active materials with regulated hydrophobic/hydrophilic balance. During ultrasonic treatment and formation of microbubbles, these materials go to a liquid/gas interface changing the surface energy of the microbubble and, as a result, final energy and its partition ratio (between thermal and chemical) during microbubble collapse [64-70].

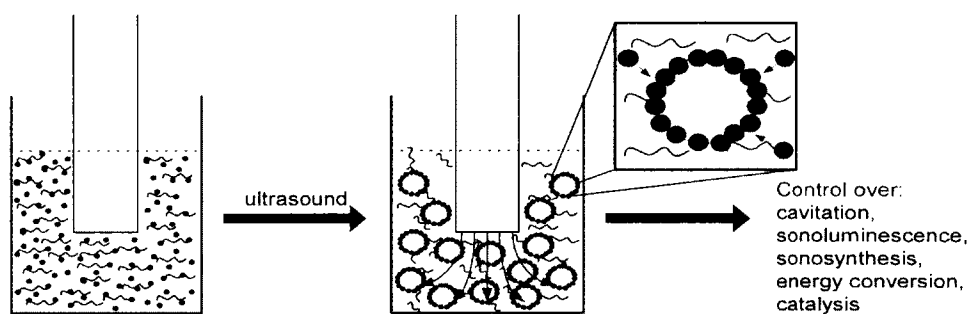


Figure 1.9 Schematic illustration of cavitation process

In our study, sonication was performed in the presence of surface-active agents to ensure their adsorption at the cavitation interface. These surface-active agents had the effect of stabilization and to increase of the lifetime of the cavitation microbubble up to second range (Figure 1.10).

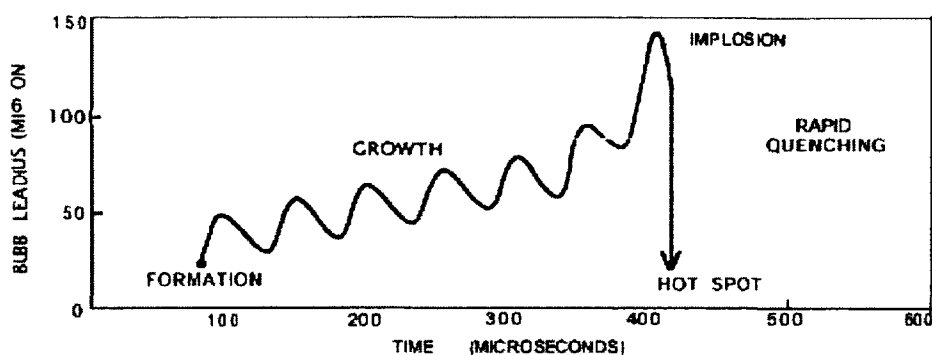


Figure 1.10 Lifetime of the cavitation microbubble [66]

The precursor reagents (bulk materials, monomers, and colloids) were added after starting the sonication in the presence of already adsorbed surface-active material (Figure 1.11).

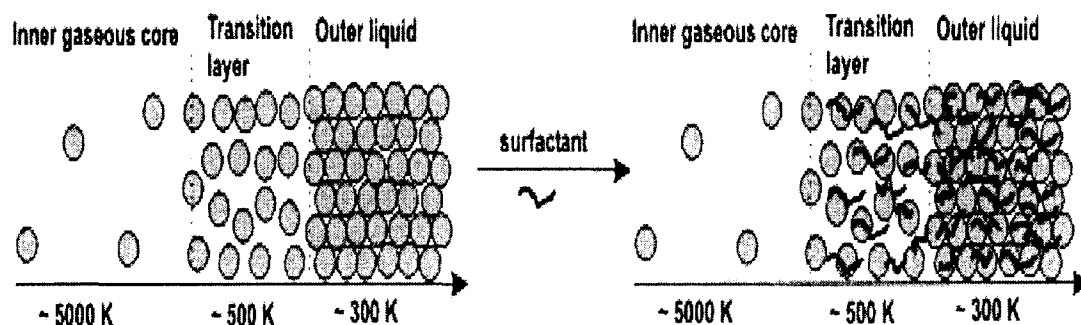


Figure 1.11 Adsorptions of surface-active materials onto the nanocolloids

To sum up, there were mainly three effects power sonication had: cavity with high temperature, jet flow generated after cavity collapse, and polyelectrolyte enrich on the cavity surface.

In order to attempt to decrease the diameter of the formed nanocores of paclitaxel, we developed two experimental techniques to increase energy of bubble collapsing (bubble formation enhancers) and elevated gas pressure which will be described further.

### 1.2.4 Methodology [70-75]

We used paclitaxel and lapatinib as representative poorly soluble anticancer drugs and aimed at establishing a simple, effective method which can be helpful for yielding advances in early detection, diagnostics, prognostics and the selection of various therapeutic strategies.

Our project focused on the study on ultrasonication assisted Layer-by-Layer technique for preparing multifunctional paclitaxel and lapatinib nanoparticles. Figure 1.12 shows the methodology. First, powerful ultra-sonication was applied for making small drug nanoparticles of desired size and suitable shape. Second, the Layer-by-Layer self-assembly of multilayer films was applied for building up the novel structures with properties tailored by controlling the molecular makeup and arrangement with nanoscale precise film thickness. In this process, a nanoarchitectural approach designing layers of different components, including ones serving as diffusion barrier and outermost layers containing targeting agents, can be realized. Third, the well prepared drug nanocolloids were delivered to the cancer cells for treatment of cancer.

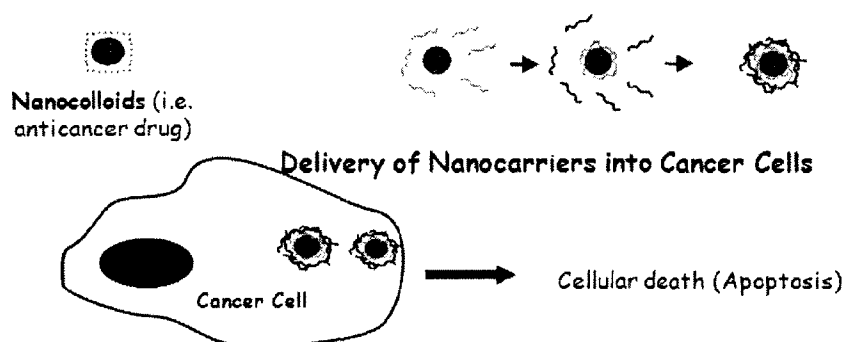


Figure 1.12 Methodology

#### 1.2.4.1 Preparation of Hydrophobic Drug Particles with Desired Size and Suitable Shape

Our first step was to prepare hydrophobic drug particles with desired size and suitable shape. Powerful ultra-sound generates micro-bubbles in liquid. These micro-bubbles will

collapse in microseconds. If any solid particle is near the bubble, jet fluid and shock waves will hit the particle and break it during collapsing [64-75]. The particle will have a wide range of size since the ultrasonic process for breaking down the particles is a mechanical process. Sonication power and time both have effect on the particle size distribution. In general, higher power and longer time will result in smaller particles. While adding polyelectrolyte into the solution, the negative surface of the newly formed surface will help keep particles away from forming aggregation. Thus smaller particle size can be achieved with better size distribution. Polycations were added during the sonication process to adsorb drug nanoparticles and were thus prevented from re-aggregation. Surface potential of particles will become more positive during this process for the influence of polycations.

#### 1.2.4.2 Design and Implementation of the Layer-by-Layer Coating Technology

Different number of layers and different polyelectrolyte types will affect the drug release rate. To obtain sustained release, the coating structure needs to be carefully designed (to obtain optimum release property). An anti-angiogenesis agent such as combretastatin-A4 will also be coated as a layer outside the core drug layer which is expected to be released before the drug to stop the cancer cell from growing larger. After that, we will use the LbL technology to efficiently bind drug nanoparticles to special targeting ligands to kill cancer cells. We will carefully design the coating structure to obtain the optimum release property. The outside layer will be coated with magnetic particles to target delivery and trace the drug particles to specific cancer cells.

#### 1.2.4.3 PEGylation and Controlled Release Study

To further improve our DDS for cancer treatment, stealthy (PEGylation) technology was carried out for increased solubility, stability and drug circulation time. The formula for PEG is  $\text{HO}-(\text{CH}_2\text{O})_n-\text{CH}_2\text{OH}$ . A controlled release study has also been carried out.

Our research is superior to micelle carrier and other drug delivery techniques in universality of method (for micelle carrier technology, different drugs require different condition to become soluble), drug concentration (more than 50% compared with less than 5%), release rate (easy and difficult controllability), and stability (high and low), and simultaneously release of more than one drugs.

### **1.3 Outline**

Chapter One introduces the motivation and some background information of this research work. It also gives a brief literature review covering the knowledge needed for this dissertation: cancer treatment and drug delivery systems, LbL nanoassembly, and sonochemistry. Our methodology for multifunctional poorly soluble drugs is shown. The research goals and the organization of this dissertation are discussed as well. Chapter Two describes materials and instruments used for the research. Chapter Three discusses the top-down approach and bubbling agent approach for preparing paclitaxel nanocores. Their optimization processes are also presented. Chapter Four describes the bottom-up approach for preparing paclitaxel and lapatinib nanocores (first concentrated solutions of these drugs were dissolved in DMSO or alcohol to make molecular solution, and then controlled nucleation of drugs were induced by water addition to decrease the solubility). The surfactant additives arrest growths of the formed cores, allowing the formation of drug particles with the diameters in the range of 150-200 nm. Chapter Five demonstrates colloid stabilization with the PEGylation and controlled release study of those drug nanocolloids using adjustment of polyelectrolyte layers in the shells. Chapter Six describes the dual drugs encapsulation paclitaxel and lapatinib. Chapter Seven concludes the results of the dissertation. Some issues and topics for future work are recommended and a list of publications and presentations on this work are given.

## CHAPTER 2

### MATERIALS AND INSTRUMENTS

#### 2.1 Materials

The two low soluble drugs, paclitaxel and lapatinib were purchased from LC Laboratories, Inc. (Woburn, MA).

There are two types of polyelectrolytes used for Layer-by-Layer self-assembly: polycations and polyanions. Poly (dimethyldiallyl ammonium chloride) (PDDA), Polyallylamine hydrochloride (PAH) are used as highzeta-potential polycations. Polylysine (PLL), PEGylated polylysine (PEG-b-PLL), Protamine sulfate ( PS ) and Chitosan are used as biocompatible polycations. Poly (acrylic acid) (PAA), Sodium polystyrene sulfonate (PSS) are used as highzeta-potential polyanions. Alginate acid (AA), Heparin, Bovine serum albumin (BSA), and Chondroitin sulfate (CS) are used as biocompatible polyanions. They are used at the concentration range from 1-3 mg/mL. All polycations and polyanions were bought from Sigma-Aldrich. PBS buffer, DMSO,  $\text{NH}_4\text{HCO}_3$ , Ethanol, Acetone, FITC , TWEEN 80 and PVP were also purchased from Sigma-Aldrich.

Reagents and Cell culture for dual drug study: The PI3K inhibitor, LY294002, and the ERK 1/2 inhibitor, UO126, were purchased from Santa Cruz Biotechnology (Santa Cruz, CA). Rhodamine (TRITC) conjugated phalloidin, were purchased from Sigma-Aldrich. The antibodies against cofilin, p-cofilin (ser-3), Akt, pAkt (ser 473), cyclin D1 and Tubulin were

purchased from Santa Cruz Biotechnology. Inhibitors for PI3K and ERK, paclitaxel were all dissolved in DMSO.

The ovarian cancer cell line OVCAR-3 and the breast cancer cell line MCF-7 were maintained in Dulbecco's modified Eagle's medium (DMEM), supplemented with 10% fetal bovin serum, 2 mM glutamine, 100U/ml penicillin and 100  $\mu$ g/ml streptomycin, and cultured at 37° C in a humidified atmosphere of 5% CO<sub>2</sub>. Cells were subcultured every three days.

## 2.2 Instruments

### 2.2.1 Ultrasonicator

A UIP1000hd Ultrasonicator (Heilscher, Germany) (Figure 2.1 (a)) was used as powerful ultrasonicator. It came with a titanium sonotrode and its working power was 15 W/cm<sup>2</sup>.

A Branson 1510 Ultrasonicator (Figure 2.1 (b)) was used as a standard ultrasonicator. An ice/water mixture was used as a cooling agent during ultrasonication. During ultrasonication, the ambient temperature is cooled down by the ice/water mixture.

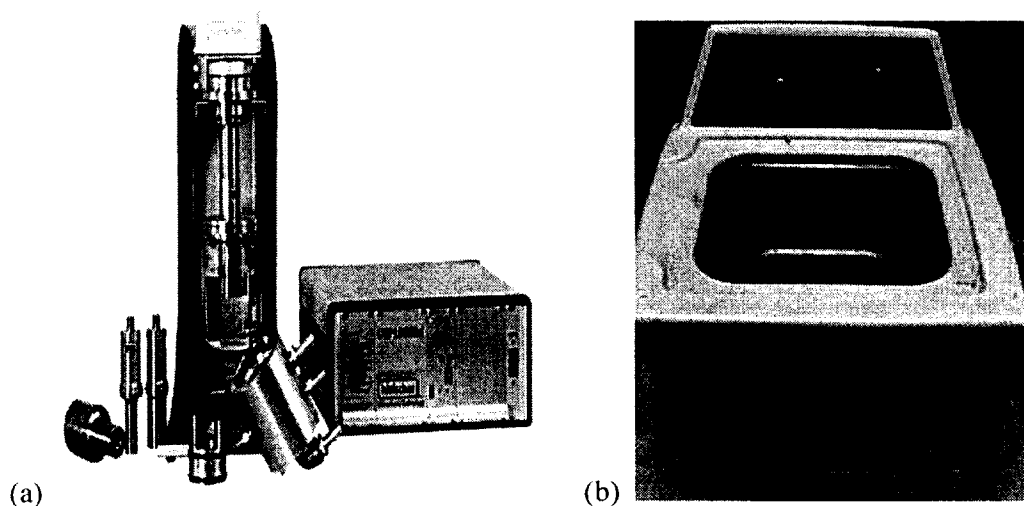


Figure 2.1 (a) powerful ultrasonicator (power: 15 W/cm<sup>2</sup>) (b) standard ultrasonicator

### 2.2.2 Centrifuge

An Eppendorf Centrifuge 5804R (Figure 2.2) was applied for centrifugation of drug nanoparticles.

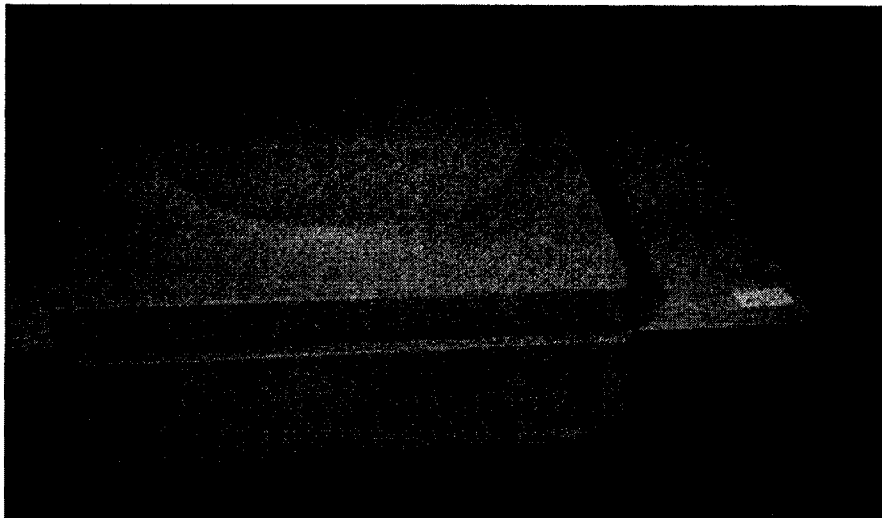


Figure 2.2 Centrifuge

The centrifugation speed range is from 0-15,000 rpm (rotate per minute). Generally, 2000 rpm was applied for precipitation of bigger particles (size larger than 500 nm) for 10 minutes. Centrifugation at 12,000 rpm for 10 minutes was applied for the separation of the drug nanoparticles from the solution (solvent, additional polyelectrolytes, surfactants and so on).

### 2.2.3 ZetaPlus Microelectrophoresis Equipment

ZetaPlus Microelectrophoresis equipment (Brookhaven) (Figure 2.3) has been applied for the measurements of particle size and  $\xi$  (zeta) -potential. Successful sequential coating of oppositely charged polyelectrolytes can be measured by the electrical surface  $\xi$ -potential changes.



Figure 2.3 ZetaPlus microelectrophoresis equipment

Figure 2.4 shows the mechanism for Zeta potential. Zeta potential refers to the electrostatic potential generated by the accumulation of ions at the surface of a particle. For determining zeta potential, a controlled electric field is applied via electrodes immersed in the sample suspension, and this causes the charged particles to move towards the electrode of opposite polarity. Viscous forces acting upon the moving particle tend to oppose this motion and equilibrium is rapidly established between the effects of the electrostatic attraction and the viscous drag. The particles, therefore, reach a constant "terminal" velocity. This velocity is dependent upon the electric field strength or voltage gradient, the dielectric constant and viscosity of the liquid, all of which are known, and the zeta potential. It is usually expressed as the particle mobility which is the velocity under unit field strength. In practice, zeta

potentials are usually negative (i.e. the surface is negatively charged), but they can lie anywhere in the range from -100 to +100 mV.

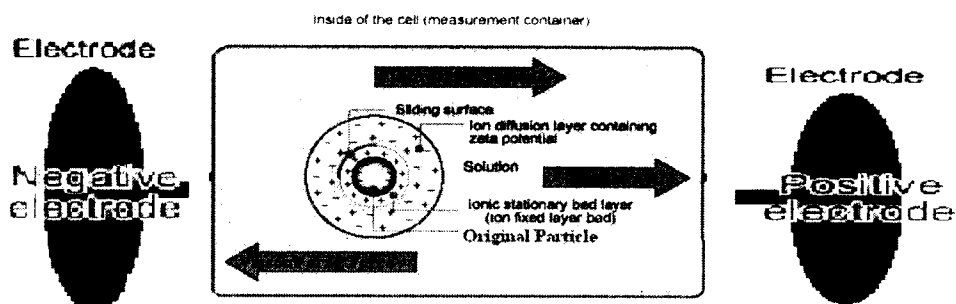


Figure 2.4 Mechanism for Zeta potential (From ref. 74)

#### 2.2.4 Light Scattering Detectors

Precision detectors PDEXpert Light Scattering Workstation (Figure 2.5) was also applied to double check the particle size.

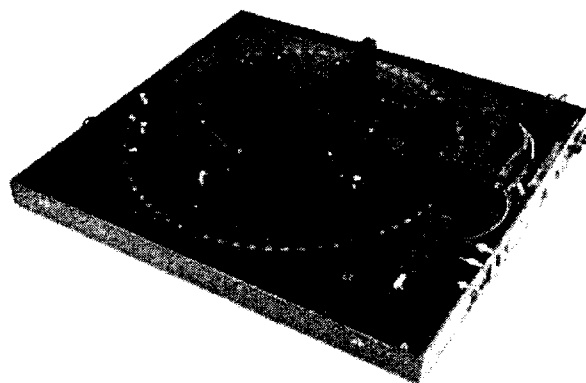


Figure 2.5 Precision light scattering detectors

The workstation provides molecular size and conformation data from the autocorrelation of dynamic light scattering signals at any user-selectable angle in five degree increments on a 360° platform. It is also known as quasi-elastic light scattering (QELS) or photon correlation

spectroscopy (PCS). It can be applied for the recording of the scattered light intensity changes on  $\mu\text{s}$  time range for individual particles' Brownian motion. It is quantified as an exponential function under the assumptions of low concentration, spherical size particle and known viscosity of its environment.

It provides accurate measurements for hydrodynamic radius ( $R_h$ ) and hydrodynamic radius distributions from any type of sample ranging from molecules (protein and antibody) to nanoparticles such as liposomes, sols, magnetic particles, emulsions etc.

### 2.2.5 Confocal Microscope

A Leica TCS SP2 laser scanning confocal microscope (Leica Microsystems, Inc.) (Figure 2.6 ) was applied for visualization of the fluorescent FITC labeled onto the outmost polycation layer of the drug nanoarchitechure for the shell composition confirmation.

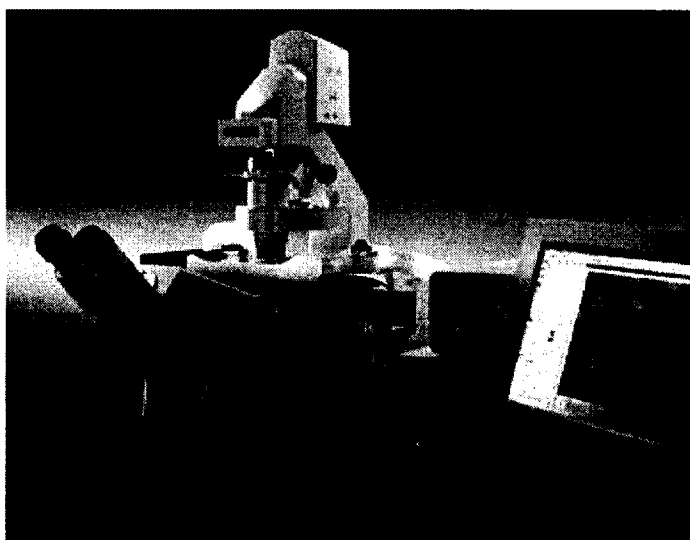


Figure 2.6 Confocal Microscope

Confocal microscopy has been widely used in the investigations of biological and medical thin optical specimens imaging for thickness up to  $100\ \mu\text{m}$ . The confocal microscopy is equipped with several high-speed acousto-optic tunable filters (AOTFs) laser

systems. Therefore, it can have excellent wavelength and excitation intensity regulation. Its minimum detectable size is around 400 nm.

### 2.2.6 Scanning Electron Microscope

A Hitachi S 4800 FESEM (field emission scanning electron microscope) (Figure 2.7) was used for particle morphology imaging and size measurement. Prior to imaging, De-Ionized water was used to wash samples for three times. Samples were then diluted 10 times and put onto silicon wafer. When the samples were dried, they were applied for imaging. An EDX detector included in the FESEM can be applied for the element composition analysis.



Figure 2.7 FESEM

### 2.2.7 X-ray Diffractometer (XRD)

A Bruker D8 Discover XRD (X-ray diffractometer) (Figure 2.8) machine was applied for non-destructive crystal structure and chemical composition determination of drug samples. The XRD is a tool for the observation samples by detecting the scattered intensity after being

hitted by X-ray beam. The XRD measurement is based on the Bragg's law:  $2d \sin\theta = n\lambda$ . For the function,  $\theta$ ,  $\lambda$  and  $d$  are the scattered angle of the X-ray, wavelength of the X-ray and  $d$ -spacing of the sample respectively. The  $d$ -spacing is the distance between crystalline planes, which gives information about the sample.

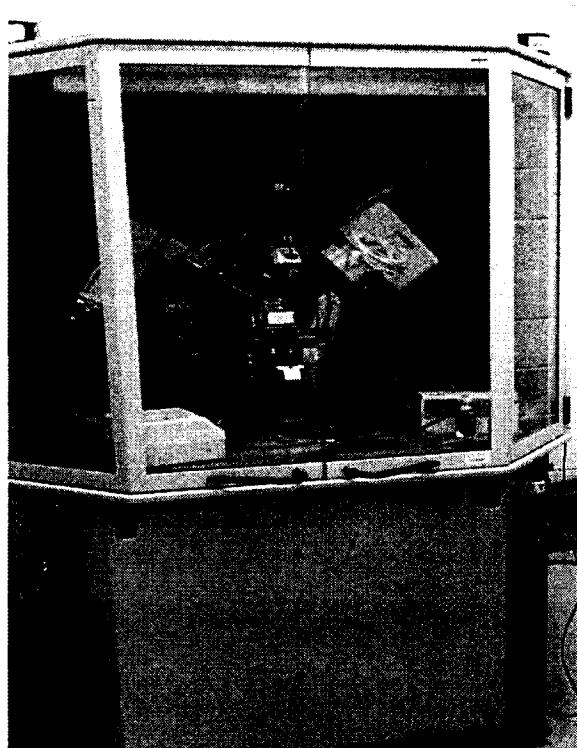


Figure 2.8 XRD

### 2.2.8 UV Spectrophotometer

An Agilent 8453 UV spectrophotometer (Figure 2.9) was used for detection of the drug concentration. Its applicable wave length is from 190 to 1100 nm. For those low soluble drugs, paclitaxel absorbance was measured at 245 nm in Ethanol and PBS. Lapatinib absorbance was measured at 365 nm in DMSO and PBS/TWEEN 80.



Figure 2.9 UV spectrophotometer

### 2.2.9 Release Chamber

The release study of those drug nanoparticles was carried out using two 1 ml standard horizontal diffusion chambers (Figure 2.10). There are mainly five components of the diffusion chambers as listed in Figure 2.9. In between these two diffusion chambers, 0.2  $\mu\text{m}$  pore size acetate membranes are used for the diffusion of drug molecular. In each diffusion chamber, a magnetic stirrer was put inside for the uniform dispersion of drug nanoparticles. The whole release set-up was placed on a magnetic stirring system, and then 1 ml of drug dispersion was added into one side of the chamber, while 1 ml of PBS was added into the other side of the chamber. After a certain time period, the drug molecular diffused onto the PBS side was taken by 1 ml pipette and put into quartz cuvette for UV absorbance measurement. One milliliter of fresh PBS was then being put back into the chamber for the diffusion test.

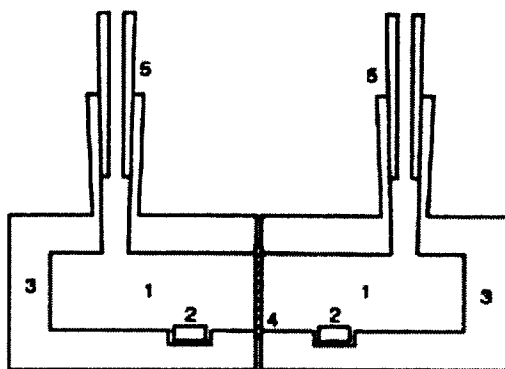


Figure 2.10 Release Chambers (1) 1ml horizontal chamber; (2) magnetic stirrer; (3) chamber side; (4) 0.2  $\mu\text{m}$  pore size acetate membranes; (5) chamber entrance for drug dispersion add-in.

## CHAPTER 3

### TOP-DOWN APPROACH FOR PREPARING PACLITAXEL NANOCORES

In this chapter the top-down approach is described. Some sections of this chapter were published in a paper written by the author of this dissertation in co-authorship with Dr. Lvov and others as “Converting Poorly Soluble Materials into Stable Aqueous Nanocolloids” in *Langmuir*, 2011, 27 (3), 1212-1217. The text sections cited from this paper is properly cited as [72], and they are not in use in any other dissertation.

Ultrasonication can be applied to create extreme physical-chemical conditions at the liquid/gas interface, whereas the bulk solution can stay at room-temperature. During high-power ultrasonication (20 kHz, 50-100 W) gas bubbles are formed and expanded, followed by cavity implosion and jet formation. This creates very high local temperature (up to 5000 K) and high pressure (up to  $10^3$  atm) in the center of the cavity, whereas the bulk solution remains at low-temperature because of localized energy release and high cooling rate. This high pressure and the jet formation crush solid materials into micro- and nanoparticles [27-31].

In this chapter, the top-down ultrasonication approach for preparing paclitaxel nanocolloid will be discussed as a representative method developed for preparing small size low soluble drug nanocolloid. The chemical structure of paclitaxel is shown in Figure 3.1.

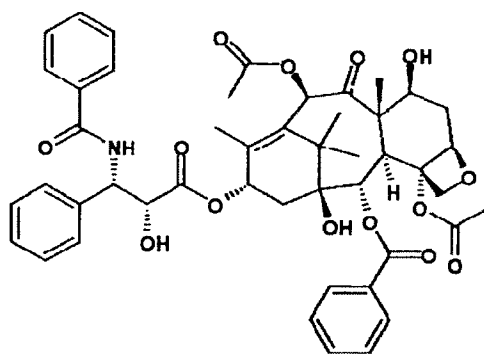


Figure 3.1 Chemical structure for paclitaxel

### 3.1 Top-Down Approach

Figure 3.2 shows the scheme for top-down approach. In this process, ultrasonication was applied to break down crystal structure of paclitaxel into nanoparticles while they are coated with polyelectrolyte to provide the system colloidal stability. Oppositely charged polyelectrolytes were applied one layer at a time for the prevention of recrystallization of those nanoparticles.

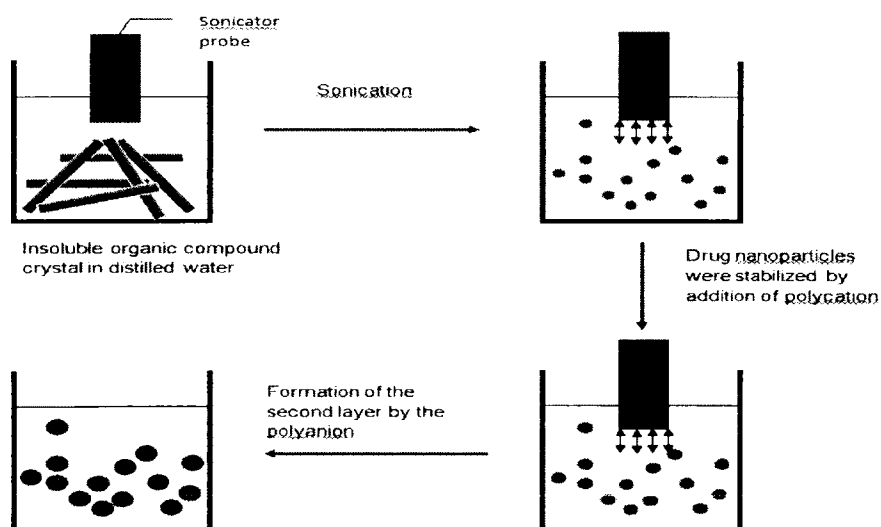


Figure 3.2 Scheme for top-down approach [72]

To be more specific, 0.5 mg/ml of paclitaxel crystal were added into De-Ionized water, and then ultrasonication with 15 W/cm<sup>2</sup> in power was applied for 45 minutes. Due to the negative surface  $\xi$ -potential of the drug particle, polycation (positive polyelectrolyte such as chitosan, protamine sulfate and polylysine) was added to the solution during ultrasonication was continuously adsorbed onto the particle surface during the crystal broken down process providing enhanced surface potential. During this process, ca. 300 nm size drug particles coated with a layer of polycation were obtained.

A set of experiments had been done to figure the minimal amount of polyelectrolyte necessary for surface recharging and further Layer-by-Layer shell build up. This minimal polyelectrolyte amount minimized the non-reacted polyelectrolyte remaining in bulk solution. Then oppositely charged polyanions (negative polyelectrolyte such as heparin, albumin and alginic acid) whose surface charge is opposite to the previously coated layer, was added into the solution with extended 15 minutes ultrasonication. This process of sequential adsorption of oppositely charged polyelectrolytes while preserving ultrasonication was repeated three to five times for stable nanocapsule formation with desired nano-architecture and functionality. Compared with the conventional Layer-by-Layer process, we minimized those tedious processes of washing and centrifugation to form a washless Layer-by-Layer process. After the completion of the Layer-by-Layer coating process, the paclitaxel drug dispersions were centrifuged at 12,000 rpm for 10 minutes to remove the excess polyelectrolytes. They were then washed and re-suspended in De-Ionized water for further experiments. The electrical surface  $\xi$ -potential and size of the nanocolloids measurements were performed using ZetaPlus microelectrophoretic instrument and light scattering machine. These machines characterized the success (or failure) of the Layer-by-Layer coating. FESEM and laser confocal microscopy imaging was applied for morphology characterization.

### 3.2 Top-Down Approach with Bubbling Agent

As described in Chapter One, the additions of chemicals which can produce more gas microbubbles increase the efficiency of ultrasonication. Figure 3.3 shows the SEM image of paclitaxel before and after top-down approach. As we can see from Figure 3.3 (a), the original paclitaxel are several microns in length. In Figure 3.3 (b) and Figure 3.3 (c), after the process using top-down approach, we were able to get paclitaxel nanoparticles around 300 nm in size. The nanoparticles have the good property of narrow size distribution. However it is very difficult to break the particle size down to less than 300 nm in size using the top-down approach. This difficulty may confine its medical application for the small size requirement.

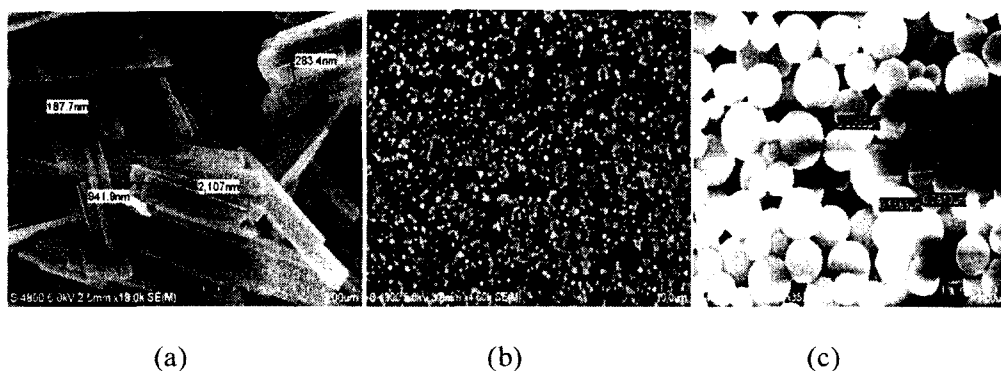


Figure 3.3 SEM image of paclitaxel before and after top-down approach. (a) Original paclitaxel; (b-c) Top-down sonication method (paclitaxel/(chitosan/alginate)<sub>2</sub>).

Figure 3.4 confirms the SEM result of paclitaxel nanoparticles after top-down approach with bubbling agent using Precision detectors PDExpert light scattering workstation. It shows that the paclitaxel nanoparticles coated with PAH/PSS had an average size of  $120 \pm 30$  nm obtained with LbL ultrasonication enhanced with bubbling agent  $\text{NH}_4\text{HCO}_3$  used at concentration 1 mg/ml. This result also shows its narrow particle size distribution.

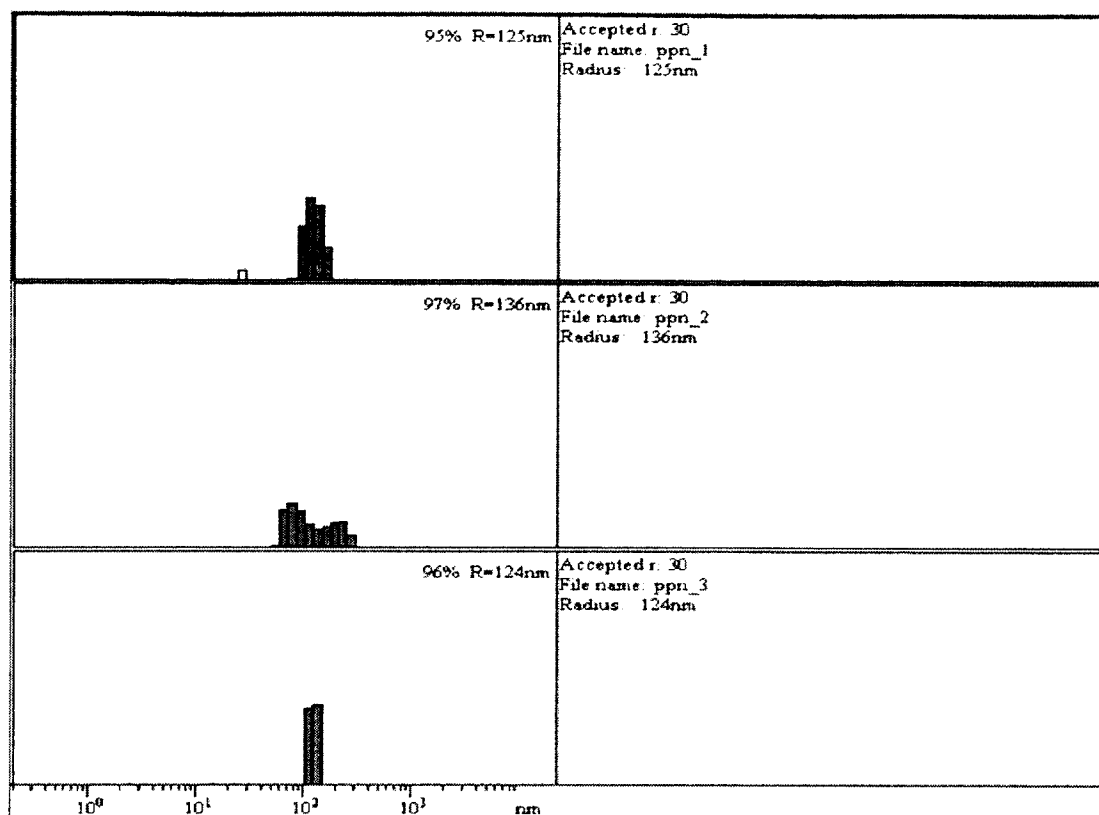


Figure 3.4 Light scattering result of paclitaxel after top-down approach with bubbling agent (X-axis: size in nm, Y-axis: ratio of particles of certain size as compared to the total particles)

Figure 3.5 shows the SEM result for using bubbling agent on large scale. We can clearly see particle size uniformity (assuming that single particle circles form these rings).

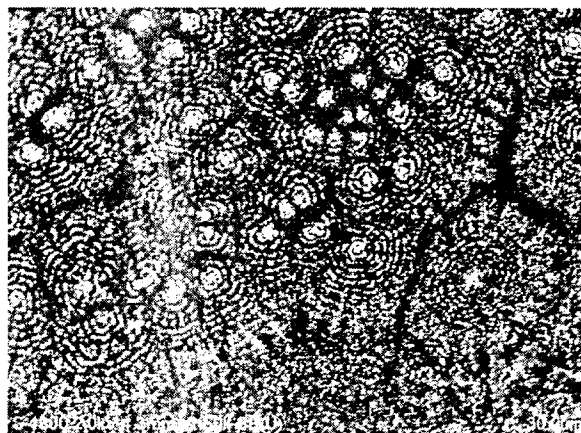


Figure 3.5 SEM image for paclitaxel nanocores formation with bubbling agent enhancement

### 3.3 Zeta Potential Monitoring the LbL Process

The best way to monitor the Layer-by-Layer process is to control the reversal change of the particle surface potential changing during the process of alternate adsorption and coating. As can be seen from Figure 3.6,  $\xi$ -potential of original paclitaxel crystal was found to be -20mV. Without the Layer-by-Layer coating, initial nanocolloids were stable only during sonication; however, aggregation came quickly when the power sonication was terminated. Therefore the Layer-by-Layer coating was applied for better stability. In the first trial for Layer-by-Layer coating, we applied synthetic polyelectrolytes (polycation: poly (allylamine hydrochloride) (PAH) and polyanion: poly (styrene sulphonate) (PSS)) since they have higher ionization and surface charge which help in anchoring on nanocolloids. This synthetic polyelectrolytes coating process is a common way for Layer-by-Layer study and had been applied in industry. After the process was elaborated, we began to use biocompatible polyelectrolytes (polycation: chitosan, polyanion: alginic acid) since for real biomedical application we need our drug formulation to be biocompatible and biodegradable.

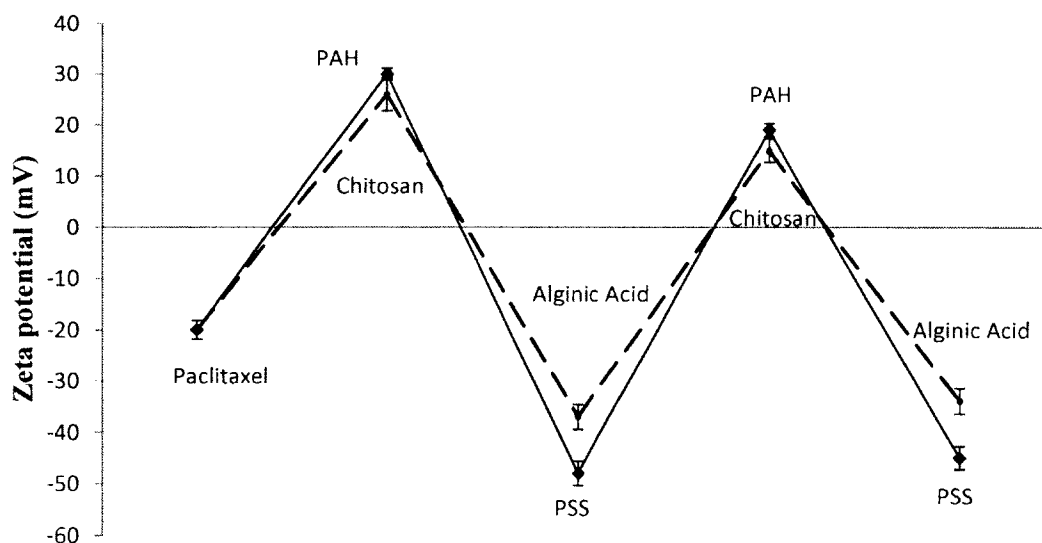


Figure 3.6  $\xi$ -potential monitoring of the Layer-by-Layer process for the nanocolloids for synthetic and natural biodegradable polyelectrolytes

Figure 3.6 shows the alternate change in surface  $\xi$ -potential of the drug nanoparticles during the adding of each polycation and polyanion solution during permanent sonication. The first polycation layer of poly (allylamine hydrochloride) (PAH) switched the surface  $\xi$ -potential to  $30 \pm 3$  mV, higher than that of biocompatible chitosan at  $24 \pm 2$  mV. The following first polyanion layer of poly (styrene sulphonate) (PSS) switched the surface  $\xi$ -potential back to  $-47 \pm 3$  mV, more negative than that of biocompatible alginic acid at  $-35 \pm 3$  mV. Both the adsorption of polycation and polyanion layer was continued and showed the regular electrical potential reversal. The changes in potential proved the successful coating of Layer-by-Layer technology. And this worked also for both natural biodegradable polyelectrolytes chitosan and alginic acid.

Figure 3.7 shows the chemical structure for chitosan and alginic acid used. Their biocompatibility and biodegradability have been helpful in cell experiment and human study. The successful coating with synthetic and biodegradable polyelectrolytes shows the versatility of materials choice for building up the architecture using Layer-by-Layer technology.

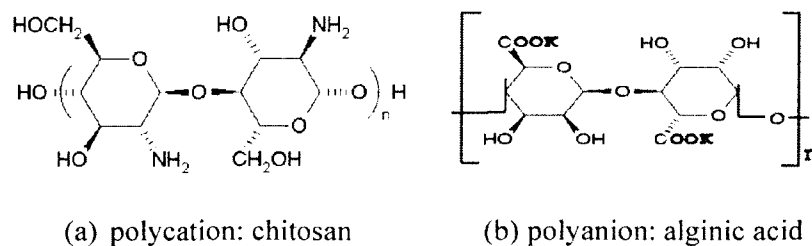


Figure 3.7 Chemical structure for biocompatible polyelectrolytes: (a) polycation: chitosan (b) polyanion: alginic acid

After the three to four bilayers coating with these polyelectrolytes, drug nanocolloids can be stable for at least one week without essential aggregation (no sediments).

For biocompatible polyelectrolytes, we also tried combinations of peptides and proteins (positive protamine sulfate (PS) and negative bovine serum albumin). The shell made of chitosan and alginic acid showed better colloidal stability than protamine sulfate and albumin combination which aggregated in two days. The better stability is due to their higher surface potential since after the final alginic acid layer coating, the nanoparticle reached the value more (in magnitude) than  $-30 \pm 3$  mV, which is considered as a threshold of stable colloid formation. Therefore, the optimization of the shell architecture for better stability was important. This surface  $\xi$ -potential characterization showed similar result for the similar architecture shell samples with and without bubbling agent, but bubbling allowed smaller initial nanocore formation.

### 3. 4 Confocal Fluorescence Image

Figure 3.8 shows the confocal fluorescence image for the paclitaxel nanoparticles coated with PAH and FITC-labeled PSS by top-down approach. We understand that we do not see a real image of the particle because it is smaller than the confocal microscope resolution (500nm). With this image, we just want to demonstrate that our paclitaxel nanocolloid is well dispersed and non-aggregated (so each separate particle image is smeared due to the convolution with instrumental function).

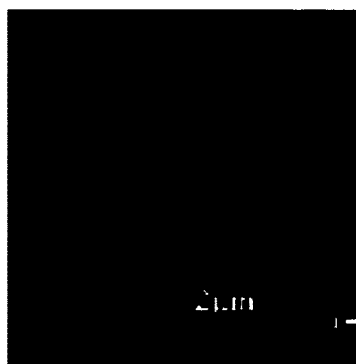


Figure 3.8 Confocal fluorescence image for top-down approach

### 3.5 Efficiency of Bubbling Agent Method

An important question is: what is the chemical stability of the samples under high local spot temperature in oxygen-saturated solutions and with the existence of bubbling agent? We needed to prove the final outcome for the bubbling agent method to be not de-composed paclitaxel. X-ray diffraction (XRD) had been applied for study of the crystalline structure of the final LbL shelled nanocolloids.

Hypothesis: The bubbling agent added during the process of sonication will evaporate and will not have an effect on the composition of the final outcome, that is, the final outcome is still paclitaxel.

Methodology: Use XRD to identify crystalline structure of the final output of bubbling agent method with pure paclitaxel and to compare it with crystal structure of the original bulk paclitaxel.

Result: The XRD result is shown in Figure 3.9. The XRD measurement is based on the Bragg's law:  $2d \sin\theta = n\lambda$ . For the function,  $\theta$ ,  $\lambda$  and  $d$  are the scattered angle of the X-ray, wavelength of the X-ray and d-spacing of the sample respectively. The d-spacing is the distance between crystalline planes, which gives information about the sample. The bottom curve shows the information of the  $2\theta$  peaks of pure paclitaxel. The top curve shows the information of the  $2\theta$  peaks of final outcome of bubbling agent method. It can be clearly seen from Figure 3.9 that the peaks of the two samples overlap well with each other. According to the Bragg's law, they have the same d-spacing, which gives information about the sample. The overlap means that the final outcome of the bubbling agent method is paclitaxel.

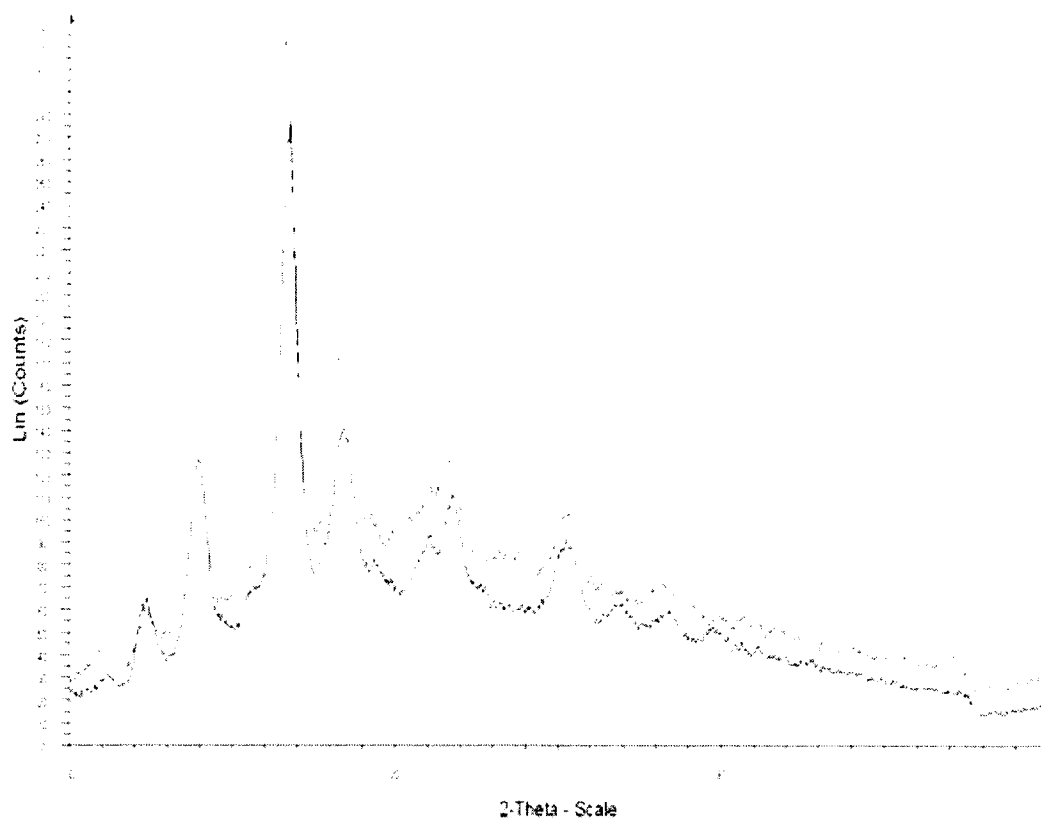


Figure 3.9 The XRD results of pure paclitaxel (bottom curve) and the final outcome of bubbling agent method (top curve)

Conclusion: The bubbling agent added during the process of sonication does not have any essential effect on the composition of the final outcome. The final outcome is still paclitaxel.

### 3.6 Mechanism of Bubbling Agent for Enhancement of Ultrasonication Capability

To maximize the ultrasonication capability for nanoparticulation, the bubble nucleation rate is a key parameter. Using  $\text{NH}_4\text{HCO}_3$  as a bubbling agent to enhance bubble nucleation allowed us decreasing size of colloid particles closer to 100 nm (Figure 3.3(d)). To be specific in experiment,  $\text{NH}_4\text{HCO}_3$  had been dissolved in the first polycation solution and then added into the drug solution during sonication. This bubbling agent was completely

decomposed and “bubbled-out” during sonication as  $\text{NH}_3$  and  $\text{CO}_2$  gases. The size distribution diagram was centered at 120 nm and its width is 60 nm.

Figure 3.10 shows the result for top-down method with bubbling agent. Its average size is  $120 \pm 30$  nm. It is much smaller than without bubbling agent.

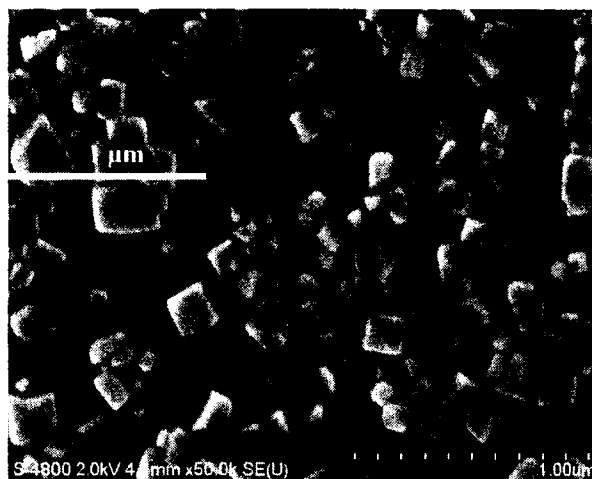


Figure 3.10 SEM image of paclitaxel coated with PAH/PSS with average size of  $120 \pm 30$  nm obtained with top-down LbL ultrasonication enhanced with bubbling agent  $\text{NH}_4\text{HCO}_3$  used at concentration 1 mg/ml [72].

Besides the gas concentration in solvent, the bubble nucleation rate  $dN/dt$  depends on gas concentration, temperature, surface tension, pressure, hydrophobicity of the substrate surface [30]:

$$dN/dt = \text{Constant} * c * \exp(-\Delta E/kT). \quad (\text{Eq. 1})$$

Here  $c$  is gas concentration,  $\Delta E = 4\pi\sigma^3 P^{-2} g(\theta)/3$  is the energy barrier for the bubble nucleation,  $T$  is the surrounding temperature,  $\sigma$  is the liquid/air surface tension.  $P$  is pressure;  $\theta$  is the contact angle of the surface.

Since we used an aqueous medium for the nanocolloid synthesis, there was a minute variation for surface tension and contact angle as compared to possible pressure variation (additional two to three atm may essentially increase ultrasonication efficiency). Therefore,

higher gas concentration through bubbling agents increases nucleation. An increase in pressure will decrease the energy barrier, also resulting in the increase of bubble nucleation, and is thus helpful for the nanoparticle formation. It was found that low wettability of materials (which is the case for more hydrophobic low soluble materials) formed the shape of a bubble resulting jet flow directing to the particle surface which may increase explosion energy [31].

Though the nanoparticulation procedure is reliable, there are number of features which have to be discussed and clarified in future studies:

1) The role of adsorbed polyelectrolytes may be not only in the particle surface re-charging but may also serve as cleaving agents, filling and widening microcracks caused by sonication. Dependence of the procedure on molecular weight of the used polyelectrolytes may be important.

2) In all our experiments, electrical surface potential ( $\xi$ -potential) of micro/nano particles after ultrasonication (but before polyelectrolyte deposition) was negative. It may be due to partial oxidation of the particle surface under ultrasonication. This assumption has to be checked and control over the depth of such oxidation may require operations in nitrogen atmosphere.

3) Even increasing ultrasonication power and extending its time did not allow smaller particle sizes: 200-nm diameter was a kind of “magic” barrier for many of our colloidal particles. We suggested that diameter barrier may be related to the nucleation size of vapor bubbles. This assumption allowed us to decrease colloid particles to 150 nm diameter using agents enhancing bubbling formation (such as  $\text{NH}_4\text{HCO}_3$ ). The process of the bubble nucleation related with materials hydrophobicity has to be analyzed to get even smaller particle sizes.

### 3.7 Conclusions

Paclitaxel nanoparticles LbL coated by biodegradable (chitosan/alginate)<sub>3</sub> shells were produced with the size in the range of 150-200 nm. Bubbling agents allowed higher ultrasonication power for smaller paclitaxel nanocores formation. These nanocolloids were stable for at least one week in water at concentrations of 0.5 mg/ml and pH 6.5. In Chapter Four, we will describe another drug nano-core formulation which helped us to avoid titanium dioxide contamination.

## CHAPTER 4

### BOTTOM-UP APPROACH FOR DRUG NANOFORMULATION

There are two approaches applied in our study. One is top-down approach with powerful ultrasonication as discussed in the previous chapter. In this approach, we used paclitaxel as a representative low soluble drug and obtained good results with LbL encapsulation of ca 150 nm diameter nanoparticles. However, a large obstacle of this method was a necessity of long ca one hour high power ultrasonication which resulted in TiO<sub>2</sub> nanoparticle detachment from the titanium electrode and contamination of the sample. Mice injection even was possible but unsafe for small animals.

The other approach is the bottom-up approach with the surfactants such as lipids, Polysorbate 80 (TWEEN 80), or albumin possessing some amphiphilic properties. We applied this approach for paclitaxel and lapatinib nanocores formation accomplished with LbL encapsulation. In this approach, a low soluble drug was dissolved in a good solvent (ethanol) for dissolution into molecular solution and then desolvation process (water addition initiating crystallization) with permanent sonication and addition was applied. Amphiphile molecules were added to the mixture to arrest drug nucleation and to provide charged sites for anchoring of the first polycation layer coating. This approach was quite different from the top-down approach in the kinetics of the nanoparticle formation (nanocrystal growth from molecular solution) rather than from breaking down bigger crystals. Some sections of this chapter were published in a paper written by the author of this dissertation in co-authorship with Dr. Lvov and others as “Top-down and Bottom-up Approaches in Production of

Aqueous Nanocolloids of Low Solubility Drug Paclitaxel”, in *Physical Chemistry Chemical Physics*, 2011, 13, 9014-9019. The text sections cited from this paper is properly cited as [73], and they are not in use in any other dissertation.

## **4.1 Bottom-Up Approach with Powerful Ultrasonication**

### **4.1.1 Method Description**

Figure 4.1 shows the scheme for bottom-up approach with powerful ultrasonication. In this process, a low soluble drug was dissolved in a good solvent (ethanol or acetone). Powerful ultrasonication was then applied with amphiphilic Polysorbate 80 and aqueous polycations were slowly added into the drug solution. Water was additionally added into the solution to decrease the solubility of the drug in the solution. With the increment of water volume in the drug solution and evaporation of solvent, solubility of the chosen drugs decreased. The solution would then reach saturation and nucleation would begin to form drug nanoparticles. The combination of powerful ultrasonication and amphiphiles stopped those nanoparticles from growing into bigger particles (“arrested” nucleation). As discussed earlier in similarity to the top-down approach, oppositely charged polyelectrolytes were then sequentially adsorbed onto the surface of drug nanoparticle to help form a high surface charge layer to provide further colloidal stability for drug particles. After 30 minutes of usual sonication treatment (not using very high power but rather usual sonication bath), centrifugation at 12,000 rotates per minute for 10 minutes were applied to precipitate these drug crystals already pre-coated with Polysorbate 80 and one polycation layer. They were then re-suspended in De-Ionized water. A second layer of polyelectrolyte (anionic) was deposited to further enhance the drug particle surface  $\xi$ -potential (recharging it to negative). Unreacted polyelectrolytes were removed by centrifugation and Layer-by-Layer drug nanoparticles with size around 150 nm were obtained both for paclitaxel and lapatinib.

Further Layer-by-Layer polyelectrolyte was applied for these stabilized nanocolloids for building up needed shell architecture using traditional process without powerful ultrasonication.

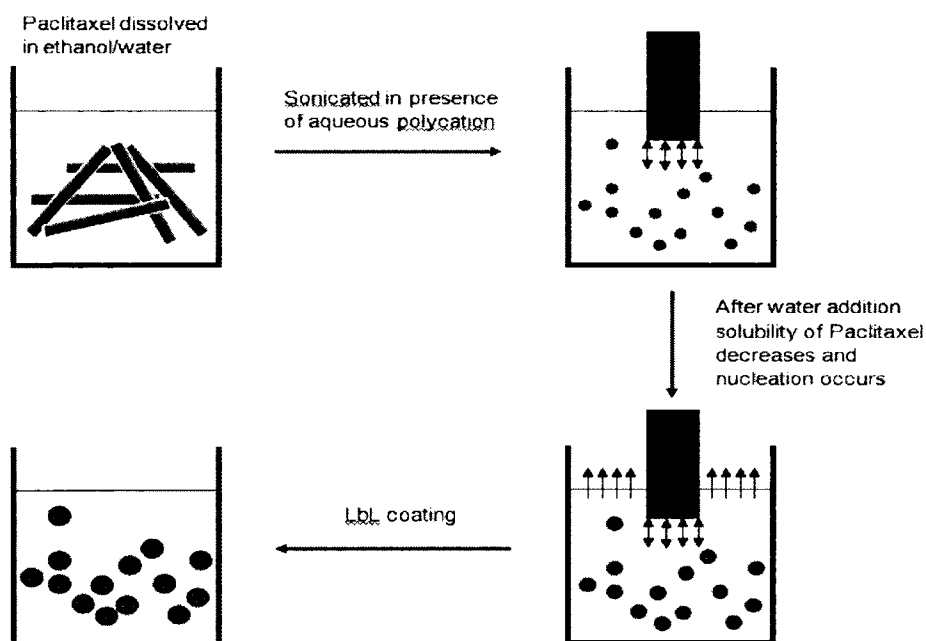


Figure 4.1 Scheme for bottom-up approach with powerful ultrasonication

Figure 4.2 shows the test result of temperature of the solution during ultrasonication and the evaporation rate of Di-Ionized (DI) water, 60% Ethanol/De-Ionized water mixture and pure ethanol. As we can see, the evaporation rate of ethanol during powerful ultrasonication was close to that of being heated to 80 °C. Therefore, the temperature in the ultrasonication solution was very close to 80 °C. The evaporation rate of De-Ionized water was much smaller than ethanol and that of 60% ethanol/De-Ionized water mixture is in between them. Typically, our dissolution process took 25-30 minutes.

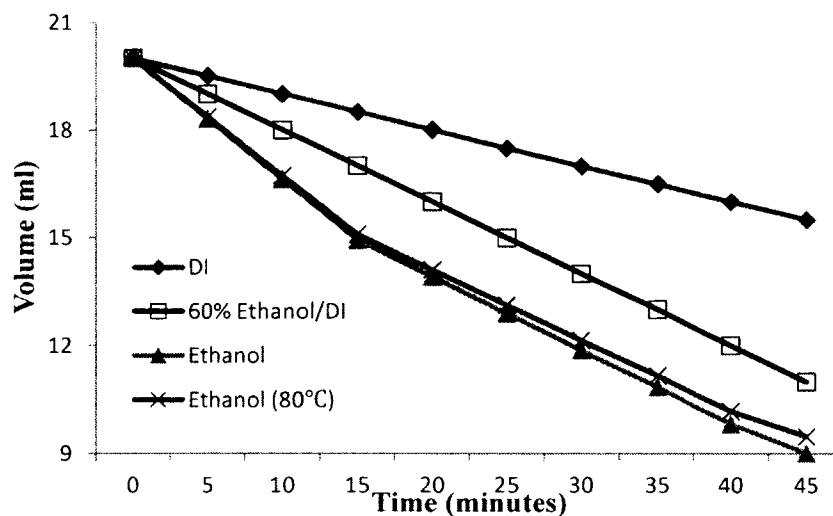


Figure 4.2 Evaporation rate of different solution during sonication

#### 4.1.2 Optimization Process

Here we would like to show our process of optimization for getting better smaller size drug nanoparticles. Our optimization process included the following parameters: solvent type, concentration, used amphiphile molecules, water instillation speed, original paclitaxel or lapatinib concentration, sonication time and the application of centrifugation. They are discussed in detail below:

##### 1. Solvent type: ethanol VS acetone.

Figure 4.3 shows the effect of different organic solvent on final drug particle size. Paclitaxel (4 mg) in 2 ml ethanol or acetone solvent was sonicated. Then 100 ul 2 mg/ml of poly (allylamine hydrochloride) (PAH) solution was added in, and 2 ml of De-Ionized water was slowly added into the solution. As can be seen, the solvent ethanol gives better dispersion and less aggregation result for drug nanoparticles than acetone.

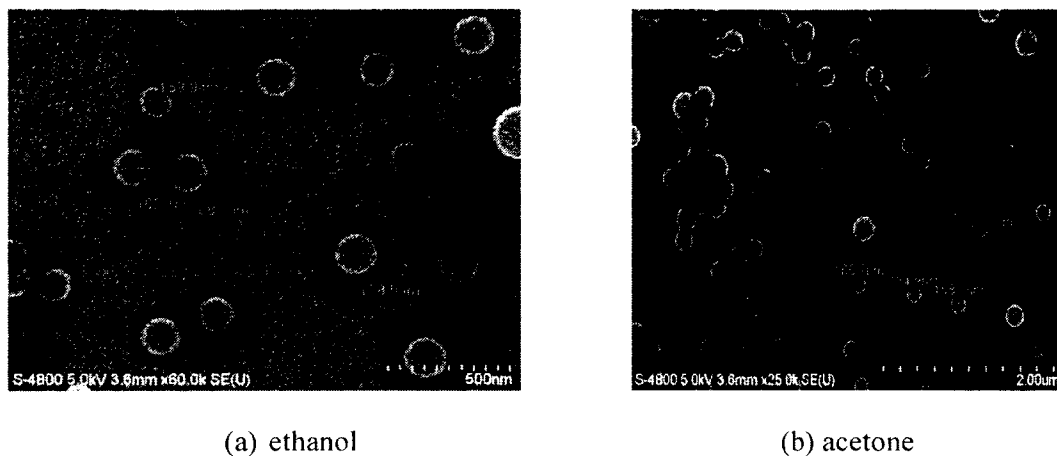
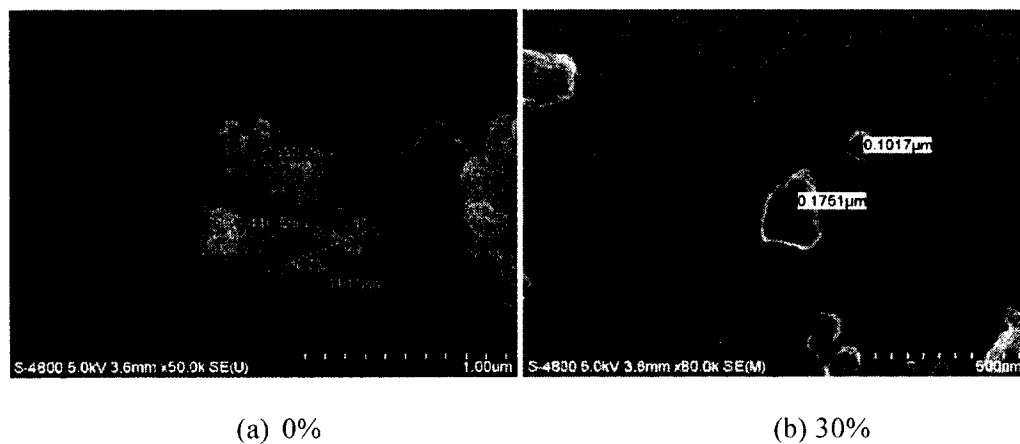
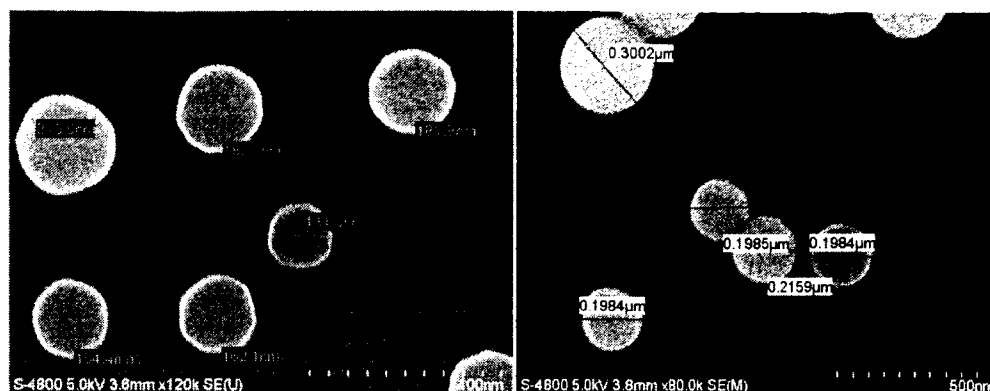


Figure 4.3 SEM image of final drug nanoparticles by different solvent type

## 2. Effect of concentration.

Figure 4.4 shows the effect of solvent concentration (0%, 30%, 60%, 90%) on the final nanoparticle size. Paclitaxel (4 mg) in 2 ml ethanol solution (0%, 30%, 60%, 90%) was sonicated. Then 100 ul 2mg/ml of poly (allylamine hydrochloride) (PAH) solution was added in, and 2 ml of DI water was slowly added into the solution. As we can see, 60% ethanol/De-Ionized water mixture gives best dispersion and particle size.





(c) 60%

(d) 90%

Figure 4.4 SEM image of final drug nanoparticles by different ethanol concentration

### 3. Water instillation speed.

Figure 4.5 shows the effect of DI water addition speed on particle size. With the increment of addition speed, particle size grows bigger. This effect can be explained by the fact that with the increment of addition speed, the solubility decreases faster leading to faster crystal nucleation rate and the possibility of aggregation gets higher leading to the increment in the final drug particle size. The low DI water addition speed at 0.5 ml/min allowed the drug molecule to form crystals slowly and protected and stabilized by polyelectrolytes with smallest size.

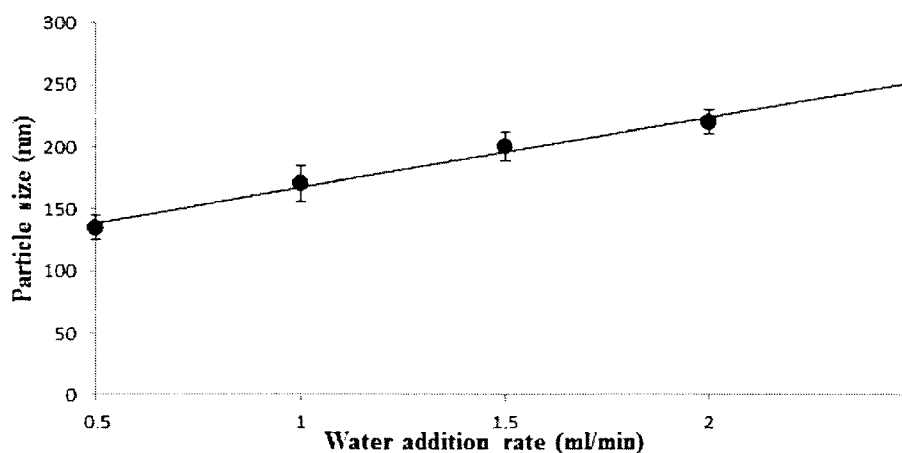


Figure 4.5 Effect of DI add in speed on particle size [73]

#### 4. Drug concentration.

As one can see from Figure 4.6, with the increment in the initial drug concentration, the aggregation tendency during nucleation process increased leading the final particle size getting larger.

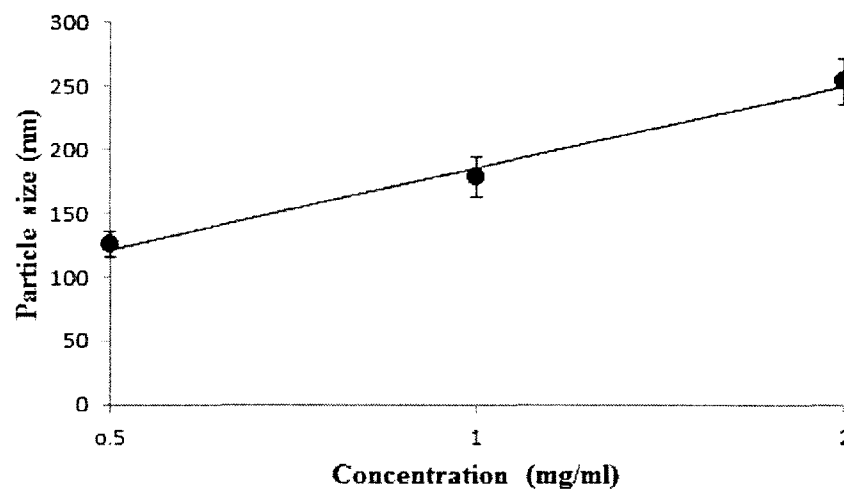


Figure 4.6 Effect of drug (paclitaxel) initial concentration on particle size [73]

#### 5. Sonication time.

With the increment of sonication time (Figure 4.7), the drug particle size decreased. After 45 minutes, there is no big change in particle size. Therefore, in our study, 45 minutes of ultrasonication were usually applied for the coating of first polyelectrolyte layer.

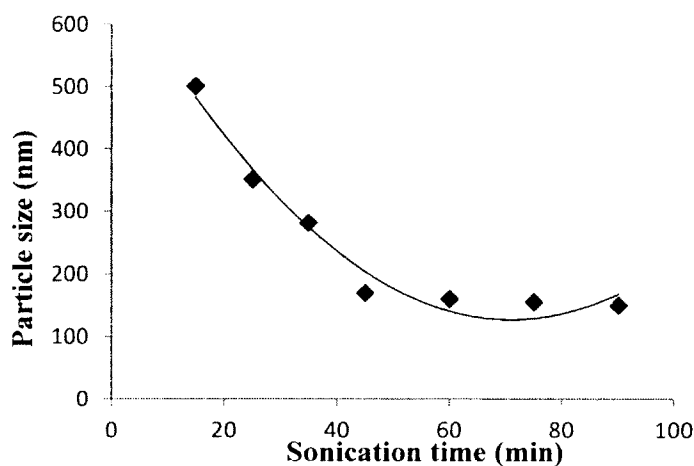


Figure 4.7 Effect of sonication time on paclitaxel particle size

#### 6. Centrifugation.

In our approach, we still had some larger particles at the edge of the container which would be harmful. Therefore, centrifugation was been applied for removing bigger particles. The result can be seen in Figure 4.8.

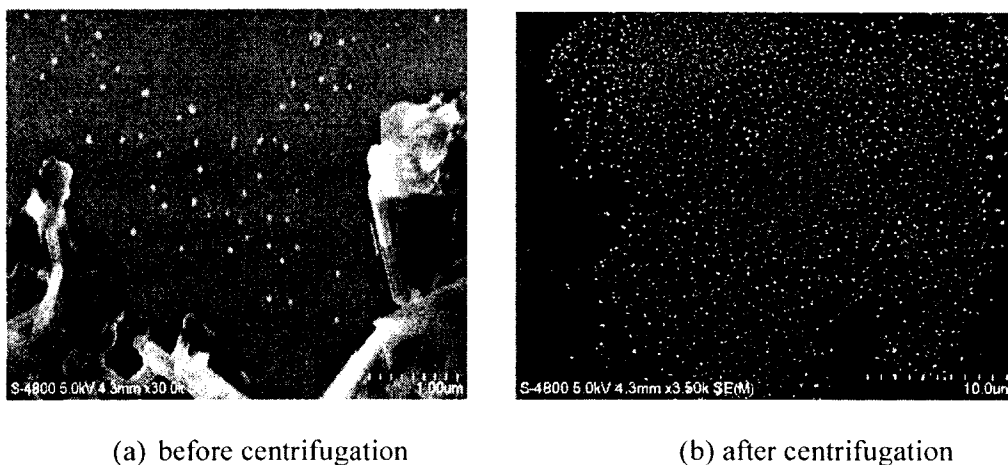


Figure 4.8 Centrifugations to eliminate bigger particles

Figure 4.9 shows the increment of centrifuge speed and time decreases the final particle size to a certain extent. Our optimization result was choosing 2000 rpm and 10 minutes as the

premium speed and time, since too high centrifuge speed and too long at a time will cost the loss of drug concentration.

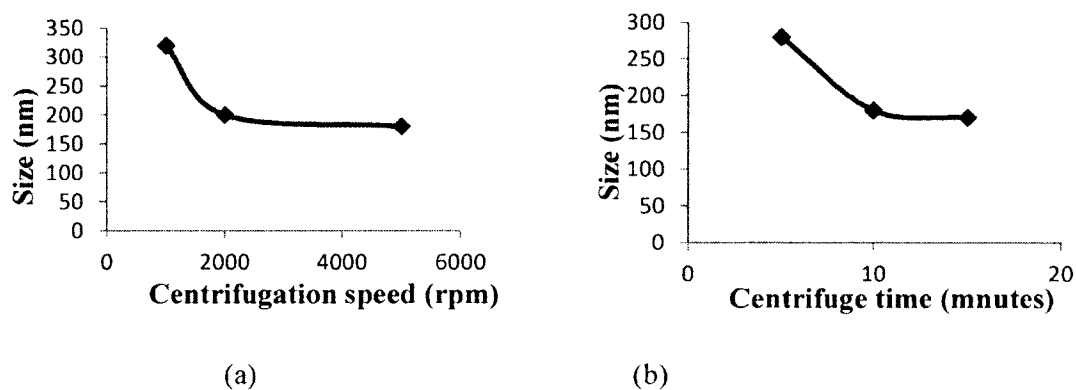


Figure 4.9 Effect of (a) centrifuge speed (r/min) and (b) time in minutes (2000 r/min) on the paclitaxel particle size (the y-axis, in nanometers)

#### 4.1.3 Bottom-up Method with Bubbling Agent Enhancement

With the optimized process above, we then applied the bubbling agent to the bottom-up approach. The procedure for bottom-up method with bubbling agent is described below:

- 1) Dissolve 0.5 mg/ml of drug in 20 ml 60% Ethanol/De-Ionized water solution and start ultrasonication for five minutes;
- 2) Add in polycation and bubbling agent solution (1mg/ml) and further apply ultrasonication for 45 minutes;
- 3) Slowly add in DI water during sonication, The solubility of the drug will decrease and crystallization will be initiated but being kept from growing into larger particle with sonication and polyelectrolyte coating;
- 4) Bottom-up method with bubbling agent will produce drugs with 30 nm in size;
- 5) Polycation coating of nanoparticles provides colloidal stability and allow further LbL shell formation.

The result for bottom-up method with bubbling agent enhanced method is shown in Figure 4.10. Some very small drug particles with the sized around 30-40 nm in size are available.

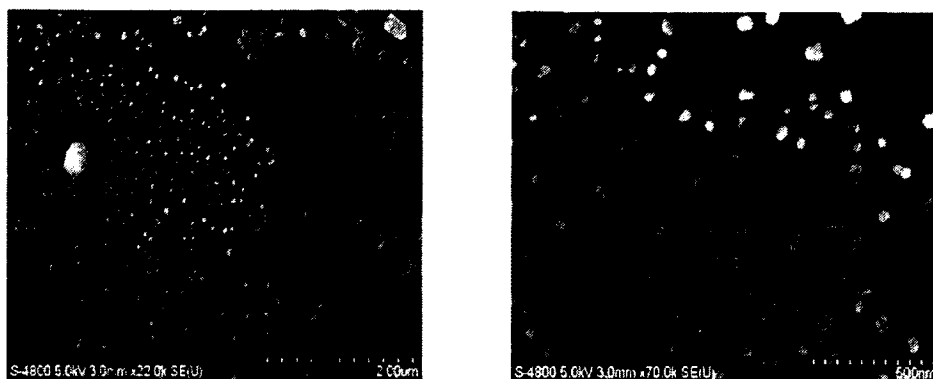


Figure 4.10 Bottom-up method with bubbling agent (images from different part of the paclitaxel sample)

#### 4.1.4 Bottom-up Approach with Magnetic Particle Milling

Preparation: 1) 0.5 mg/ml Pac in 20 ml 60% Ethanol/DI water. Sonicate for five minutes. 2) Add in 2/0.5/1 mg/mg/ml PAH/  $\text{Fe}_3\text{O}_4$ /DI 3ml drop by drop in three minutes. 3) Add in 0.5/0.125/1 mg/mg/ml PAH/ $\text{Fe}_3\text{O}_4$ /DI 20 ml using syringe for 45 minutes. Notes:  $\text{Fe}_3\text{O}_4$  was not completely dissolved in DI. Take upper liquid for experiment. 4) Take the sample after sonication, centrifugation, filtration, and centrifugation plus filtration samples, denoted as 1, 2, 3 and 4 for SEM.

Figure 4.11 shows the SEM image of bottom-up method with magnetic particles for sample 3 after filtration. We can see many 20 nm particles on the edges, which could be  $\text{Fe}_3\text{O}_4$  after sonication. Drug particles around 200 nm in size were obtained. For the sample after centrifugation and filtration process in Figure 4.12, we still see some drug surrounded by  $\text{Fe}_3\text{O}_4$ , but the concentration may not be high enough. This process can be further studied and improved.

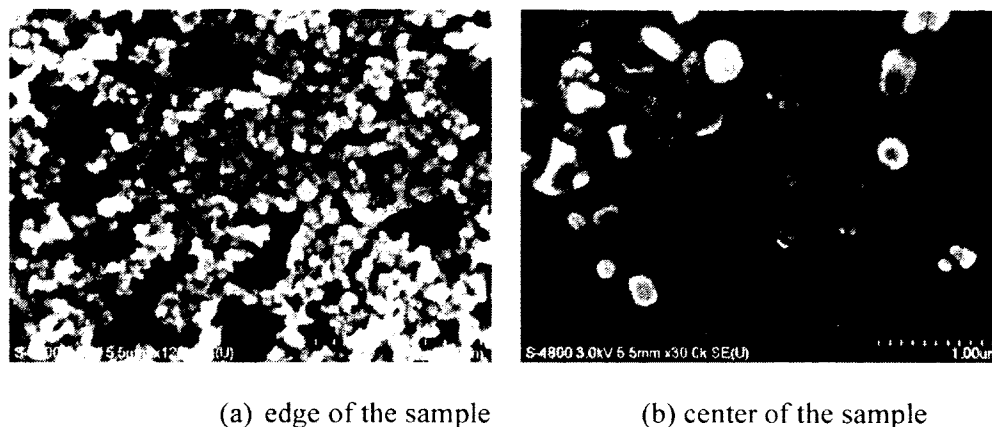


Figure 4.11 SEM image of bottom-up method with magnetic particles

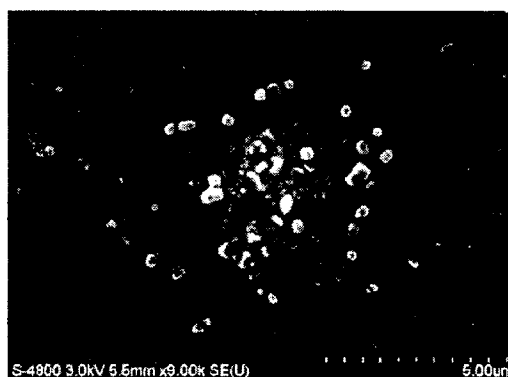


Figure 4.12 SEM sample of magnetic particle coating on the drug after centrifugation and filtration process

#### 4.2 Bottom-up with Surfactants Assisted Sonication Approach

Another bottom-up approach applied in our research is using those surfactants such as albumin, polysorbate 80 (TWEEN 80) and polyvinylpyrrolidone (PVP) during sonication. We applied this approach for paclitaxel and lapatinib. In this approach, we use a regular sonicator rather than a powerful ultrasonicator. Since the samples prepared by powerful ultrasonicator usually has black precipitate of  $\text{TiO}_2$  which polluted of the drug nanocapsules. It is difficult to remove them because they have close particle sizes. Therefore, we used regular sonication and combined our LbL approach with traditional emulsification process with addition of biodegradable surfactants to anchor polyelectrolytes on the surface of the

formed drug nanoparticles. This chapter is mostly devoted to our second anticancer drug at work: lapatinib. Chapter Six of this dissertation will show, for the first time, the combined action of these two drugs assembled within one LbL nanocapsule.

Figure 4.13 shows the chemical structure of lapatinib. It is a drug with very low solubility. It is widely used as an orally active drug for breast cancer.

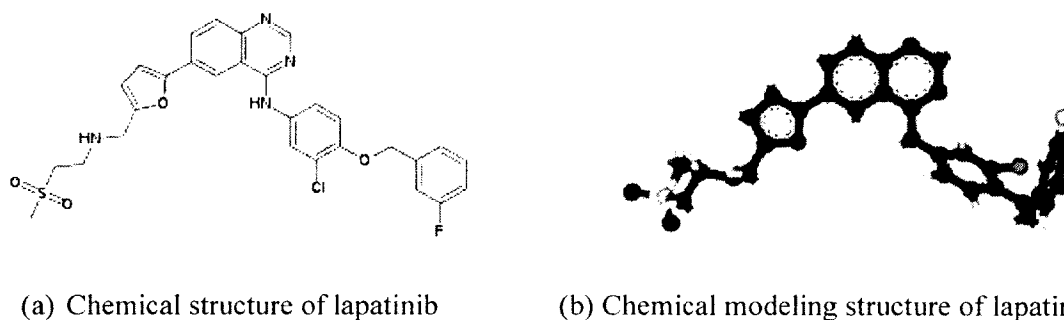


Figure 4.13 Lapatinib structural formulas

Let us give a brief introduction of the surfactants used in this study. The chemical structure of polysorbate 80 (TWEEN 80) and polyvinylpyrrolidone (PVP) are shown in Figure 4.14. Polysorbate 80 (TWEEN 80) is an emulsifier and nonionic surfactant. It is a viscous and soluble yellow liquid widely used in the food industry. It is derivative of oleic acid and polyethoxylated sorbitan. Its hydrophilic polyethers groups (polyoxyethylene groups) are biocompatible. Polyvinylpyrrolidone (PVP) is a water-soluble polymer. It is polymerized from its monomer N-vinylpyrrolidone.

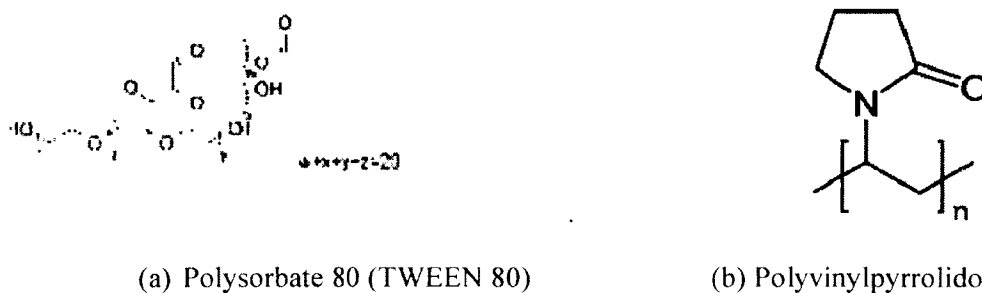


Figure 4.14 Polysorbate 80 and polyvinylpyrrolidone

For this approach, a small amount of albumin and polyvinylpyrrolidone was added into PBS (Phosphate buffered saline) buffer solution and then regular sonication was applied. A low soluble drug was dissolved in a good solvent (DMSO) for dissolution into molecule and then added into the surfactant solution during sonication. Biocompatible polyelectrolyte PLB16-5 (PEG and PLL (Polylysine) block copolymer PLL [16kDa]-b-PEG [5kDa] as shown in Figure 4.15) was added for LbL coating.

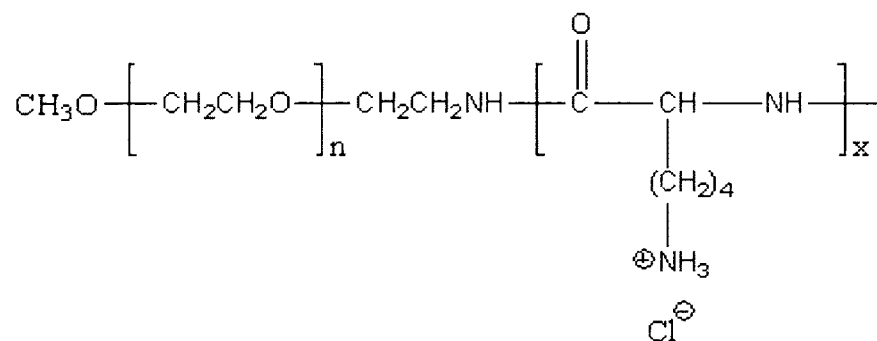


Figure 4.15 PLL -block-PEG (PLB)

### 4.3 Conclusions

In this chapter, we described LbL nanoencapsulation of another anticancer drug: lapatinib. In Chapter Seven we will demonstrate LbL assembly of paclitaxel and lapatinib in one LbL capsule.

## CHAPTER 5

### CAPSULE PEGYLATION AND CONTROLLED RELEASE STUDY FOR LAPATINIB AND PACLITAXEL

#### 5.1 PEGylation

##### 5.1.1 PEGylation Process

To overcome difficulties with drug nanoformulation colloidal stability in high molarity PBS (Phosphate Buffered Saline) buffer, we developed LbL shells with PEGylation. For this we used block copolymer of cationic PLL with PEG. No essential changes in the LbL deposition method were necessary. The detailed procedure for PEGylated shell assembly is shown below:

- 1) Two point five microliters of PBS, 10  $\mu$ l 60 mg/ml of albumin/PBS, 50  $\mu$ l of PVP (80 mg/ml) added together and sonicate for two minutes.
- 2) During sonication, add 200  $\mu$ l lapatinib/DMSO (7 mg/ml), keep sonication for 20 minutes.
- 3) Using around 20  $\mu$ l PLB (PEG and polylysine block copolymer) (60 mg/ml in acidic PBS), 20  $\mu$ l heparin (60 mg/ml in acidic PBS) for layer by layer coating by sonicating for one minute each time.
- 4) Taking half milliliter sample, centrifuge at 2,000 rpm for 10 minutes, and keep the supernatant, we get nanoparticles 150 nm in size.

5) Centrifuging the above supernatant at 10,000 rpm for 10 minutes, get the bottom sample, sonicate and add in the same amount of PBS, and get particle size at 125 nm as shown in Figure 5.1.

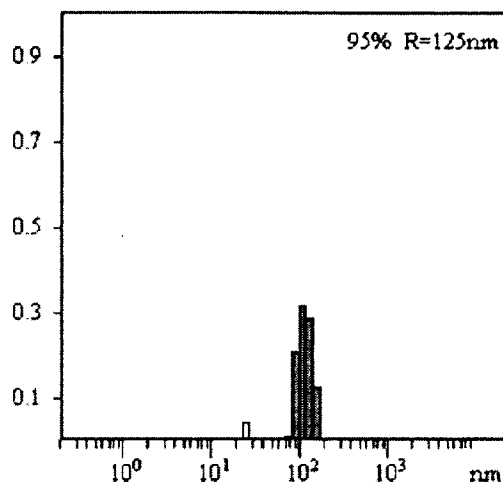


Figure 5.1 Lapatinib particle size after PEGylation (X-axis: size in nm, Y-axis: ratio of particles of certain size as compared to the total particles)

6) The steps three to five were repeated to make 3.5 bilayers on top of the drug particles with heparin being the outmost layer. Drug particles around 180 nm in size,  $-36 \mu\text{V}$  in surface charge were obtained. Figure 5.2 shows the SEM image for lapatinib nanoparticles with 3.5 bilayers of PLB (polyethylene glycol and polylysine block copolymer) and heparin.

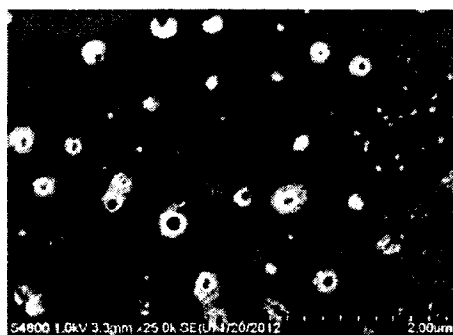


Figure 5.2 SEM image for lapatinib nanoparticles after Layer-by-Layer coating; the shell composition is as follows: lapatinib/albumin/ (PLB16-5/heparin)<sub>3.5</sub>

### 5.1.2 Monitoring of the Assembly Process with PEGylation

The relationship between zeta potential and the amount of polyelectrolyte (PE) volume has been shown in Figure 5.3. The initial zeta potential for drug particle without any PLB16-5 (PEG and PLL (Polylysine) block copolymer PLL [16kDa]-b-PEG [5kDa]) coating is around  $-36 \pm 2$  mV with albumin coating as the outer layer. With the addition of PLB (Polyethylene glycol (PEG) solution), the zeta potential increased gradually to around  $38 \pm 2$  mV, and with the addition of negative polyelectrolyte heparin, the zeta potential decreased gradually to around  $-39 \pm 2$  mV. The amount of heparin used was a little bit larger than that of PLB (Polyethylene glycol (PEG) solution). This process can be repeated as shown in Figure 5.3. This method allowed researchers to avoid the intermediate sample centrifugation because due to step-wise polycation/polyanion addition, we were able to find the point of complete particle recharging and switched to the oppositely charged polyelectrolyte.

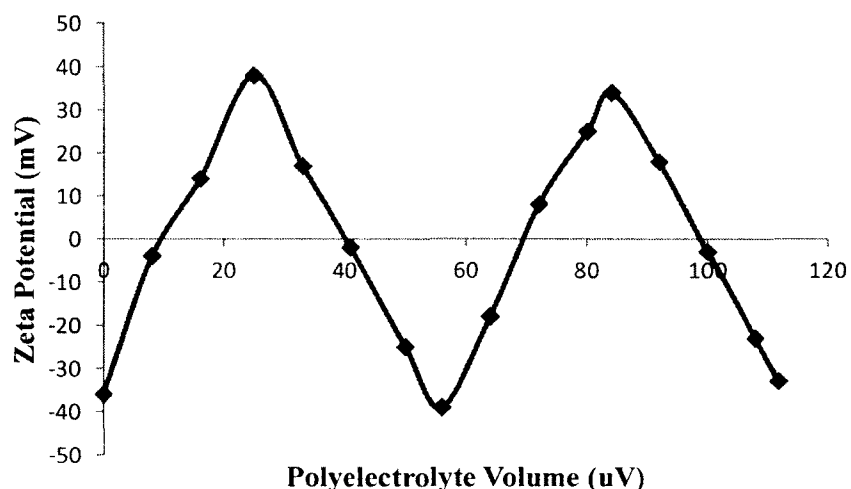


Figure 5.3 Zeta potential (y-axis, unit: mV) VS Polyelectrolyte (PE) volume (X-axis, unit: uL). Zeta potential monitoring of lapatinib drug during coating, at each point at the graph we added 0.02 mL polyelectrolytes (first cationic, then anionic, and further again cationic and anionic, following the particle recharging process), the shell composition is as follows: lapatinib/albumin/ (PLB16-5/heparin)<sub>2</sub>

## 5.2 Controlled Release Study

### 5.2.1 Concentration Study and Productivity of Our Method

In our study, we want to figure the productivity of our drug of the Layer-by-Layer coating. The most common method for detection the concentration is to use UV spectroscopy for the calibration and testament of the concentration of the drug. The calibration curve for lapatinib in DMSO is shown in Figure 5.4. The result was applied for the study of concentration of lapatinib in the solution.

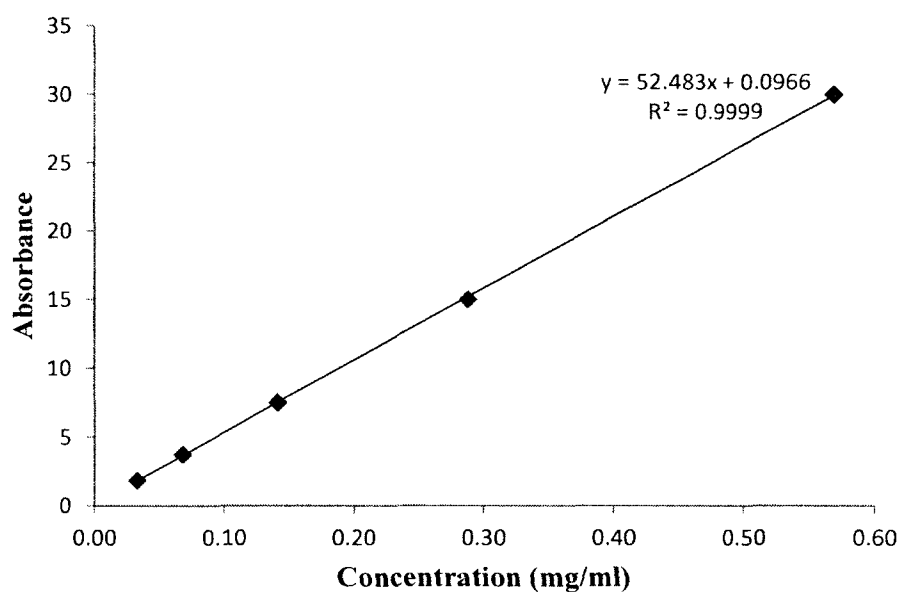


Figure 5.4 UV calibration result for lapatinib in DMSO (concentration mg/ml)

The initial lapatinib nanoparticle concentration is 0.45 mg/ml. After the Layer-by-Layer coating, final centrifugation at 12000 rpm for 10 minutes, and remove the upper liquid, re-disperse in same amount of PBS, the nanoparticle concentration is 0.25 mg/ml, which is around 56% of productivity.

### 5.2.2 Release Test for Lapatinib in PBS Buffer

Lapatinib release study in 80 mg/ml PBS-TW80:

Add 0.05 ml nano-lapatinib into 2 ml 80 mg/ml PBS TW80, test its UV absorbance. It is used as the total concentration for release in UV test.

Add 0.05 ml nano-lapatinib into 150 ml PBS-TW80 for release test. Each time take 2 ml for UV tests.

Draw the release curve according to the Absorbance data as shown in Figure 5.5.

The release time for 97.4% release is, therefore, four hours, and the release equation is a log equation:  $y=0.2735\ln(x)-0.512$ . And the confidence of this release curve is  $R^2=0.9264$ .

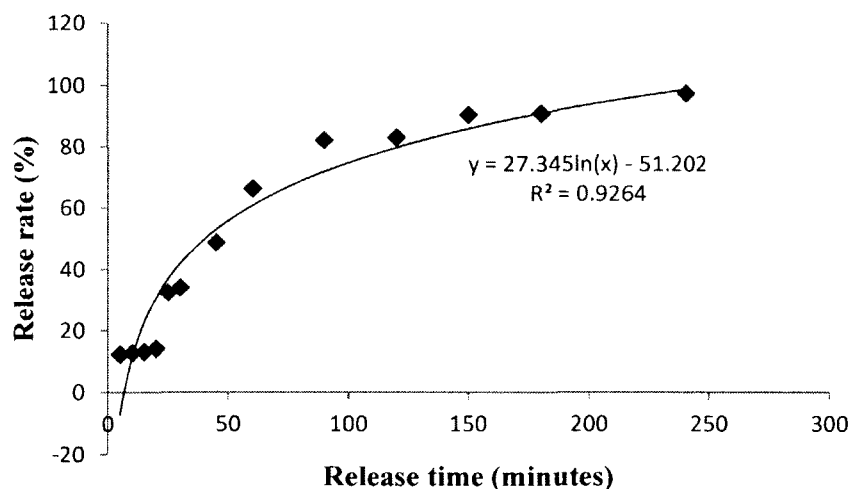


Figure 5.5 Lapatinib nanocapsule release study in 80 mg/ml PBS-TW80

### 5.2.3 Release of Drug from Different Formulation (Effect of LbL Shell)

This section was published in a paper written by the author of this dissertation in co-authorship with Dr. Lvov and others as “Top-down and Bottom-up Approaches in Production of Aqueous Nanocolloids of Low Solubility Drug Paclitaxel,” in *Physical*

*Chemistry Chemical Physics*, 2011, 13, 9014-9019. The text section cited from this paper is properly cited as [73], and they are not in use in any other dissertation.

The release profiles of original paclitaxel powder, paclitaxel nanocolloids with one polycation layer and three polycation/polyanion bilayer coating were analyzed in standard sink conditions (initial drug concentration was 2 mg/ml). The release curves fitting were done with exponential Peppas' model. Seventy percent of original paclitaxel powder was released within eight hours (Figure 5.6).

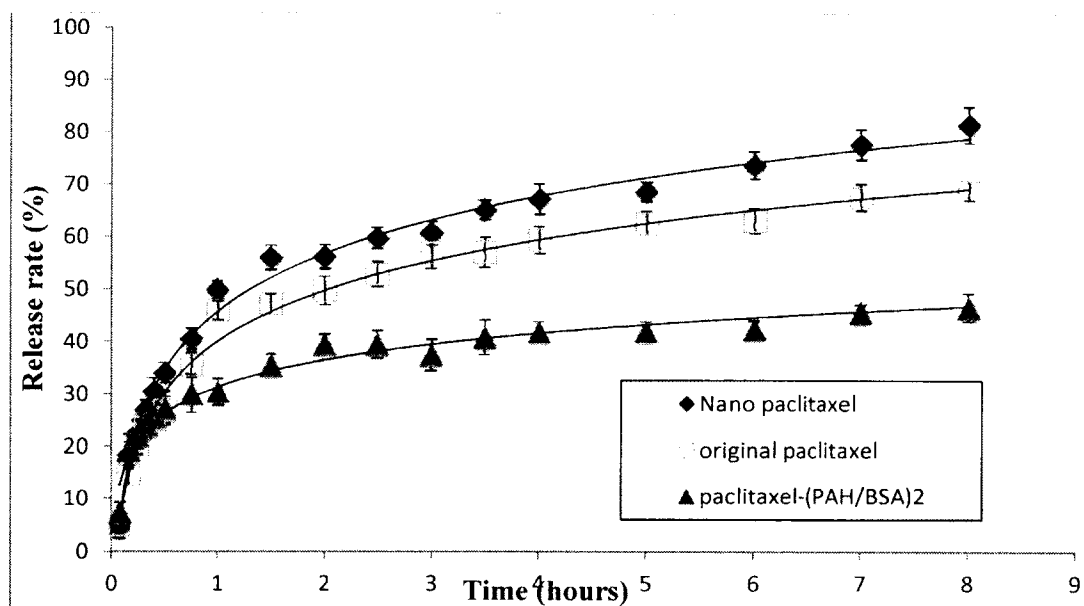


Figure 5.6 Release from paclitaxel nanocolloidal particles produced with SLbL top-down approach: PAH coating-1, original paclitaxel without coating-2, and (PAH/BSA)<sub>3</sub> coating-3 [73].

Nanoparticulated paclitaxel coated with one polyelectrolyte layer lead to slightly faster release due to smaller particle size in nanoformulation as compared with micrometer size of the original paclitaxel. Paclitaxel nanocolloids coated with three bilayers of PAH / BSA showed lower drug release rate due to increasing thickness of the capsule wall. For example, in eight hours only 40% of the two layers coated sample was released as compared with 80% for one layer coated sample. LbL technique allows for control of drug release rate from

polyelectrolytes-stabilized nanoparticles by changes the number of coating layers or the shell composition.

Under sink conditions, 50% of non-coated paclitaxel crystals (without sonication) were solubilized within two hours, while three LbL coating bilayers extended this time to more than ten hours (extrapolation). Similar release rate results were obtained for bottom-up approach in paclitaxel nanoparticulation. Paclitaxel coated with one layer of PAH after bottom-up approach (particle size was  $100 \pm 20$  nm) showed slightly faster release than top-down approach (particle size is  $220 \pm 20$  nm) due to the smaller particle size.

Conclusions: In the proposed paclitaxel and lapatinib formulation, we obtained 150-200 nm drug particles, but our nanocapsules contained high drug content of 80-90% due to very thin capsule walls (of ca 10 nm, as it was estimated from Quartz Crystal Microbalance measurements of the LbL multilayers of corresponding compositions). The drug release time from LbL capsules was found to be between 10 and 20 hours depending on the shell thickness.

## CHAPTER 6

### DUAL DRUGS ENCAPSULATION OF PACLITAXEL AND LAPATINIB

In this chapter, the preparation and characterization of dual drug paclitaxel and lapatinib is shown. In a multidrug-resistant (MDR) ovarian cancer cell line, OVCAR-3, paclitaxel/lapatinib nanocolloids mediated an enhanced cell growth inhibition in comparison with the paclitaxel-only treatment. A series of *in vitro* cell assays were used to test the efficacy of these formulations. The small size and functional versatility of these nanoparticles, combined with their ability to incorporate various drugs, indicated that paclitaxel/lapatinib nanocolloids may have *in vivo* therapeutic applications. Some sections of this chapter were published in a paper written by the author of this dissertation as “Lapatinib/Paclitaxel Polyelectrolyte Nanocapsules for Overcoming Multidrug Resistance in Ovarian Cancer,” in *Nanomedicine: Nanotechnology, Biology, and Medicine* (2011 Nov 16) [74].

Figure 6.1 shows how the drug particles are formulated (basically based on the former sonication assisted Layer-by-Layer approach) and the *in vivo* toxicity test of paclitaxel/lapatinib colloidal nanoparticles. It will be discussed in detail in the following sections of this chapter.

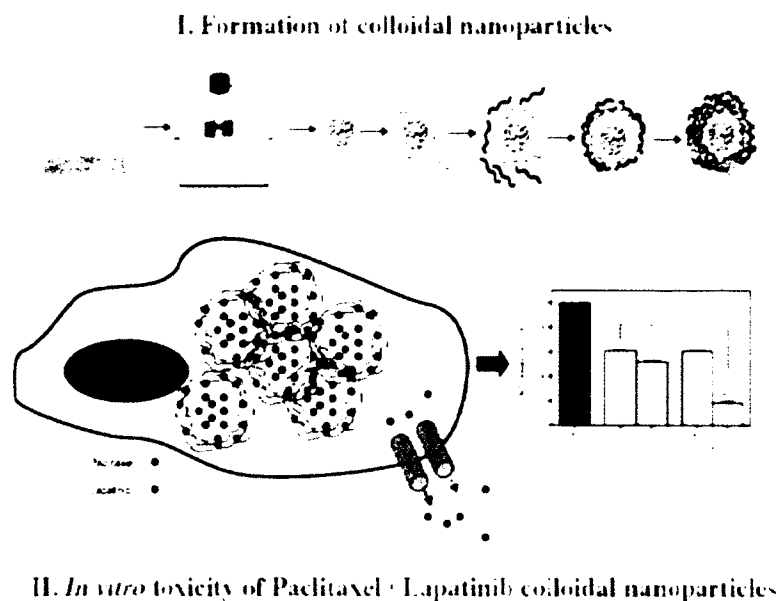


Figure 6.1 Formulation and *in vivo* toxicity test of paclitaxel/lapatinib colloidal nanoparticles [74] (The bottom left picture: red dots: lapatinib, black dots: paclitaxel. The bottom right picture is shown in Figure 6.9)

## 6.1 Introduction

Ovarian cancer is one of the most common gynaecological malignancies in women and the leading cause of gynaecological cancer-related deaths in developing countries [76]. This mortality rate is due to the lack of early symptoms for ovarian cancer that becomes clinically evident until it reaches an advanced stage. The picture is complicated by the failure of the current available therapies that are not very effective. The major obstacle is the presence of several mechanisms of drug resistance, some of which have been well described, for many of the currently chemotherapies used for the treatment of ovarian cancer including paclitaxel [77]. Paclitaxel is a drug of natural origin isolated from the bark of *Taxusbrevifolia* [78] and currently used for the treatment of ovarian cancer and breast cancer. Paclitaxel promotes microtubule assembly and stability, an effect that results in the disruption of the normal microtubule network required for mitosis.

Efforts have been made over the past years to overcome drug resistance associated with paclitaxel treatment and a number of specific factors have been identified as causes of paclitaxel resistance; however, the underlying complex mechanisms are far from fully understood. Paclitaxel resistance has been associated with the overexpression of P-glycoprotein, altered expression of specific tubulin isotypes, activation of the Toll-like receptor (TLR)-MyD88 signaling pathway and HIF-1 $\alpha$  stimulation by hypoxia [79-83].

Furthermore, paclitaxel presents a poor solubility in water and it is formulated for its current clinical administration in a mixture of Cremophor EL/absolute ethanol (50% v/v). This preparation has been associated with several side effects including nephrotoxicity and neurotoxicity [84].

To overcome toxicity, to increase bioavailability and to control drug release, several approaches for packing paclitaxel are under investigation. Since 2005, albumin-based nanoparticles were approved by the US Food and Drug Administration and, during these years, new nanoparticle formulations, such as polymeric nanoparticles, micelles, dendrimers and liposomes, demonstrated to possess numerous benefits over conventional methods and early nanoparticles products [85-88].

Among the wide panel of novel formulations under investigation, previous studies have shown that Layer-by-Layer nanoassembly technique can be used efficiently for the nano-encapsulation of poorly soluble anti-cancer drugs [72].

In particular, stable nanocolloids of paclitaxel were prepared by sonication assisted Layer-by-Layer (SLbL) self assembly technology. Under powerful ultrasonication, the air-bubble dissolved in water underwent the formation and implosion of cavity, followed by the jet flow and thus extreme physico-chemical environment was created. Drug crystals were broken into smaller and smaller particles. During this process, polyelectrolyte of opposite charge to the drug was added and absorbed onto the drug crystals through electrostatic forces:

this helps for preventing aggregation of the newly formed nanoparticles. Since the ultrasonication is based on the collapse of air-bubbles, a bubbling agent such as  $\text{NH}_4\text{HCO}_3$  was mixed with the polyelectrolyte to increase the intensity of ultrasonication [72]. By this method, drug nanoparticles around  $150 \pm 50$  nm in size were achieved. Generally speaking, initial drug particles are negative in charge. After the first polyelectrolyte coating (in this case, polycation), the surface potential becomes positive. Then a second layer polyelectrolyte (in this case, polyanion), was coated and the surface charge reversed back to negative. This surface charge reversal can be repeated several times to demonstrate the successful coating of different polyelectrolyte layers which can build up such architecture and maintain properties such as controlled release by tailoring layers composition and number. The Layer-by-Layer self assembly technology can also be applied for combining two drugs in one nanocolloid system for enhancing synergistically drug efficiency [73].

For all these reasons, we hypothesized that paclitaxel clinical efficacy can be increased through a strategy that combines improvements in paclitaxel cellular delivery and combination of targeted therapies to inhibit one or more signalling pathways involved in paclitaxel resistance. Of all these mechanisms of drug resistance, overexpression of P-glycoprotein (P-gp), a member of the ATP-binding cassette (ABC) transporters [89], has been associated with a poor response to chemotherapy [90]; therefore, its impairment is likely to have a significant impact on paclitaxel clinical action. However, until now, many P-gp inhibitors failed during pre-clinical and clinical studies [91]. Recently, lapatinib, an epidermal growth factor receptor (EGFR) and Erb-2 dual tyrosine kinase inhibitor have been shown to inhibit the function of ABC transporters including P-gp [92].

In this work, the efficacy of paclitaxel-loaded nanocolloid formulations has been tested in two ovarian cancer cell lines *in vitro* compared to that of paclitaxel given alone.

Furthermore, a co-therapy strategy which results from the combination of paclitaxel and lapatinib in nanocolloids showed to be very effective in enhancing paclitaxel efficacy.

Overall, results of this study showed that paclitaxel-nanocolloids increased antitumor efficacy of paclitaxel and that the combination with lapatinib, can significantly overcome multidrug resistance in ovarian cancer cell lines. These results are encouraging for the development of multifunctional nanocolloids that could be used in the clinical practice.

## **6.2 Methods**

### **6.2.1 Preparation of Nanocolloids**

To build up the nanocapsules for a simultaneous controlled release of two drugs, we used a SLBL technique. Biodegradable chitosan (polycation) and alginic acid (polyanion) were chosen for a biocompatible and biodegradable coating on drug NPs.

A Heilscher UIP 1000hd Ultrasonicator (Germany) was applied at its maximum power ( $15 \text{ Wcm}^{-2}$ ) to break the drug colloid into smaller nanoparticles. Water/ ice mixture was used for the cooling of the beaker with drug particles under the powerful ultraasonicator to prevent overheating and oxidation of the drug.

#### 1) Paclitaxel samples.

Paclitaxel (40 mg), chitosan (6 mg) (MW=2500) and  $\text{NH}_4\text{HCO}_3$  (40 mg) were added to 30 ml De-Ionized (DI) water, stirred for five minutes and then sonicated in water/ice bath for 45 minutes (to make paclitaxel/chitosan). After 45 minutes, six ml alginic acid solution (one mg/ml) was added in during sonication; sonicated for 25 minutes (to make paclitaxel /chitosan/ alginic acid).

The coating process of chitosan and alginic acid were repeated to make (paclitaxel/chitosan/alginic acid/chitosan/alginic acid /chitosan/alginic acid) nanocolloid.

2) Paclitaxel/lapatinib dual drug nanocolloids preparation: (paclitaxel/chitosan/alginate acid/chitosan/lapatinib/chitosan/alginate acid).

Paclitaxel (40 mg), chitosan (6 mg) and  $\text{NH}_4\text{HCO}_3$  (40 mg) were added in 30 ml De-Ionized (DI) water, stirred for five minutes and then sonicated in water/ice bath for 45 minutes (to make paclitaxel/chitosan complex). After 45 minutes, 6 ml alginate acid solution (1 mg/ml) was added during sonication for 25 minutes (to make paclitaxel/chitosan/alginate acid). Six milliliter of 1 mg/ml chitosan solution was added, and then sonicated for 25 minutes (to make paclitaxel/chitosan/alginate acid/chitosan). Lapatinib solution (20 ml, 0.5 mg/ml) was added for sonication for 25 minutes (to make paclitaxel/chitosan/alginate acid/chitosan/lapatinib). Chitosan (6 ml, 1mg/ml) solution was added under sonication for 25 minutes (to produce paclitaxel/chitosan/alginate acid/chitosan/lapatinib/chitosan). Six milliliter of AA solution (in 1 mg/ml concentration) was added, and then sonicated for 25 minutes (to make paclitaxel/chitosan/alginate acid/chitosan/lapatinib/chitosan/alginate acid). Samples were centrifuged at 2000 rpm for 20 minutes to remove lower solid. The samples were then centrifuged at 10000 rpm for 10 minutes to remove upper liquid.

### 6.2.2 Cell Viability Assay

Cells were seeded at a density of  $5 \times 10^3$  per well in a 96-well plate containing 100  $\mu\text{l}$  of full medium and allowed to adhere to the plate overnight. For determining cell viability, the MTT assay was used. After treatment with paclitaxel or LbL-paclitaxel nanocolloids for 24 hours, the culture medium was aspirated and 100  $\mu\text{l}$  of fresh medium containing 10  $\mu\text{l}$  of MTT solution (stock five mg/ml in PBS) was added to each well. Cells were then incubated for further two to three hours. After removal of MTT solution, 100  $\mu\text{l}$  of DMSO were added to the wells maintained in agitation for 15 minutes. Absorbance of the converted dye was measured at a wavelength of 570 nm with background subtraction at 690 nm. The relative cell viability was expressed as a percentage of the untreated control wells.

### 6.2.3 Reverse Transcription-PCR

Total cellular RNA was isolated by IllustratriplePrep extraction kit following manufacturer's instruction and immediately used. Purified DNA and protein pellets were stored at -80° C for further analysis.

Reverse transcription polymerase chain reaction was then performed by using the High Capacity RNA-to-cDNA Master Mix (Applied Biosystem). Approximately one µg of total RNA was converted to cDNA.

PCR was conducted on a MyCycler thermal cycler (Bio-Rad). The final volume of 25 µl included one µl of cDNA template, 12.5 µl of PCR Master Mix (Promega), and one µl of a mix containing primers.

The primers used for PCR amplification were designed using the Primer blast program (<http://www.ncbi.nlm.nih.gov/tools/primer-blast/>) and were as follows: Cofilin sense 5' GTGGGCGATGTGGGCCAGAC 3', antisense 5' CCAGGGTGCAGCGGTCCTTG 3' (280 base pairs, bp, Tm 60°); Cyclin D1 sense 5' CGCTTCCTGTCGCTGGAGCC 3', antisense 5' CTTCTCGGCCGTCAGGGGA 3' (111 bp, Tm 60°); GAPDH sense 5' GCATGGCCTTCCGTGTCCCC 3', antisense 5' CAATGCCAGCCCCAGCGTCA 3' (216 bp, Tm 60°).

PCR was carried out using the following conditions: denaturation at 95 °C for 30 s, annealing at 60 °C for 30 s, and extension at 72 °C for 45 s. PCR samples were loaded onto a 1.2 % agarose gel containing ethidium bromide and analysed. All PCR experiments were run in triplicate. GAPDH was used as an internal loading control.

### 6.2.4 Immunoblotting Assay

Proteins were extracted in RIPA buffer (50 mM Tris-base, 150 mM NaCl, 0.1% SDS, 1% Triton X-100, 0.5% sodium deoxycholate, one mM sodium orthovanadate, 10 mM sodium fluoride, 1% protease inhibitor cocktail) and lysates were clarified by centrifugation at

13000 g for 15 minutes at 4°C. Protein concentration was determined using the Bradford protein assay. Proteins (50 µg) were separated on 10% polyacrylamide gel and transferred to nitrocellulose membranes (Amersham Biosciences). The membranes were blocked overnight in 5% non-fat milk in TBST buffer (Tris Buffer Saline and 0.1 % Tween 20) at 4°C under agitation, and subsequently probed by the appropriately diluted primary antibodies in blocking buffer. The blots were then incubated with HRP-conjugated secondary antibody for two hours at room temperature. Target proteins were detected by enhanced chemiluminescence reagents and visualized on Hyperfilm ECL films (Amersham).

#### 6.2.5 Confocal Microscopy

Exponentially growing ovarian cancer cells were seeded on 25 mm square glass cover slips placed in 35 mm diameter culture dishes. After treatment, cells were fixed for five minutes with 3.7% formaldehyde in phosphate-buffered saline (PBS) solution, permeabilized with a 0.1% solution of Triton X-100 in PBS, and incubated for 30 minutes at room temperature with phalloidin-TRITC (Sigma) (one µg/ml in PBS from one mg/ml DMSO stock solution). After that, cells were washed three times in PBS. The preparations were mounted in 50% glycerol in PBS. Images were acquired by laser confocal microscopy using a TCS SP5 (Leica Microsystem GmbH, Mannheim, Germany).

#### 6.2.6 Statistical Analysis

Statistical analysis was performed using GraphPad Prism 4.1 (GraphPad Software, San Diego, CA, USA). Differences between group means were compared by Student's t-test. Student's t-test was used for the statistical analysis of RT-PCR and western blot data. Data are presented as mean ± standard error of the mean (s.e.m.). A probability level of  $P < 0.05$  was considered significant.

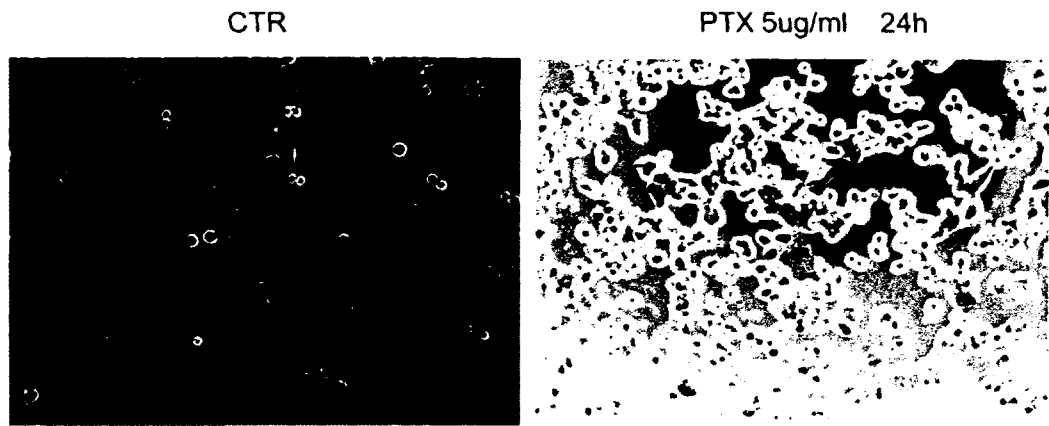
### 6.3 Results

The aim of this study is to develop new strategies based on nanocolloids technology to overcome multiple drug resistance (MDR) associated with paclitaxel in ovarian cancer. Preliminary experiments were performed to identify cellular targets of paclitaxel action. The identification of these targets will be useful as markers of nanocolloids action respect to paclitaxel alone.

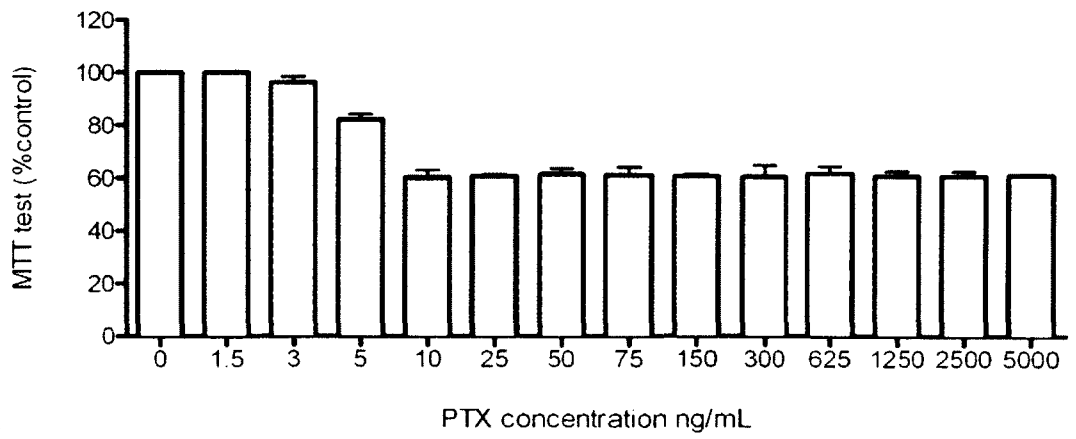
An ovarian cancer cell line, OVCAR-3, was chosen for its drug-resistance phenotype and used as model system in this study. The MDR phenotype of this cell line was confirmed by the presence at mRNA level of TLR4 and P-glycoprotein (P-gp) (Figure 6.2 E), which were associated with paclitaxel chemoresistance [79, 81-82]. The expression levels of these mRNA. MDR1 mRNA is greatly expressed in OVCAR-3 with respect to MCF-7 while no significant differences were observed for TLR-4.

The over-expression of the glycoprotein P-gp, a member of the ATP-binding cassette (ABC) protein family, has profound implications in the clinical practice. In fact, the presence of drug efflux pumps that mediate the active efflux of chemotherapeutics is one of the most extensively described mechanisms of drug resistance and strategies to modulate or blocking this process that have been investigated actively in oncology [93]. In ovarian cancer, P-gp overexpression at the mRNA and protein level has been implicated in chemoresistance, correlated inversely with patient survival and associated with resistance to paclitaxel [94-96].

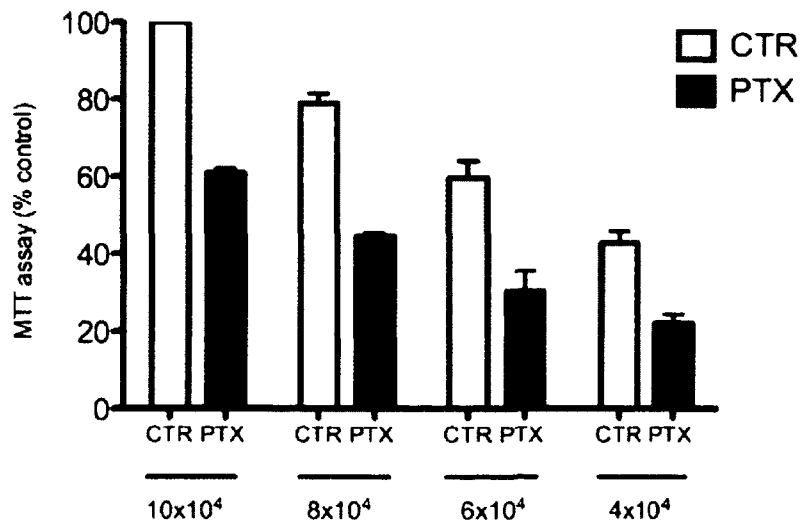
Dose-response studies highlighted the resistant nature of this cell line (Figure 6.2 B). Exponentially growing OVCAR-3 cells were exposed to increasing concentration of paclitaxel (from 1.5 ng/ ml to 5000 ng/ ml) for 24 hours and MTT cell viability assay was performed. As shown in Figure 6.2, the cancer cell line exhibited a characteristic dose-response curve, in fact, treatment with paclitaxel at concentration above 10 ng/ml did not induce a proportional reduction of cell viability.



A)



B)



C)

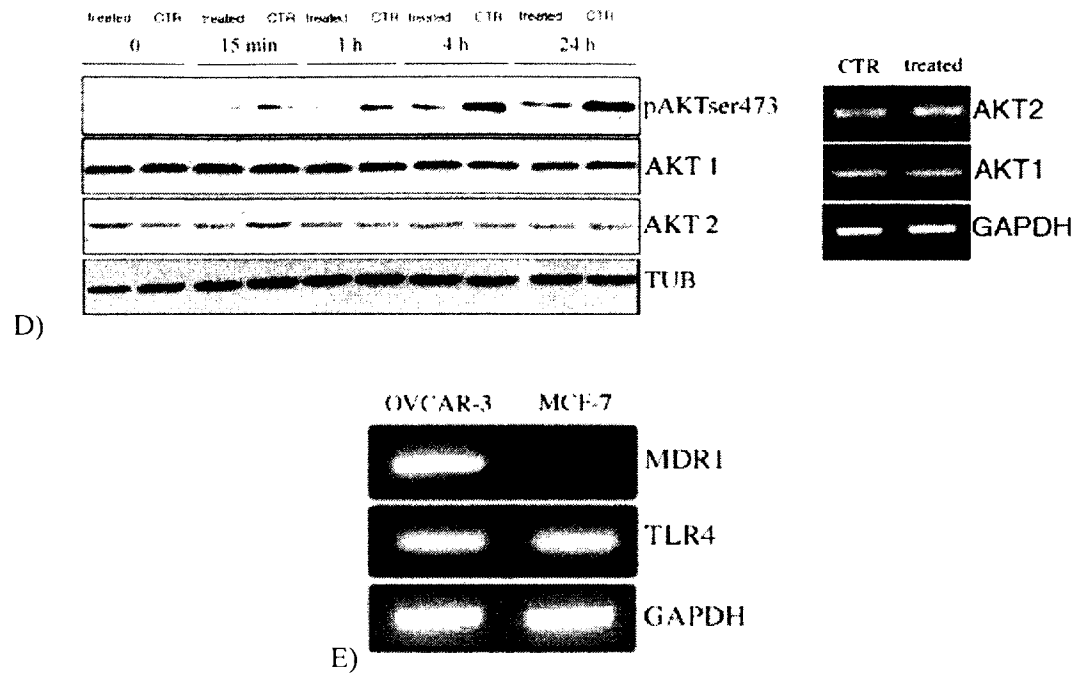


Figure 6.2 Paclitaxel inhibits cell growth of OVCAR-3 cells

A) Evaluation of the effects of paclitaxel on OVCAR-3 cell morphology using phase-contrast microscopy after 24 hours of incubation (magnification 10 x). Cell death was observed after paclitaxel treatment as evidenced by the increasing number of floating cells. B) Paclitaxel reduces cell viability. OVCAR-3 were seeded overnight into 24-well plates and incubated with paclitaxel at the indicated concentrations. After 24 hours, cell viability was detected by MTT test. OVCAR-3 demonstrated a plateau in survival at concentrations of paclitaxel above 5 ng/ml. Values are mean  $\pm$  s.e.m. of three independent experiments performed in triplicate. C) Paclitaxel reduces cell viability. OVCAR-3 were seeded overnight into 24-well plates at the indicated concentrations and incubated with paclitaxel for 24 hours at 5  $\mu$ g/ml. The response of OVCAR-3 to paclitaxel is independent of the number of cell seeded. Values are mean  $\pm$  s.e.m. of three independent experiments performed in triplicate. D) Paclitaxel reduces Akt phosphorylation at ser 473. OVCAR-3 cells were cultured in DMEM media supplemented with 10% FBS for 24 hours followed by starvation for 12 hours in serum-free media. Cells were switched to the media in the absence (CTR) or presence (treated) of paclitaxel 5  $\mu$ g/ml for 15 minutes, 1 hour, 4 hours and 24 hours, respectively. The whole cell lysates were prepared, and western blotting was performed as described in the Materials and Methods. Blots were stripped and re-probed with total Akt isoforms. The level of tubulin was used to indicate relative amounts of protein loaded. Experiments were performed three times and blot is a representative of one independent experiment. (Right) paclitaxel effects on the expression of Akt 1, Akt 2. RT-PCR showed mRNA levels of Akt isoforms after paclitaxel treatment. The expression of GAPDH is shown as internal control. E) Expression of MDR1 and TLR4 measured by RT-PCR in untreated OVCAR-3 and MCF-7 cells. The expression of GAPDH is shown as internal control.

Comparable findings were obtained in a similar experiment, in which the drug concentration was maintained fixed and the number of cell seeded on the plate was changed (Figure 6.2 C). Ovarian cancer cells seeded at four different concentrations and treated with paclitaxel at 5 ng/ml for 24 hours showed a similar survival ratio between control and treated cells. This result means that cytotoxicity due to paclitaxel is less dependent on the concentration of the drug at concentrations above 10 ng/ml. In the case of OVCAR-3, the IC<sub>50</sub> could not be determined because even at concentrations of paclitaxel upper than 20 ng/ml more than 50% of the cells remained viable (data not shown). In contrast, an IC<sub>50</sub> of 100-200 ng/ml has been determined by MTT (data not shown) for MCF-7 (drug sensitive) cells suggesting that the multidrug resistance transporter MDR-1 is associated with resistance to paclitaxel in OVCAR-3.

In recent years, the phosphatidylinositol 3-kinase (PI3K)/Akt pathway has risen to prominence as a regulator of cell survival and growth in many different cell types. In ovarian cancer, constitutive Akt activity or gene amplification was frequently detected in tumor samples and associated with chemoresistance and poor prognosis [97, 98]. Akt promotes cell survival and growth through a variety of mechanisms, including the regulation of proapoptotic proteins Bad and caspase-9 and cyclin D1 expression [97].

To determine the effects of paclitaxel on this signaling pathway, an experiment of western blot was conducted to investigate the phosphorylation status of Akt ser 473 after paclitaxel treatment. Ovarian cancer cell lines were grown under normal conditions and were deprived of serum overnight. Cells were then treated or not (control) with paclitaxel in presence of serum. Western blot analysis showed that levels of pAkt ser 473 were reduced compared to those in control cells that, on the contrary, increase when stimulated with serum at the indicated times (Figure 6.2 D).

No differences were noted in the levels of total Akt 1 and Akt 2 isoforms at both mRNA and protein levels, suggesting that paclitaxel-regulation of this pathway results largely from post-transcriptional regulation.

To investigate whether the encapsulation of paclitaxel in nanocolloids leads to a general improvement of the efficacy of the drug, we assayed the cytotoxicity of the LbL-paclitaxel toward the OVCAR-3 cell line and compared the results with that of paclitaxel free.

To assess this point, two types of LbL-nanocolloids were fabricated and tested: paclitaxel-chitosan and paclitaxel-chitosan-alginate. In particular, chitosan is a positively charged natural carbohydrate polymer with minimal toxicity that shows strong electrostatic interaction with the negatively charged mucosal surface [98]. Chitosan has been largely used as biomaterials and the much higher expression of mucin, heavily glycosylated extracellular protein, in ovarian tumors compared to the surrounding normal tissue [99] can provide a rationale for using chitosan as delivery system in ovarian tumors. Both preparations were tested on ovarian cancer cells for their ability to increase paclitaxel efficacy. The results obtained by MTT test were comparable for the two types of nanocolloids, and for this reason, we will use the general name of LbL-paclitaxel nanocolloids to design both formulations. As shown in Figure 6.3, paclitaxel and LbL-paclitaxel have a similar trend of cytotoxicity in ovarian cells with a higher cytotoxicity for LbL-paclitaxel than paclitaxel alone. It should be noted that, since cells incubated for 24 hours with empty LbL-nanocolloids (drug free) does not show any significant difference in cell viability compared to control cells. We exclude a role of empty nanocolloids to explain the difference between paclitaxel and LbL-paclitaxel.

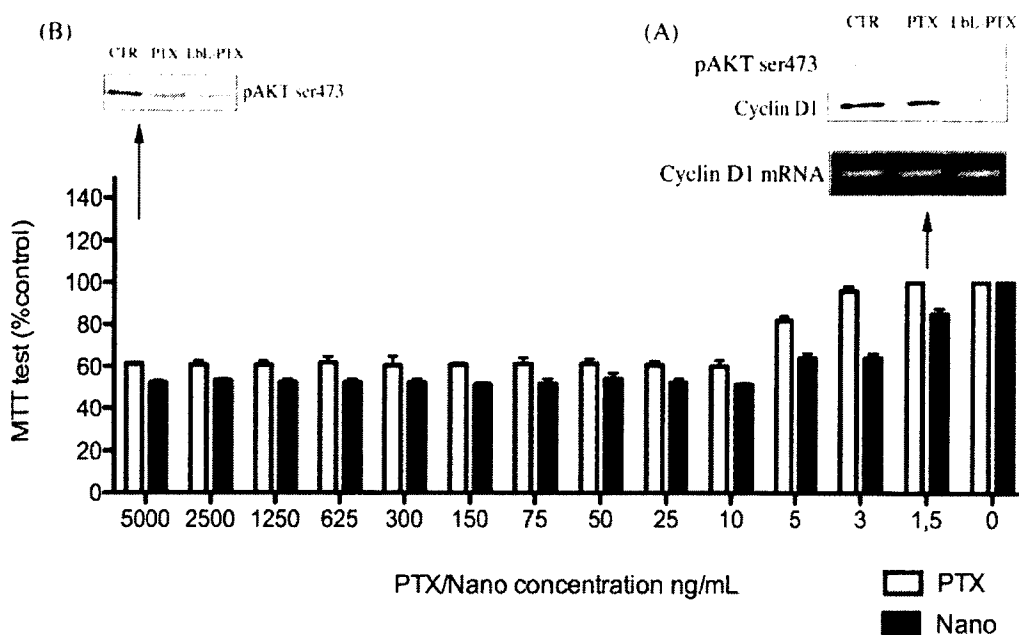


Figure 6.3 Citotoxic effect of LbL-paclitaxel nanocolloids on OVCAR-3 and SKOV-3 cancer cells and regulation of pAkt ser 473 and cyclin D1 expression

Citotoxic effect of paclitaxel alone or LbL-paclitaxel nanocolloids at the indicated concentrations was measured by the MTT assay as described in Section 6.2. Control cells were treated with paclitaxel free or paclitaxel-LbL nanocolloids. Values are mean  $\pm$  s.e.m. of three independent experiments performed in triplicate. The cell viability is related to control wells treated with vehicle (DMSO) or empty LbL-nanocolloids (drug free).

Regulation of pAkt ser 473 and cyclin D1 by paclitaxel or LbL-paclitaxel nanocolloids: Ovarian cancer cells were treated with paclitaxel or LbL-paclitaxel nanocolloids at the concentration of 1.5 ng/ml for 24 hours. Whole cell lysates (50  $\mu$ g in each lane) were subsequently subjected to western blotting analysis with antibodies to pAkt ser 473 and cyclin D1. RT-PCR analysis of cyclin D1 mRNA expression levels was performed as described in Section 6.2.

Moreover, we observed that the treatment of ovarian cancer cells with LbL-paclitaxel results in cell growth inhibition at the concentration of 1.5 ng/ml where the same concentration of paclitaxel free does not affect cell viability.

Comparison of ovarian cancer cells treated with LbL-paclitaxel and paclitaxel at the concentration of 1.5 ng/ml revealed a down-regulation of pAkt ser 473 only for LbL-paclitaxel treated cells. Akt pathway is known to play a pivotal role in the regulation of cyclin D1 expression in ovarian cancer cells [100]. Therefore, we examined if paclitaxel or LbL-paclitaxel nanocolloids regulate cyclin D1 expression. After 24 hours of treatment at the concentration of 1.5 ng/ml only LbL-paclitaxel nanocolloids were able to decrease cyclin D1 protein level. Cyclin D1 mRNA level remains unaffected after treatment suggesting the regulation at the protein level.

We next determined if increased LbL-paclitaxel nanocolloids cytotoxicity respect to paclitaxel free could be explained by a higher down-regulation of the Akt pathway. Western blot analysis of pAkt ser 473 from ovarian cells treated with paclitaxel and LbL-paclitaxel nanocolloids at five  $\mu\text{g/ml}$  showed a significant difference in the pospho-protein level in control with respect to treated cells with a further down-regulation in LbL-paclitaxel treated samples (Figure 6.3 B), a finding that correlates with the increased cytotoxicity of nanocolloids compared to paclitaxel free.

The enhanced cytotoxicity of drug-nanoparticles could be explained considering the different mechanisms of drug-nanocolloids uptake compared to paclitaxel free. Several mechanisms have been described including the increased accumulation of the nanoparticles in the cells and their entrapment in the endosomes/lysosomes rendering the drug inaccessible for P-gp [101].

A possible link between the activation of PI3K/Akt pathway and actin remodeling has been described [102-103]. It has been shown that PI3K/Akt pathway induced cell migration

through the remodeling of actin filaments and that actin is a cellular target of this kinase [104-105]. It is possible that the involvement of this pathway in paclitaxel action could have consequences on the organization of actin cytoskeleton after paclitaxel treatment. TRITC-phalloidin staining of F-actin followed by confocal microscopy analysis revealed some differences in the cell shape and organization of actin filaments for paclitaxel free and LbL-paclitaxel cells compared to control (Figure 6.4 A). Not treated cells show regular shaped bodies, with a readily visible actin staining in the periphery, actin protusions (yellow arrows, Figure 6.4 A) and the absence of bundles of actin filaments. Rounded cells appeared after paclitaxel treatment together with the formation of blebs (green arrows, Figure 6.4 A). No actin protusions are more visible in treated cells. Furthermore, a more distinct net of actin filaments is visible in the cytoplasm of OVCAR-3 treated with LbL-paclitaxel nanocolloids.

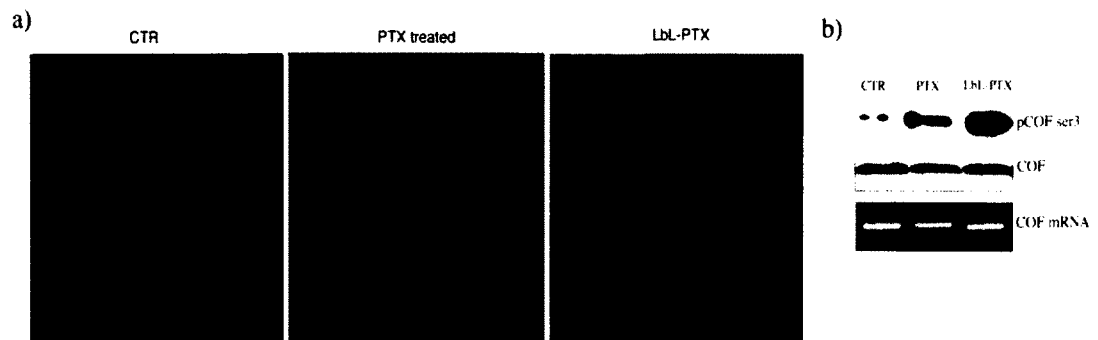


Figure 6.4 Effects of paclitaxel or LbL-paclitaxel nanocolloids on actin cytoskeleton: (A) Ovarian cancer cells plated on glass coverslips were treated with paclitaxel or LbL-paclitaxel nanocolloids at the concentration of 5  $\mu\text{g}/\text{ml}$  for 24 hours and then fixed. Cells were stained with TRITC-phalloidin. (B) The phosphorylation status of cofilin at ser 3 was assessed with a phosphospecific antibody, and then the blot was reprobred for total cofilin levels. The mRNA level of cofilin was assessed by using a specific set of primer.

The organization of actin filaments is governed by a plethora of proteins that regulate the rate of actin polymerization. One of the key proteins in this scenario is cofilin, which can regulate the rate of actin-filament turnover and the net polymerization of actin. In particular,

actin dynamics is regulated by phosphorylation of cofilin at serine, which renders phospho-cofilin inactive towards F-actin [106]. We examined by western blot the phosphorylation status of cofilin after paclitaxel or LbL-paclitaxel nanocolloids treatment. As shown in Figure 6.4 B, cofilin phosphorylation increased after paclitaxel treatment and, in particular, after the exposure with LbL-paclitaxel. This result is consistent with the morphological actin-changes observed by confocal microscopy and raises questions about the role of the actin cytoskeleton in mediating paclitaxel sensitivity. Moreover, the significant effect of LbL-nanoparticles on cofilin phosphorylation will prompt us to investigate the role of actin cytoskeleton in mediating the uptake the LbL-nanoparticles into OVCAR-3 cells.

In summary, the Akt pathway is a target of paclitaxel and LbL-paclitaxel action; the modulation of this pathway after paclitaxel treatment can affect the cell growth as observed by MTT.

Moreover, LbL-paclitaxel nanocolloids lower the minimum dose necessary to obtain a significant reduction of cell viability an issue that can be important for future possible application *in vivo* in order to minimize the cytotoxicity and adverse side effects associated with paclitaxel. On the other hand, although the cell growth inhibition of paclitaxel free and LbL-paclitaxel nanocolloids reached a statistical difference, nanocolloids did not produce a sustained growth inhibition in ovarian cancer cells suggesting that LbL-paclitaxel nanocolloids are susceptible to efflux by P-gp. Thus, the combination with an interrelated drug is required to optimize the therapeutic activity of nanoparticle-encapsulated drug.

In search for novel strategies to overcome resistance of ovarian tumor cells, we tested the cytotoxic activity of paclitaxel in combination with two small molecule chemical inhibitors, UO126, an extracellular signal-regulated kinase (ERK) 1/2 inhibitor, and LY29004, a PI3K inhibitor. Both signal-pathways have been described and well characterized for their role in drug-resistance [97, 107].

In addition, the combination with lapatinib, an inhibitor of the intracellular tyrosine kinase domains of both the EGFR and Her-2 receptors, was further explored to increase the cytotoxic efficacy of paclitaxel. The combination of lapatinib with paclitaxel has been explored in the clinical practice. In fact, clinical trials demonstrated the efficacy of lapatinib and paclitaxel in HER-2-positive locally advanced or metastatic breast cancer [103]. Moreover, the ability of lapatinib to reverse multidrug resistance due to ABCB1 and ABCG2 transporters, including P-gp, has been recently described with the potential to increase the cytotoxic effects of several chemotherapeutic drugs including paclitaxel [108]. This finding supports the idea to combine paclitaxel and lapatinib in our cell line that shows a high expression of P-gp. As shown in Figure 6.5, an improvement of paclitaxel efficacy is obtained when the drug is administrated in combination with the ERK 1/2 inhibitor UO126, suggesting that this pathway may play a role in the generation of paclitaxel resistance, and a greatly enhanced of paclitaxel efficacy is obtained in combination with lapatinib. On the contrary, there are no significant differences in cell viability between cells treated with LY29004 alone or with LY29004 plus paclitaxel suggesting that LY29004 alone is the major determinant of the observed decrease in cell viability.

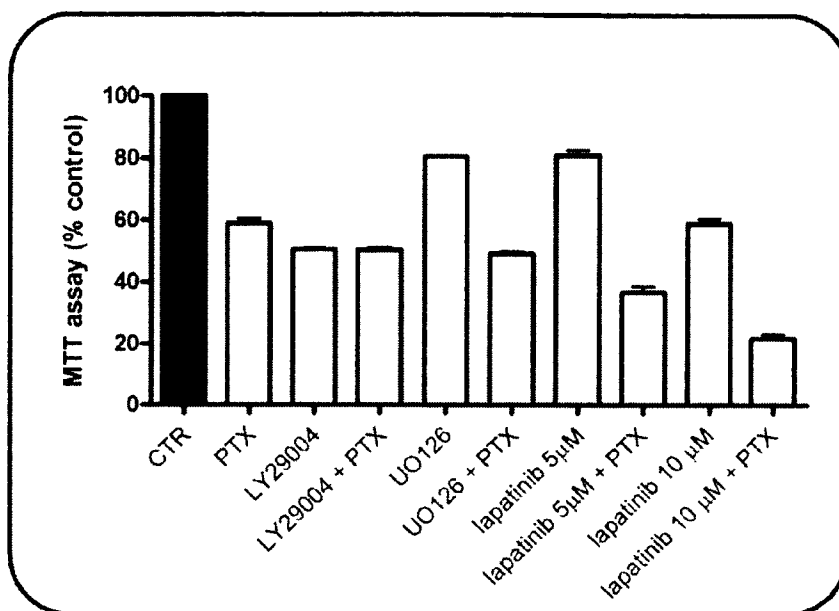


Figure 6.5 MTT test was used to test the efficacy of paclitaxel in combination with the ERK 1/2 inhibitor UO126, the PI3K inhibitor LY29004 and the drug lapatinib. MTT test was performed as described in Materials and Methods. Ovarian cancer cells were grown on 96-well plates and treated for 24 hours at the following concentration of chemicals: paclitaxel 5 µg/ml, UO126 and LY29004 at 10 µM and lapatinib at 5 µM and 10 µM. Values are mean  $\pm$  s.e.m. of three independent experiments performed in triplicate

Next, we determined if the therapeutic potential of LbL-paclitaxel nanocolloids could be further increased by the co-delivery of paclitaxel and lapatinib. For this purpose, nanocolloids containing paclitaxel and lapatinib were prepared by LbL-technology. As shown in Figure 6.6, the particle size of paclitaxel with one layer coating was  $125 \pm 50$  nm, much smaller as compared with several micrometers of original paclitaxel powder. We monitored the Layer-by-Layer coating process using the zeta potential analyzer (Figure 6.8 (a)), light scattering machine (Figure 6.8 (b)) and SEM (Figure 6.7). These results show that the consecutive coating process had been successful. After Layer-by-Layer coating with biocompatible and biodegradable layers of chitosan, alginate acid and lapatinib, the particle diameter was around 250 nm. Such architectural nanocapsules allowed dual delivery of these two drugs.

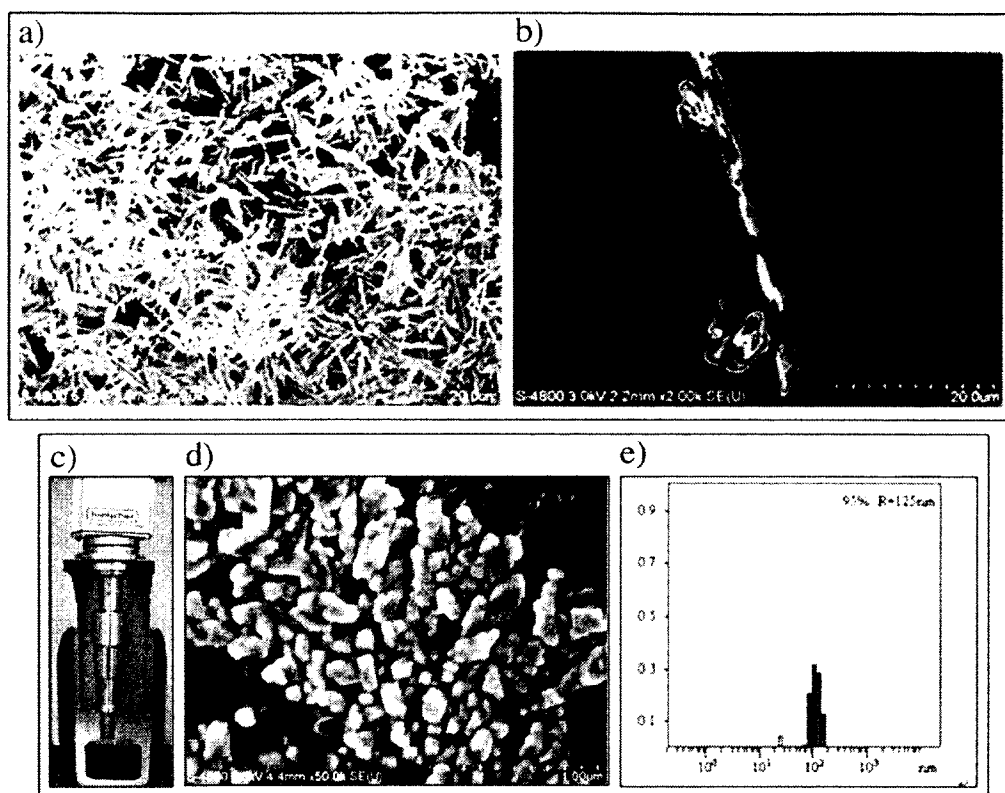


Figure 6.6 SEM images of paclitaxel (a) and lapatinib (b) before treatment. Ultrasonication assisted coating of first layer on paclitaxel: (c) Sonicator, (d) SEM image, (e) Light scattering result

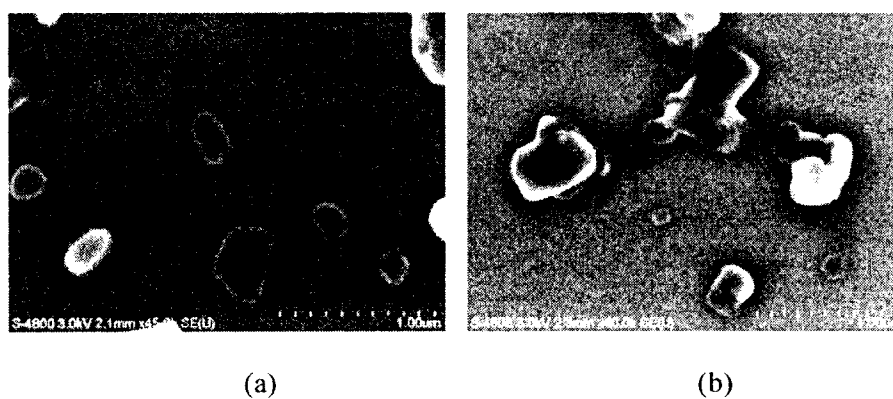


Figure 6.7 SEM image of Layer-by-Layer coating of paclitaxel nanoparticles: (a) paclitaxel-(chitosan-alginate)<sub>3</sub> and (b) paclitaxel-(chitosan-alginate)<sub>3</sub>-lapatinib-alginate

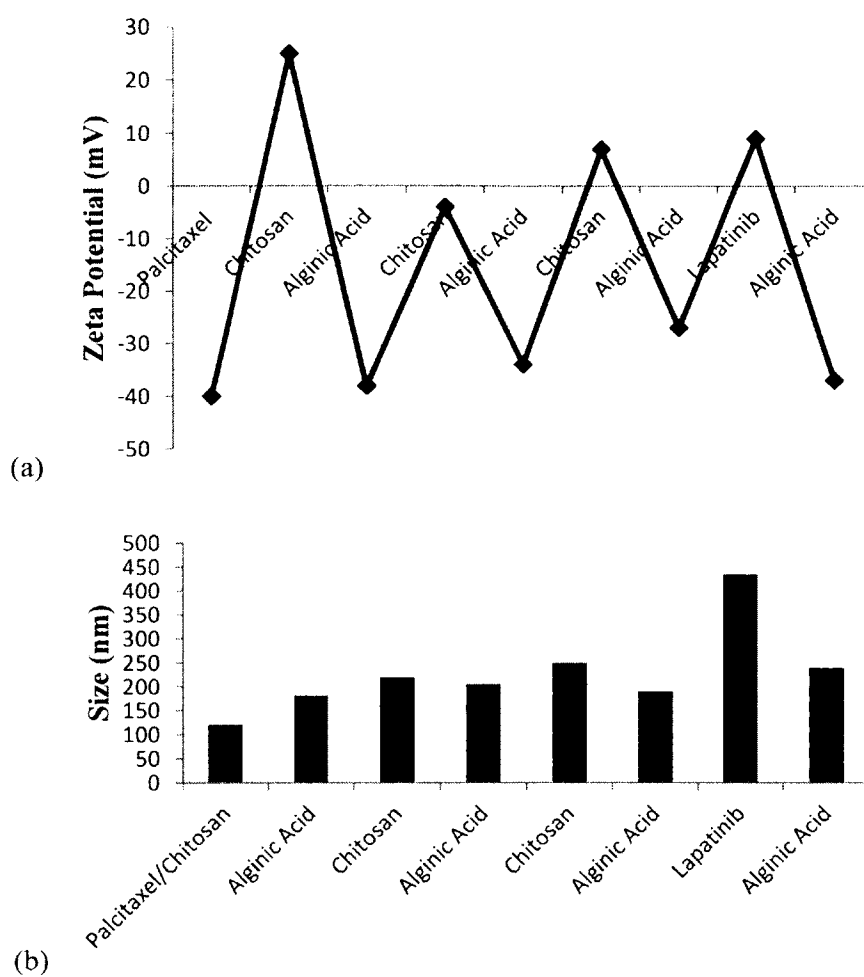


Figure 6.8 Layer-by-Layer coating of paclitaxel nanoparticles: (a) Zeta-potential and (b) Diameter as a function of coated layers

Results obtained by MTT test confirmed the enhanced cytotoxic activity of this nanopreparation compared to paclitaxel free and LbL-paclitaxel (Figure 6.9).

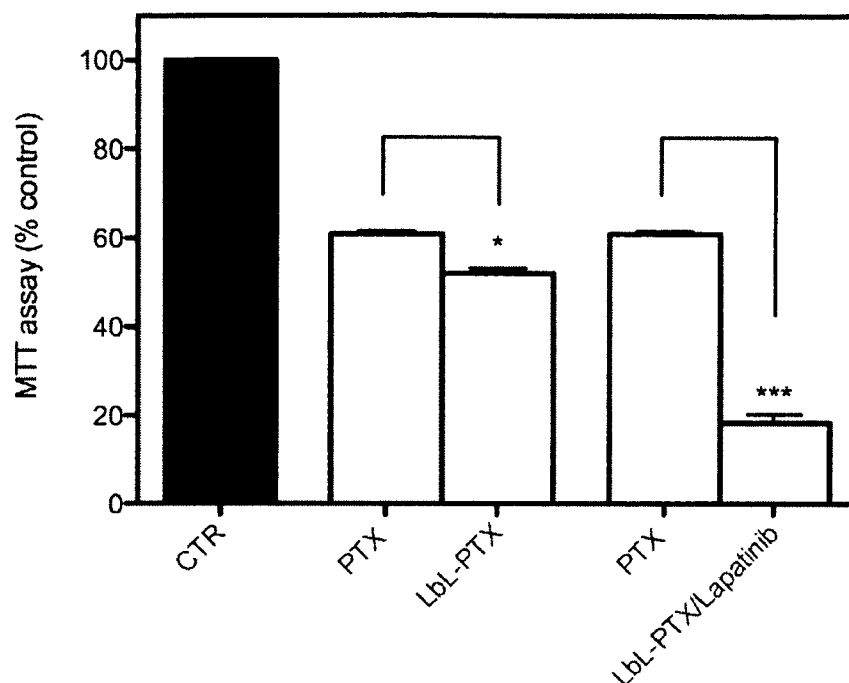


Figure 6.9 LbL-paclitaxel/lapatinib nanocolloids demonstrate significant cytotoxic activity in P-gp overexpressing ovarian cancer cells as determined by MTT test. Values are mean  $\pm$  s.e.m. of three independent experiments performed in triplicate ( $p < 0.05$  \*;  $p < 0.01$  \*\*;  $p < 0.001$  \*\*\*).

#### 6.4 Discussion

Ovarian cancer still remains one of the most fatal malignancies among women. Improving the efficacy of current therapeutics will have a great impact in the management of the disease. Paclitaxel is widely used for the treatment of patients with ovarian cancer, but despite substantial clinical efficacy the optimal administration regimen remains elusive. Many questions remain concerning the way to administer the drug and the molecular mechanisms at the basis of chemoresistance.

Among the proteins related to the chemoresistance process, the overexpression of P-gp has profound implications in clinical practice. In fact, the presence of drug-efflux pumps that mediate the active efflux of chemotherapeutics is one of the most extensively described

mechanisms of drug resistance, and strategies to modulate or block this process have been investigated actively in oncology [111]. In ovarian cancer, the expression of P-gp has been implicated in chemoresistance, correlated inversely with patient survival and associated with resistance to paclitaxel [102-114].

These observations set the stage for the development of efficacious instruments to increase paclitaxel efficacy by limiting adverse side effects and increasing its cytotoxic action. In this regard, nanotechnology has been recognized as a fundamental tool in cancer research [115] and the potential of nanocarriers to increase drug efficacy is well described [116-118].

### 6.5 Conclusions

Here, we describe a SLbL method to efficiently convert paclitaxel into drug NPs. It allows clinicians to combine many necessary factors for an efficient drug-delivery system: i) control of nanocolloid size within 100-300 nm, ii) high drug content of approximately 70% wt, iii) shell biocompatibility and biodegradability, and iv) sustained controlled release. Overall, these characteristics, including the small size and the net negative charge, that can be advantageous for their penetration to and within tumors, make NPs attractive candidates for possible *in vivo* applications.

In addition, in this research we elaborated nanoformulation of two drugs in one nanocapsule locating paclitaxel in the core and lapatinib on the shell periphery. The rationale for considering combination therapy is to overcome major problems associated with paclitaxel administration, such as the counteraction of paclitaxel resistance and, in combination with dose-escalation, the potential reduction of systemic toxicities. Moreover, with this strategy both drugs can be temporally co-localized in the tumor cells for optimal synergy, limiting possible differences in the pharmacokinetics and tumor accumulation of the two different agents.

Given the molecular complexity of cancer, drug combinations are most likely to translate into a significant clinical benefit. To further increase the therapeutic potential of nanocapsules, a research objective that remains to be explored regards the realization of a target delivery system. Surface functionalization by targeting ligands or antibodies is an attractive opportunity to direct NPs toward cancer-specific cells or tumor-specific clones with substantially greater selectivity in tumor killing versus toxicity to normal host tissues. Several types of targeting ligands should be used for this purpose, including peptides and antibodies. These ligands enable NPs to bind specific receptors and to be internalized by endocytosis, enhancing the intracellular accumulation of drugs. The feasibility of the LbL method makes easy the realization of functionalized NPs by using polymers with free reactive groups for the outer layer of LbL NPs. On the contrary, a relevant concern is the identification of reliable ligands to impart a precise biological function to NPs. Significant research efforts have been made in a recent study from the National Cancer Institute Pilot Project for the acceleration of translational research, where 75 possible tumor antigens were recognized [119]. Some of these tumor-associated antigens, including MUC1, CA 125, NY-ESO-1, and human epidermal GFR 2 (HER2)/neu are potential targets in ovarian cancer. In particular, due to its role in cellular transformation and tumorigenicity, MUC1 received great attention in those years. Recently, a monoclonal antibody anti-MUC1 has been utilized alone or in combination with docetaxel (DTX) in preclinical models of ovarian cancer, leading to a significant increase in survival. Furthermore, a MUC1 aptamer-guided nanoscale drug-delivery system was developed to enhance the paclitaxel delivery to MUC1- overexpressing MCF-7 cells *in vitro* [120-121].

To characterize the clinical potential of nanocolloids loaded with paclitaxel and lapatinib, preclinical studies in animal tumor models are necessary, including a detailed evaluation of pharmacokinetics and pharmacodynamics and active intracellular intracellular delivery of

LbL nanocolloids after intravenous or intraperitoneal administration. Extensive future research is warranted. Because many women experience recurrences during ovarian cancer therapy due to drug-resistance mechanisms, we postulate that our approach aiming at limiting this problem may serve the purpose of improving the treatment of ovarian tumors.

## CHAPTER 7

### CONCLUSIONS AND FUTURE WORK

#### 7.1 Conclusions

In this dissertation, the application of ultrasonication assisted Layer-by-Layer technology for the preparation of multifunctional nanoparticulated forms of poorly water-soluble anticancer drugs paclitaxel and lapatinib had been developed. Powerful ultra-sonication performed in the presence of surface-active bubbling agents resulted in formation of small drug nanoparticles of desired size. To stabilize them, the Layer-by-Layer self-assembly of multilayer films was built up with properties tailored by controlling the molecular makeup and arrangement with nanoscale precise film thickness. In this process, the nano-architectural approach designing layers of different components, including ones serving as diffusion barrier and outermost layers charging, were realized.

Two different approaches with powerful ultrasonication, top-down approach (sonicating bulk drug crystals in polyelectrolyte solution) and bottom-up approach (sonicating drug in a water-miscible organic solvent followed by slowly water add-in) had been successfully applied for the preparation of the nanoparticles of paclitaxel and lapatinib, correspondingly. For the top-down approach, 200 nm diameter was a kind of “magic” barrier for colloidal particles prepared. We suggested that it may be related to the nucleation size of the solvent vapor microbubbles. This assumption allowed us to decrease paclitaxel colloid particles to 120 nm diameter using agents enhancing bubbling formation (such as  $\text{NH}_4\text{HCO}_3$ ). However, a large obstacle of these powerful ultrasonication methods were a necessity of long time (one

hour) high power ultrasonication resulted in TiO<sub>2</sub> nanoparticle detachment from titanium electrode and contamination of the sample. Such formed paclitaxel nanoparticles were LbL coated with 10-20 nm polycation/polyanion shell to provide aqueous colloidal stability and slower particle dissolution. Mice injection was possible but demanded TiO<sub>2</sub> purification.

With the bottom-up approach (based on desolvation of the drug diluted in alcohol), less powerful sonication was used, and prepared particle sizes of 140-150 nm were obtained both for lapatinib and paclitaxel. Less sonification time (ca 15 minutes) allowed avoiding TiO<sub>2</sub> contamination. Regular sonication combined with our LbL approach and traditional emulsification process with addition of biodegradable surfactants to anchor polyelectrolytes on the surface of the formed drug nanoparticles had been applied to avoid the Ti pollution created by powerful ultrasonication. The bottom-up approach using polymeric excipients combined with non-ionic and anionic surfactants along with regular sonication allows preparing uniform 140-150 nm colloid cores of lapatinib. The amphiphiles attach to the hydrophobic nanoparticles and serves as anchors for LbL shell. In contrast to untangled amphiphiles, LbL polyelectrolyte shells do not detach easily from the surface and retain integrity upon dilution in another media. The inner LbL layers and surfactants minimize the surface free energy, thereby preventing crystal form changes and nanoparticles coalescence, while the outermost layers enhance colloidal stability.

To overcome difficulties with drug nanoformulation colloidal stability in high molarity PBS buffer, we developed LbL shells with PEGylation for lapatinib. For these shells, we used block-copolymer of cationic polylysine with PEG. The best stable in PBS buffer nanoformulations of lapatinib have shells consisting of a block copolymer of poly-L-lysine (PLL) and PEG of different length (PLB) as a positive component of the shell and heparin as a negative component. Better colloidal stability of lapatinib dispersions in PBS was obtained while using PLB copolymer at every bilayer with the shell architecture of (PLB/heparin)<sub>3.5</sub>.

In the proposed paclitaxel and lapatinib formulation, we obtained 150-200 nm with high drug content of 80-90 % due to very thin capsule walls (of ca 10 nm). The drug release time from the LbL capsules was found to be between 10 and 20 hours depending on the shell thickness. Washless LbL assembly had been used: 1) addition of polycation in the amount that is enough to reverse surface charge of the dispersion to a high positive (+30 mV) value; 2) addition of polyanion in the amount that is enough to reverse surface charge of the dispersion to a high negative (-30 mV) value. No intermediate washing of nanoparticles was done until the shell was complete.

We elaborated nanoformulation of two drugs in one nanocapsule locating paclitaxel in the core and lapatinib on the shell periphery. With this formulation of combining in one nanoparticle dual drug we reached the drugs efficiency synergy. In a multidrug-resistant (MDR) ovarian cancer cell line, OVCAR-3, lapatinib/paclitaxel nanocolloids mediated an enhanced cell growth inhibition in comparison with the paclitaxel-only treatment.

## **7.2 Future Work**

Upon completion of this research, the following ideas for future work were suggested. The first idea is the application of the bubbling agent for the bottom-up approach with regular ultrasoincaton to get even smaller particle sizes without the pollution of powerful ultrasonication. The second idea is trying different encapsulation methods for the preparation of dual drugs.

To further increase the therapeutic potential of nanocapsules, a target delivery system for anticancer drugs paclitaxel and lapatinib remains to be explored. Surface functionalization by targeting ligands or antibodies is an attractive opportunity to direct nanoparticles toward cancer-specific cells or tumor-specific clones with substantially greater selectivity in tumor killing versus toxicity to normal host tissues. Several types of targeting ligands should be

used for this purpose, including peptides and antibodies. The feasibility of the LbL method makes easy the realization of functionalized nanoparticles by using polymers with free reactive groups for the outer layer of LbL shell. Significant research efforts have been made in a recent study from the National Cancer Institute Pilot Project for the acceleration of translational research, where 75 possible tumor antigens were recognized [119-121].

## REFERENCES

- [1] <http://www.cancer.org/Research/CancerFactsFigures/ACSPP-031941> accessed on April 1st (2012).
- [2] R. Siegel, D. Naishadham, A. Jemal. "Cancer Statistics." *CA: A Cancer Journal for Clinicians*. 62:10-29 (2012).
- [3] D. Peer, J. Karp, S. Hong, O. Farokhzad, R. Margalit, R. Langer. "Nanocarriers as an emerging platform for cancer therapy." *Nature Nanotechnology*. 2, 751-760 (2007).
- [4] T. Allen, P. Cullis. "Drug delivery systems: entering the mainstream." *Science*. 303 (5665), 1818-1822. (2004).
- [5] C. Alexiou, R. Jurgons, C. Seliger, H. Iro. "Medical Applications of Magnetic Nanoparticles." *Journal of Nanoscience and Nanotechnology*. 6, 2762–2768 (2006).
- [6] P. Anand, C. Sundaram, S. Jhurani, A. Kunnumakkara, B. Aggarwal, B. Bharat. "Curcumin and cancer: An "old-age" disease with an 'age-old' solution." *Cancer Letters*. 267, 133-164 (2008).
- [7] V. Torchilin. "Multifunctional nanocarriers." *Advanced Drug Delivery Review*. 58, 1532-1555 (2006).
- [8] V. Torchilin. "Micellar nanocarriers: pharmaceutical perspectives." *Pharmaceutical Research*. 24, 1-16 (2007).
- [9] S. Croy, G. Kwon. "Polymeric Micelles for Drug Delivery." *Current Pharmaceutical Design*. 12, 4669-4684 (2006).

- [10] N. Nasongkla, E. Bey, J. Ren, H. Ai, C. Khemtong, J. Guthi, S. Chin, A. Sherry, D. Boothman, J. Gao. "Multifunctional polymeric micelles as cancer-targeted, MRI-ultrasensitive drug delivery systems." *Nano Letters*. 6, 11, 2427-2430 (2006).
- [11] C. A. Lipinski. "Drug-like properties and the causes of poor solubility and poor permeability." *Journal of Pharmacological and Toxicological Methods* 44, 235-249 (2000).
- [12] V. Vergaro, X. Zhang, Y. Lvov and S. Leporatti. "Drug-loaded polyelectrolyte microcapsules for sustained targeting of cancer cells." *Advanced Drug Delivery Review* 63, 9, 847-864 (2011).
- [13] C. Lipinski, F. Lombardo, B. Dominy, P. Feeney. "Experimental and computational approaches to estimate solubility and permeability in drug discovery and development settings." *Advanced Drug Delivery Review*. 46, 3-26 (2001).
- [14] <http://www.freedoniagroup.com/brochure/22xx/2294smwe.pdf> accessed on April 1st, 2012.
- [15] W.H.De Jong, P. J.A. Borm. "Drug delivery and nanoparticles: applications and hazards." *International Journal of Nanomedicine*. 3, 2, 133-149 (2008).
- [16] C. Medina, M. J. Santos-Martinez, A Radomski, O. I. Corrigan, M. W. Radomsk. "Nanoparticles: pharmacological and toxicological significance." *British Journal of Pharmacology*. 150, 552-558. (2007).
- [17] S.C. McBain, H.H.P. Yiu, J. Dobson. "Magnetic nanoparticles for gene and drug delivery." *International Journal of Nanomedicine*. 4, 1-7 (2009).
- [18] J. Lee, Y. Huh, Y. Jun, J. Seo, J. Jang, H. Song, S. Kim, E. Cho, H. Yoon, J. Suh, J. Cheon, "Artificially engineered magnetic nanoparticles for ultra-sensitive molecular imaging." *Nature Medicine*. 13, 1, 95-99 (2007).

- [19] D.J Bharali, M.Khalil, M. Gurbuz, T.M. Simone, S.A. Mousa. "Nanoparticles and cancer therapy: a concise review with emphasis on dendrimers." *International Journal of Nanomedicine*. 4, 1-7 (2009).
- [20] M.G. Ozawa, A.J. Zurita, E. Dias-Neto, D.N. Nunes, R. L. Sidman, J. G. Gelovani, W. Arap, R.Pasqualini. "Beyond Receptor Expression Levels: The Relevance of Target Accessibility in Ligand-Directed Pharmacodelivery Systems." *Trends in Cardiovascular Medicine*. 18, 4, 126-133 (2008).
- [21] R. Parthe, J.L. Conyers. "Biomedical applications for functionalized fullerene-based nanomaterials." *International Journal of Nanomedicine*. 4, 261-275 (2009).
- [22] E. Bekyarova, Y. Ni, E.B Malarkey, V. Montana, J. L.McWilliams, R.C. Haddon, V. Parpura. "Applications of carbon nanotubes in biotechnology and biomedicine." *Journal of Biomedical Nanotechnology*. 1, 1, 3-17 (2005).
- [23] F. Balavoine, P. Schultz, C.Richard, V. Mallouh, Th. W. Ebbesen, C. Mioskowski. "Helical crystallization of proteins on carbon nanotubes: A first step towards the development of new biosensors." *Angewandte Chemie International Edition*. 38, 1912-1915 (1999).
- [24] Z. Guo, P. Sadler, S. Tsang. "Immobilization and visualization of DNA and proteins on carbon nanotubes." *Advanced Materials*. 10, 701- 703 (1998).
- [25] J.J. Davis, M.L.H. Green, H.A.O. Hill, Y.C. Leung, P.J.Sadler, J. Sloan, A.V. Xavier, S.C. Tsang, "The immobilization of proteins in carbon nanotubes." *Inorganica Chimica Acta*. 272, 261-266 (1998).
- [26] V. Vergaro, E. Abdullayev, Y.M. Lvov, A. Zeitou, R. Cingolani, R. Rinaldi, S. Leporatti. "Cytocompatibility of halloysite clay nanotubes." *Biomacromolecules* 11, 820-826 (2010).

- [27] V. Vergaro, F. Scarlino, C. Bellomo, M. Maffia, X. Zhang, Y. Lvov, S. Leporatti. "Drug-loaded polyelectrolyte microcapsules for sustained targeting of cancer cells" *Advanced Drug Delivery Reviews*. 63, 847-864 (2011).
- [28] M. Ferrari. "Cancer nanotechnology: opportunities and challenges." *Nature Review Cancer*. 5, 3, 161-71 (2005).
- [29] F. Caruso, R. Caruso, H. Mohwald. "Nanoengineering of inorganic and hybrid hollow spheres by colloidal templating." *Science* 282, 1111-1114 (1998).
- [30] Y. Lvov, A. Antipov, H. Mohwald, G. Sukhorukov. "Urease encapsulation in nanoorganized microshells." *Nano Lett.* 1, 125-128 (2001)
- [31] G. Decher. "Fuzzy nanoassemblies: toward layered polymeric multicomposites." *Science* 227, 1232-1237 (1997).
- [32] Y. Lvov, G. Decher, H. Möhwald. "Assembly, structural characterization and thermal behavior of layer-by-layer deposited ultrathin films." *Langmuir*. 9, 481-486 (1993).
- [33] Y. Lvov, K. Ariga, I. Ichinose, T. Kunitake. "Assembly of multicomponent protein films by means of electrostatic layer-by-layer adsorption." *Journal of the American Chemical Society*. 117, 6117-6122 (1995).
- [34] K. Varshramyan, Y. Lvov. "Nanomanufacturing by layer-by-layer assembly - from nanoscale coating to device applications." Proceedings of the Institution of Mechanical Engineers, Part N. *Journal of Nanoengineering and Nanosystems*, 1, 220, 29-37 (2006).
- [35] M. McShane, Y. Lvov. "Layer-by-Layer Electrostatic Self-Assembly," in book: "Dekker Encyclopedia of Nanoscience & Nanotechnology," v. 4, Ed. J. Schwartz, C. Contescu, M. Dekker Publ. NY, 1-21 (2005).
- [36] P. Bertrand, A. Jonas, A. Laschewsky, R. Legras. "Ultrathin polymer coatings by complexation of polyelectrolytes at interfaces: suitable materials, structure and properties." *Macromolecular Rapid Communications*. 21, 319-348 (2000).

- [37] S. Sukhishvili. "Responsive polymer films and capsules via layer-by-layer assembly." *Current Opinion in Colloid & Interface Science*. 10, 37-44 (2005).
- [38] Z. Tang, Y. Wang, P. Podsiadlo, N. Kotov. "Biomedical applications of layer-by-layer assembly: from biomimetics to tissue engineering." *Advanced Materials*. 18, 3203–3224 (2006).
- [39] B. De Geest, N. Sanders, G. Sukhorukov, J. Demeester, S. De Smedt. "Release mechanisms for polyelectrolyte capsules." *Chemical Society Reviews*. 36, 636-649 (2007).
- [40] P. Hammond. "Form and function in multilayer assembly: new applications at the nanoscale." *Advanced Materials*. 16, 1271-1293 (2004).
- [41] G. Sukhorukov, A. Rogach, M. Garstka, S. Springer, W. Parak, A. Munoz-Javier, O. Kreft, A. Skirtach, A. Susa, Y. Ramaye, R. Palankar, M. Winterhalter. "Multifunctionalized polymer microcapsules: novel tools for biological and pharmacological applications." *Small*. 3, 944-955 (2007).
- [42] C.S. Peyratout, L. Daehne. "Tailor-made polyelectrolyte microcapsules: from multilayers to smartcontainers." *Angewandte Chemie International Edition*. 43, 3762-3783 (2004).
- [43] G.B. Sukhorukov, A. Fery, M. Brumen, H. Mohwald. "Physical chemistry of encapsulation and release." *Physical Chemistry Chemical Physics*. 6, 4078-4089 (2004).
- [44] B. De Geest, S. De Koker, G. Sukhorukov, O. Kreft, W. Parak, A. Skirtach, J. Demeester, S. De Smedt, W. Hennink. "Polyelectrolyte microcapsules for biomedical applications." *Soft Matter*. 5, 282-291 (2009).
- [45] L. De Cock, S. De Koker, B. De Geest, J. Grooten, C. Vervaet, J. Remon, G. Sukhorukov, M. Antipina. "Polymeric Multilayer Capsules in Drug Delivery." *Angewandte Chemie International Edition*. 49, 2-22(2010).

- [46] M. Delcea, A. Yashchenok, K. Videnova, O. Kreft, H. Möhwald, A. Skirtach. "Multicompartmental Micro- and Nanocapsules: Hierarchy and Applications in Biosciences." *Macromolecular Bioscience*. 10,465-474 (2010).
- [47] M. Hwald, G. Sukhorukov. "Polymericmicrocapsules with light responsive properties for encapsulation and release." *Advances in Colloid and Interface Science*. 158, 2-14 (2010).
- [48] C. Mora-Huertasa, H. Fessia, A. Elaissaria. "Polymer-based nanocapsules for drug delivery." *International Journal of Pharmaceutics*. 385, 113-142 (2010).
- [49] P. Gil, L. del Mercato, P. del\_Pino, A. Javier, W. Parak. "Nanoparticle-modified polyelectrolyte capsules." *Nanotoday*. 3: 3-4, 12-21 (2008).
- [50] T. Allen, P. Cullis. "Drug delivery systems: entering the mainstream." *Science*. 303, 1818-1822 (2004).
- [51] G. Hughes. "Nanostructure-mediated drug delivery." *Nanomedicine*. 1, 1, 22-30 (2005).
- [52] R. Langer, D.A. Tirrell. "Designing materials for biology and medicine." *Nature*. 428, 487-492 (2004).
- [53] E. Pridgen, R. Langer, O. Farokhzad. "Biodegradable polymeric nanoparticle delivery systemsfor cancer therapy." *Nanomedicine*. 2, 5, 669-680 (2007).
- [54] F. Caruso, R. Caruso, H. Mohwald. "Nanoengineering of inorganic and hybrid hollow spheres bycolloidal templating." *Science*. 282, 1111-1114 (1998).
- [55] E. Donath, G. Sukhorukov, F. Caruso, S. Davis, H. Mohwald. "Novel hollow polymer shells bycolloid-templated assembly of polyelectrolytes." *Angewandte Chemie International Edition*. 37, 2201-2205 (1998).
- [56] D. Volodkin, A. Petrov, M. Prevot, G. Sukhorukov. "Matrix polyelectrolyte microcapsules: newsystem for macromolecule encapsulation." *Langmuir*. 20, 8, 3398-3406 (2004).

- [57] G. Sukhorukov, H. Mohwald. "Multifunctional cargo systems for biotechnology." *Trends in Biotechnology*. 25, 3, 93-98 (2007).
- [58] T. Borodina, E. Markvicheva, S. Kunizhev, H. M $\ddot{o}$ hwald, G. Sukhorukov, O. Kreft. "Controlled Release of DNA from Self-Degrading Microcapsules." *Macromolecular Rapid Communications*. 28, 18-19, 1894-1899 (2007).
- [59] G. Sukhorukov, D. Volodkin, A. Gunther, A. Petrov, D. Shenoy, H. Mohwald. "Porous calcium carbonate microparticles as templates for encapsulation of bioactive compounds." *Journal of Materials Chemistry* 14, 1, 2073-2081 (2004).
- [60] D.V. Volodkin, N.I. Larionova, G.B. Sukhorukov. "Protein encapsulation via porous CaCO<sub>3</sub> microparticles templating." *Biomacromolecules*. 5, 1962-1972 (2004).
- [61] D. Shenoy, A. Antipov, G. Sukhorukov, H. Mohwald. "Layer-by-Layer Engineering of Biocompatible, Decomposable Core-Shell Structures." *Biomacromolecules*. 4, 265-272 (2003).
- [62] Y. Ma, W. Dong, M. Hempenius, H. Mohwald, G. Vancso. "Redox-controlled molecular permeability of composite-wall microcapsules." *Nature Materials*. 5, 724-729 (2006).
- [63] A. Agarwal, Y. Lvov, R. Sawant, V. Torchilin. "Stable nanocolloids of poorly soluble drugs with high content drug prepared using the combination of sonication and layer-by-layer technology." *Journal of Controlled Release* 128, 255-260, (2008).
- [64] K. Suslik. "Sonochemistry." *Science*. 247, 1439-1445 (1990).
- [65] K. Suslik, David A. Hammerton, Raymond E. Cline, Jr. "The sonochemical hot spot." *Journal of the American Chemical Society*. 108, 5641-5642 (1986).
- [66] K. Suslick. "*Scientific American*." 2, 260, 80-86 (1989).
- [67] D. Shchukin, H. Mohwald. "Sonochemical nanosynthesis at the engineered interface of a cavitation." *Physical Chemistry Chemical Physics*. 8, 3496-3506 (2006).

- [68] D. Radziuk; H. Möhwald; D. Shchukin. "Sonochemical Design of Engineered Gold-Silver Nanoparticles." *Journal of Physical Chemistry C*. 112, 2462-2468 (2008).
- [69] D. Shchukin, K. Kohler, H. Möhwald, G. Sukhorukov. "Gas-Filled Polyelectrolyte Capsules." *Angewandte Chemie International Edition*. 44, 3310-3314 (2005).
- [70] X. Teng, D. Shchukin, H. Mohwald. "Encapsulation of water-Immiscible Solvents in Polyglutamate/Polyelectrolyte Nanocontainers." *Advanced Functional Materials*. 17, 1273-1278 (2007).
- [71] Z. Zheng, X. Zhang, D. Carbo, C. Clark, C. Nathan, Y. Lvov. "Sonication assisted synthesis of polyelectrolyte coated curcumin nanoparticles." *Langmuir*. 26, 11, 7679-7681 (2010).
- [72] Y. Lvov, P. Pattekari, X. Zhang, Vladimir Torchilin. "Converting Poorly Soluble Materials into Stable Aqueous Nanocolloids." *Langmuir*. 27, 3, 1212-1217 (2011).
- [73] P. Pattekaria, Z. Zheng, X. Zhang, T. Levchenko, V. Torchilin, Y. Lvov. "Top-down and Bottom-up Approaches in Production of Aqueous Nanocolloids of Low Solubility Drug Paclitaxel." *Physical Chemistry Chemical Physics*. 13, 9014-9019 (2011).
- [74] D. Vergara, C. Bellomo, X. Zhang, Y. Lvov, S. Leporatti. "Lapatinib/Paclitaxel Polyelectrolyte Nanocapsules for Overcoming Multidrug Resistance in Ovarian Cancer." *Nanomedicine: Nanotechnology, Biology, and Medicine*. 8, 6, 891-899 (2012).
- [75] [http://niton.com/en/products/zecom\\_s.htm](http://niton.com/en/products/zecom_s.htm) accessed on 04/01/2012
- [76] A. Jemal, R. Siegel, J. Xu, E. Ward. "Cancer statistics." *CA – A Cancer Journal for Clinicians*. 60, 277-300 (2010).
- [77] P. Vasey. "Resistance to chemotherapy in advanced ovarian cancer: mechanisms and current strategies." *British Journal of Cancer*. 89, 23-28 (2003).

- [78] M. Wani, H. Taylor, M. Wall, P. Coggon, A. McPhail. Plant antitumor agents. VI. The isolation and structure of taxol, a novel antileukemic and antitumor agent from *Taxus brevifolia*. *Journal of the American Chemical Society*. 93, 2325-2327 (1971).
- [79] V. Sandor, T. Fojo, S. Bates. "Future perspectives for the development of P-glycoprotein modulators." *Drug Resistance Updates*. 1, 190-200 (1998).
- [80] G. Ferrandina, G. Zannoni, E. Martinelli, A. Paglia, V. Gallotta, S. Mozzetti, G. Scambia, C. Ferlini. "Class III beta-tubulin overexpression is a marker of poor clinical outcome in advanced ovarian cancer patients." *Clinical Cancer Research*. 12, 2774-2779 (2006).
- [81] M. Szajnik, M. Szczepanski, Czystowska M, Elishaev E, Mandapathil M. "Nowak-Markwitz E, Spaczynski M, Whiteside TL. TLR4 signaling induced by lipopolysaccharide or paclitaxel regulates tumor survival and chemoresistance in ovarian cancer." *Oncogene*. 28, 4353-63 (2009).
- [82] M. Kelly, A. Alvero, R. Chen, D. Silasi, V. Abrahams, S. Chan, I. Visintin, T. Rutherford, G. Mor. "TLR-4 signaling promotes tumor growth and paclitaxel chemoresistance in ovarian cancer." *Cancer Research*. 66, 3859-3868 (2006).
- [83] L. Huang, Q. Ao, Q. Zhang, X. Yang, H. Xing, F. Li, G. Chen, J. Zhou, S. Wang, G. Xu, L. Meng, Y. Lu, D. Ma. "Hypoxia induced paclitaxel resistance in human ovarian cancers via hypoxia-inducible factor 1alpha." *Journal of Cancer Research and Clinical Oncology*. 136, 447-456 (2010).
- [84] L. Zuylen, J. Verweij, Sparreboom A. "Role of formulation vehicles in taxane pharmacology." *Investigational New Drugs*. 19, 125-141 (2001).
- [85] A. Zahr, M. Pishko. "Encapsulation of paclitaxel in macromolecular nanoshells." *Biomacromolecules*. 8, 2004-2010 (2007).

- [86] X. Li, P. Li, Y. Zhang, Y. Zhou, X. Chen, Y. Huang, Y. Liu. "Novel mixed polymeric micelles for enhancing delivery of anticancer drug and overcoming multidrug resistance in tumor cell lines simultaneously." *Pharmaceutical Research*. 27, 1498-1511 (2010).
- [87] T. Ooya, J. Lee, K. Park. "Hydrotropic dendrimers of generations 4 and 5: synthesis, characterization, and hydrotropic solubilization of paclitaxel." *Bioconjugate Chemistry*. 15, 1221-1229 (2004).
- [88] H. Zhao, J. Wang, Q. Sun, C. Luo, Q. Zhang. "RGD-based strategies for improving antitumor activity of paclitaxel-loaded liposomes in nude mice xenografted with human ovarian cancer." *Journal of Drug Targeting*. 17, 10-8 (2009).
- [89] J. Zhao, Y. Cui, A. Wang, J. Fei, Y. Yang, L. Junbai. "Side Effect Reduction of Encapsulated Hydrocortisone Crystals by Insulin/Alginate Shells." *Langmuir*. 27, 1499-1504 (2011).
- [90] K. Linton. "Structure and function of ABC transporters." *Physiology (Bethesda)*. 22, 122-130 (2007).
- [91] T. Simşek, G. Ozbilim, H. Gülkesen, H. Kaya, F. Sargin, S. Karaveli. "Drug resistance in epithelial ovarian cancer: P-glycoprotein and glutathione S-transferase. Can they play an important role in detecting response to platinum-based chemotherapy as a first-line therapy." *European journal of gynaecological oncology*. 22, 436-438 (2001).
- [92] R. Krishna, L. "Mayer. Multidrug resistance (MDR) in cancer. Mechanisms, reversal using modulators of MDR and the role of MDR modulators in influencing the pharmacokinetics of anticancer drugs." *European Journal of Pharmaceutical Sciences*. 11, 265-283 (2000).

- [93] C. Dai, A. Tiwari, C. Wu, X. Su, S. Wang, D. Liu, C. Ashby, Y. Huang, R. Robey, Y. Liang, L. Chen, C. Shi, S. Ambudkar, Z. Chen, L. Fu. "Lapatinib (Tykerb, GW572016) reverses multidrug resistance in cancer cells by inhibiting the activity of ATP-binding cassette subfamily B member 1 and G member 2." *Cancer Research*. 68, 7905-7914 (2008).
- [94] G. Bantchev, Z. Lu, Y. Lvov. "Layer-by-Layer Nanoshell Assembly on Colloids through Simplified Washless Process." *Journal of Nanoscience and Nanotechnology*. 9, 396-403 (2009).
- [95] G. Leonard, O. Polgar, S. Bates. "ABC transporters and inhibitors: new targets, new agents." *Current Opinion in Investigational Drugs*. 3, 1652-1659 (2002).
- [96] E. Yakirevich, E. Sabo, I. Naroditsky, Y. Sova, O. Lavie, M. Resnick. "Multidrug resistance-related phenotype and apoptosis-related protein expression in ovarian serous carcinomas." *Gynecologic Oncology*. 100, 152-159 (2006).
- [97] P. Surowiak, V. Materna, C. Denkert, I. Kaplenko, M. Spaczyński, M. Dietel, M. Zabel, H. Lage. "Significance of cyclooxygenase 2 and MDR1/P-glycoprotein coexpression in ovarian cancers." *Cancer Letters*. 235, 272-280 (2006).
- [98] van der Zee AG, Hollema H, Suurmeijer AJ, Krans M, Sluiter WJ, Willemse PH, Aalders JG, de Vries EG. "Value of P-glycoprotein, glutathione S-transferase pi, c-erbB-2, and p53 as prognostic factors in ovarian carcinomas." *Journal of Clinical Oncology*. 13:70-78 (1995).
- [99] D. Altomare, H. Wang, K. Skele, A. De Rienzo, A. Klein-Szanto, A. Godwin, J. Testa. "Akt and mTOR phosphorylation is frequently detected in ovarian cancer and can be targeted to disrupt ovarian tumor cell growth." *Oncogene*. 23, 5853-5857 (2004).

- [100] Z. Yuan, M. Sun, R. Feldman, G. Wang, X. Ma, C. Jiang, D. Coppola, S. Nicosia, J. Cheng. "Frequent activation of Akt 2 and induction of apoptosis by inhibition of phosphoinositide-3-OH kinase/Akt pathway in human ovarian cancer." *Oncogene* 19, 2324-2330 (2000).
- [101] B. Hennessy, D. Smith, P. Ram, Y. Lu, G. Mills. "Exploiting the PI3K/Akt pathway for cancer drug discovery." *Nature Reviews Drug Discovery*. 4, 988-1004 (2005).
- [102] O. Felt, P. Buri, R. Gurny. "Chitosan: a unique polysaccharide for drug delivery." *Drug Development and Industrial Pharmacy*. 24, 979-993 (1998).
- [103] S. Chauhan, D. Kumar, M. Jaggi. "Mucins in ovarian cancer diagnosis and therapy." *Journal of Ovarian Research*. Dec 24; 2:21 (2009).
- [104] N. Gao, D. Flynn, Z. Zhang, X. Zhong, V. Walker, K. Liu, X. Shi, B. Jiang. "G1 cell cycle progression and the expression of G1 cyclins are regulated by PI3K/AKT/mTOR/p70S6K1 signaling in human ovarian cancer cells." *American Journal of Physiology - Cell Physiology*. 287:281-291 (2004).
- [105] H. Onyüksel, E. Jeon, I. Rubinstein. "Nanomicellar paclitaxel increases cytotoxicity of multidrug resistant breast cancer cells." *Cancer Letters*. 274:327-330 (2009).
- [106] Y. Qian, L. Corum, Q. Meng, J. Blenis, J. Zheng, X. Shi, D. Flynn, B. Jiang. "PI3K induced actin filament remodeling through Akt and p70S6K1: implication of essential role in cell migration." *American Journal of Physiology - Cell Physiology*. 286:153-163 (2004).
- [107] A. Amiri, F. Noei, S. Jeganathan, G. Kulkarni, D. Pinke, J. Lee. "eEF1A 2 activates Akt and stimulates Akt-dependent actin remodeling, invasion and migration." *Oncogene* 26, 3027-3040 (2007).

- [108] F. Vandermoere, I. Yazidi-Belkoura, Y. Demont, C. Slomianny, J. Antol, J. Lemoine, H. Hondermarck. "Proteomics exploration reveals that actin is a signaling target of the kinase Akt." *Molecular & Cellular Proteomics*. 6, 114-124 (2007).
- [109] V. Cenni, A. Sirri, M. Riccio, G. Lattanzi, S. Santi, A. de Pol, N. Maraldi, S. Marmioli. "Targeting of the Akt/PKB kinase to the actin skeleton." *Cellular and Molecular Life Sciences*. 60, 2710-2720 (2003).
- [110] J. Van Rheenen, J. Condeelis, M. Glogauer. "A common cofilin activity cycle in invasive tumor cells and inflammatory cells." *Journal of Cell Science*; 122:305-311 (2009).
- [111] S. Abrams, L. Steelman, J. Shelton, E. Wong, W. Chappell, J. Bäsecke, F. Stivala, M. Donia, F. Nicoletti, M. Libra, A. Martelli, J. McCubrey. "The Raf/MEK/ERK pathway can govern drug resistance, apoptosis and sensitivity to targeted therapy." *Cell Cycle*. 9, 1781-1791 (2010).
- [112] A. Di Leo, H. Gomez, Z. Aziz, Z. Zvirbule, J. Bines, M. Arbushites, S. Guerrero, M. Koehler, C. Oliva, S. Stein, L. Williams, J. Dering, R. Finn, M. Press. "Phase III, double-blind, randomized study comparing lapatinib plus paclitaxel with placebo plus paclitaxel as first-line treatment for metastatic breast cancer." *Journal of Clinical Oncology*. 26, 5544-5552 (2008).
- [113] G. Leonard, O. Polgar, S. Bates. "ABC transporters and inhibitors: new targets, new agents." *Current Opinion in Investigational Drugs*. 3, 1652-9 (2002).
- [114] E. Yakirevich, E. Sabo, I. Naroditsky, Y. Sova, O. Lavie, M. Resnick. "Multidrug resistance-related phenotype and apoptosis-related protein expression in ovarian serous carcinomas." *Gynecologic Oncology*. 100, 152-9 (2006).
- [115] P. Surowiak, V. Materna, C. Denkert, I. Kaplenko, M. Spaczyński, M. Dietel. "Significance of cyclooxygenase 2 and MDR1/P-glycoprotein coexpression in ovarian cancers." *Cancer Letters*. 235,272-80 (2006).

- [116] A. van der Zee, H. Hollema, A. Suurmeijer, M. Krans, W. Sluiter, P. Willemse, et al. "Value of P-glycoprotein, glutathione S-transferase pi, c-erbB-2, and p53 as prognostic factors in ovarian carcinomas." *Journal of Clinical Oncology*. 13, 70-8 (1995).
- [117] M. Ferrari. "Cancer nanotechnology: opportunities and challenges." *Nature Reviews Cancer*. 5, 161-71 (2005).
- [118] J. Heath, M. Davis. "Nanotechnology and cancer." *Annual Review of Medicine*. 59, 251-65 (2008).
- [119] V. Vergaro, F. Scarlino, C. Bellomo, R. Rinaldi, D. Vergara, M. Maffia, et al. "Drug-loaded polyelectrolyte microcapsules for sustained targeting of cancer cells." *Advanced Drug Delivery Reviews*. 63, 847-64 (2011).
- [120] I. Palamà, S. Leporatti, E. de Luca, N. Di Renzo, M. Maffia, C. Gambacorti-Passerini, et al. "Imatinib-loaded polyelectrolyte microcapsules for sustained targeting of BCR-ABL+ leukemia stem cells." *Nanomedicine (Lond)*. 5, 419-31 (2010).
- [121] M. Cheever, J. Allison, A. Ferris, O. Finn, B. Hastings, T. Hecht, et al. "The prioritization of cancer antigens: a national cancer institute pilot project for the acceleration of translational research." *Clinical Cancer Research*. 15, 5323-37 (2009).
- [122] L. Wang, H. Chen, M. Pourgholami, J. Beretov, J. Hao, H. Chao, et al. "Anti-MUC1 monoclonal antibody (C595) and docetaxel markedly reduce tumor burden and ascites, and prolong survival in an *in vivo* ovarian cancer model." *PLoS One*. 6, e24405 (2011).
- [123] C. Yu, Y. Hu, J. Duan, W. Yuan, C. Wang, H. Xu, X. Yang. "Novel aptamer-nanoparticle bioconjugates enhances delivery of anticancer drug to muc1-positive cancer cells *in vitro*." *PLoS One*. 6, e24077 (2011).

## VITA

Xingcai Zhang finished his college in Quanzhou, China in 2001 and earned his Master of Science degree in Materials Physics and Chemistry at Sun-Yet Sen University in 2006. During 1999-2006, Mr. Zhang was recognized more than 10 times by the school or university administration as well as by the Ministry of Education of People's Republic of China for his successes in studies and research. He is the winner of National Scholarship, Dupont Scholarship, Shanghai Heshibi Huibang Scholarship; Xianluan Scholarship, Excellent student scholarship for College Students, First Prize in 2003 Fujian College English Contest ; Second Prize in National College English Contest, First Prize for Excellent Students in College, Excellent student in Advanced Mathematics, First Class Merit-based Scholarship, Excellent student in English and other awards. He worked as a Quality Manager in the Painting Department of multinational company Guangzhou Honda Automobile Co., Ltd, which got No.1 ranking by J.D. Power Initial Quality Survey. He was sent to Tokyo, Japan for his excellent job in quality management. He also interned at Fujian Petrochemical Company Limited (FPCL) (integrated petrochemical project between China Petroleum & Chemical Co., ExxonMobil and Aramco Overseas Company), German BSD Company, and Ourchem Consulting Company Limited etc. In the autumn of 2008 he was enrolled into Engineering Ph.D. program at Louisiana Tech University under the supervision of Dr. Yuri Lvov. Mr. Zhang's area of interest is the development of ultrasonication assisted Layer-by-Layer technology for the preparation of multi-functional anticancer drugs paclitaxel and lapatinib, etc. He also got his masters' degree in Micro/Nano System Engineering (Nov. 2011), Mathematics and Statistics (Aug. 2012) at Louisiana Tech University. Mr. Zhang has had

many publications and attended many conferences during his graduate studies. His publications are listed as follows:

### Book Chapter

- X. Zhang "On-Job-Training Book for Painting Department," Guangzhou Honda Automobile Co., Ltd , 2008 (Book)

### Peer-Reviewed Journals

- Z. Zheng, X. Zhang, Y. Lvov et al. "Sonication assisted synthesis of polyelectrolyte coated curcumin nanoparticles." *Langmuir*. 2010, 26(11), 7679-7681 (IF:4.268).
- Y. Lvov, P. Pattekari, X. Zhang, Vladimir Torchilin. "Converting Poorly Soluble Materials into Stable Aqueous Nanocolloids." *Langmuir*. 2011, 27 (3), 1212-1217 (IF:4.268).
- P. Pattekaria, Z. Zheng, X. Zhang, T. Levchenko, V. Torchilin, Y. Lvov. "Top-down and Bottom-up Approaches in Production of Aqueous Nanocolloids of Low Soluble Drug Paclitaxel." *Physical Chemistry, Chemical Physics*. 2011, 13, 9014-9019 (IF:4.06).
- V. Vergaro, etal, X. Zhang, Y. Lvov and S. Leporatti. "Drug-loaded polyelectrolyte microcapsules for sustained targeting of cancer cells." *Advanced Drug Delivery Review*. 2011, 63, 9, 847-864 (IF:13.577).
- D. Vergara, C. Bellomo, X. Zhang , Y. Lvov, S. Leporatti. etal. Lapatinib/Paclitaxel Polyelectrolyte Nanocapsules for Overcoming Multidrug Resistance in Ovarian Cancer. *Nanomedicine: Nanotechnology, Biology, and Medicine*. 2012, 8, 6, 891-899 (IF: 6.202).
- X. Zhang, P. Pattekari, Y. Lvov "Making Aqueous Nanocolloids from Low Soluble Materials: Bibubbling method assisted LbL Encapsulation." *Nanomedicine* (To be submitted 2013) (IF: 6.202).
- Z. Gong, S. Karandikar, X. Zhang, V. Kotipalli, Y. Lvov, L. Que. "Composite nanomaterial thin film-based biosensors." *IEEE Sensors*. 2010, 29-32 (IF: 1.917).
- X. Zhang, M. Rong, M. Zhang, "Progress in self-healing materials." *Aerospace Materials and Technology*. 2006, 36, 1.

### Conference Proceedings

- X. Zhang, Y. Lvov. "Stable low soluble drug nanocolloids preparation using bubbling agent assisted ultrasonication and Layer-by-Layer technology." *67th ACS Southwest Regional Meeting*. November 9-12, 2011. DoubleTree Hotel, Austin, Texas.
- X. Zhang, Y. Lvov. et al. "Preparation of Stable Nanocolloids for Low Soluble Drugs Using Sonication Assisted Layer-by-Layer Technology." *Materials Science and Technology 2010 Conference and Exhibition*. October 17-21, 2010. Houston, Texas.
- V. Vergaro, X. Zhang, G. Maruccio, Y. Lvov, S. Leporatti. "Nanotechnology for Cancer Therapy: Nanocarriers and Cytomechanics." *2nd World Conference on Nanomedicine and Drug Delivery (WCN-2011)* March 11-13, 2011, Kerala, India.
- V. Vergaro, E. Abdullayev, X. Zhang, Y. Lvov, S. Leporatti. "Nanocarriers for Cancer Therapy PMSE Symposium Clay/Polymer Nanocomposites." *241st National American Chemical Society Meeting*, Anaheim, March 27-30, 2011.
- P. Pattekari, X. Zhang, Z. Zheng, B. Shah, Y. Lvov. "Stable nanoparticles of low soluble anticancer drugs using ultrasonication assisted layer-by-layer technique." *13th International Conference on Organized Molecular Films (LB-13)*, July 18-21, 2010 Quebec City, Canada.
- Z. Gong, X. Zhang, Y. Lvov, L. Que. "Fabrication of micro and nanodevices using nanocomposite materials by combining layer-by-layer nanoassembly and optical lithography." *Materials Science and Technology 2010 Conference and Exhibition*. October 17-21, 2010. Houston, Texas.
- V. Vergaro, Z. Zheng, X. Zhang, Y. Lvov et al. "Nanocarriers for Cancer Therapy." *Particles 2010*. May 22-25, 2010. Regal Sun Resort, Lake Buena Vista, Florida.
- Y. Lvov, P. Pattekari, X. Zhang, Z. Zheng. "Making Aqueous Nanocolloids from Low Soluble Materials: LbL Encapsulation." *5th International Conference on Surfaces, Coatings and Nanostructures Materials (NANOSMAT-5)*. Reims, France, Oct 19-21, 2010.
- Z. Gong, S. Karandikar, X. Zhang, V. Kotipalli, Y. Lvov, L. Que. "Composite nanomaterial film-based biosensors." *IEEE Sensors 2010 Conference*. November 1-4, 2010. Waikoloa, HI.